Studies on effect of GGBFS content on the performance of Geopolymer Concrete

a Thesis submitted

in partial fulfilment of the requirements for the award of the degree of

DOCTOR OF PHILOSOPHY

in

CIVIL ENGINEERING

by

Diksha

(Roll No.: 2K18/Ph.D./CE/16)

under the supervision of

Prof. Nirendra Dev

&

Prof. Pradeep Kumar Goyal

DEPARTMENT OF CIVIL ENGINEERING

DELHI TECHNOLOGICAL UNIVERSITY

SHAHBAD DAULATPUR, BAWANA ROAD, DELHI - 110042 (INDIA)

JULY 2025

DELHI TECHNOLOGICAL UNIVERSITY

(Formerly Delhi College of Engineering)
Shahbad Daulatpur, Main Bawana Road, Delhi-42

CANDIDATE'S DECLARATION

I **Diksha** hereby certify that the work which is being presented in the thesis entitled **Studies on effect of GGBFS content on the performance of Geopolymer Concrete** in partial fulfillment of the requirements for the award of the Degree of Doctor of Philosophy, submitted in the Department of **Civil Engineering**, Delhi Technological University is an authentic record of my own work carried out initially during the period from **02/08/2018** to **02/07/2025** under the supervision of **Prof. Nirendra Dev & Prof. Pradeep Kumar Goyal.**

The matter presented in the thesis has not been submitted by me for the award of any other degree of this or any other Institute.

Diksha

Candidate's Signature

This is to certify that the student has incorporated all the corrections suggested by the examiners in the thesis and the statement made by the candidate is correct to the best of our knowledge.

Nirendra Dev

Signature of Supervisor

Deepak Kumar

Signature of External Examiner

ACKNOWLEDGEMENT

It is my proud privilege to express my heartfelt indebtedness to my research supervisors Prof. Nirendra Dev, Professor, Department of Civil Engineering, DTU Delhi and Prof. Pradeep Kumar Goyal, Department of Civil Engineering, DTU Delhi, for their excellent guidance, valuable suggestions and encouragement in the course of the study and preparation of this thesis. Indeed, I am greatly honored to be their research student and greatly influenced by their penchant for excellence. Their unwavering support and help in the face of all kinds of odds and uncertainties are humbly acknowledged. I avail this opportunity to express my deep sense of gratitude and sincere thanks to my research supervisors for their inspiration, expert guidance, moral support and continuous encouragement, which were vital factors in the successful completion of the present work.

Sincere thanks to Respected Shri Vinai Kumar Saxena, Hon'ble Chancellor, Delhi Technological University, Delhi and Prof. Prateek Sharma, Hon'ble Vice-Chancellor, Delhi Technological University, Delhi. I would like to thank Prof. K. C. Tiwari, Professor and Head, Department of Civil Engineering, Delhi Technological University, Delhi. I am thankful to the Delhi Technological University for providing an opportunity for research through its research fund and sponsoring me to pursue my research. I would also like to thank the DTU Library for providing me with the literature of research content and online journals. The co-operation and encouragement of my colleagues at Delhi Technological University, Delhi, are gratefully acknowledged. I express my special thanks to my friends for their help and valuable support. I express my warm regards and profound gratitude to my esteemed father and my family members for their moral support, encouragement and blessings. I humbly thank all those who, in any manner, directly or indirectly, put a helping hand to complete this research work.

(Diksha)

Abstract

Geopolymer concrete (GPC) is an innovative, sustainable, cementless, and eco-friendly material that significantly reduces carbon emissions by entirely replacing cement in concrete production. Cement manufacturing is a major contributor to CO_2 emissions, and GPC offers a viable alternative. In this experimental investigation, the fresh, chemical, and mechanical properties of GPC were evaluated across various parameters to determine the optimum mix design. The study examined fly ash-to-GGBFS (alccofine) ratios ranging from 100/0 to 75/25, liquid-to-binder (L/B) ratios from 0.35 to 0.65, superplasticizer contents from 0.5% to 2.0%, sodium hydroxide molarity from 8M to 14M, and sodium silicate-to-sodium hydroxide ratios from 0.5 to 3. Durability tests included exposure to seawater, magnesium sulfate (sulfate attack), acid attack, and wetting-drying conditions. Workability was assessed using slump and density tests, while mechanical properties were evaluated through compressive strength, splitting tensile strength, flexural strength, elastic modulus, and rebound hammer tests. Durability tests measured residual compressive strength, visual inspections, and density variations. The results revealed that oven-cured samples consistently outperformed ambient-cured samples, with the 75/25 fly ash-to-alccofine ratio achieving the highest engineering strength. The compressive strength peaked at an L/B ratio of 0.55, with strength increasing up to this point before declining randomly at higher ratios. A mix containing 1.5% superplasticizer and a 0.45 L/B ratio demonstrated superior strength compared to other combinations. Increasing the NaOH molarity up to 12M enhanced compressive strength, but strength declined beyond this point under both curing conditions. Similarly, strength improved with higher alkaline ratios, peaking at a ratio of 2, before decreasing. Mechanical strength also increased with curing temperature, reaching an optimum at 100°C, after which it began to decrease. Durability tests showed that seawater exposure initially increased strength and density but led to degradation after 12 weeks. Alccofine-based GPC exhibited better resistance to seawater and sulfate attacks compared to other compositions. Both types of specimens followed similar patterns of strength and mass loss under these conditions, with alccofine-based samples demonstrating superior stability. Under wetting-drying cycles, alccofine-based GPC also exhibited greater durability and resistance to degradation. For the final optimum values, the Advanced machine learning techniques, including Artificial Neural Networks (ANN), Gene Expression Programming (GEP), Support Vector Regression (SVR), Bi-LSTM, and Self-Improved Jelly Search Optimization (SIJSO), demonstrated significant

potential in predicting the mechanical properties of GPC. These methods offer powerful tools for optimizing mix designs and enhancing performance. This study underscores the potential of Alccofine as a high-performance supplementary material and highlights the role of advanced ML techniques in advancing sustainable construction practices.

Abbreviations

Abbreviation	Definition
GPC	Geopolymer Concrete
FA	Flyash
GGBFS	Ground Granulated Blast Furnace Slag
MK	Metakaolin
NaOH	Sodium Hydroxide
Na_2SiO_3	Sodium Silicate
KOH	Potassium Hydroxide
K_2CO_3	Potassium Carbonate
Na_2CO_3	Sodium Carbonate
XRD	X-Ray Diffraction
SEM	Scanning Electronic Microscope
EDS	Energy-Dispersive X-Ray Spectroscopy
OPC	Ordinary Portland Cement
PPC	Portland Pozzolana Cement
PCE	Poly-Carboxylate Ester
G	Specific Gravity
P	Bulk Density
SNF	Sulphonated Naphthalene Formaldehyde
CSH	Calcium Silicate Hydrate
UPV	Ultrasonic Pulse Velocity
ASTM	American Standard Testing Materials
IS	Indian Standard
TGA	Thermogravimetric Analysis
LBR	Liquid-To-Binder Ratio
FTIR	Fourier-Transform Infrared Spectroscopy
FLGC	Flyash-Based Lightweight Geopolymer Concrete
UTM	Universal Testing Machine

CTM	Compression Testing Machine
ML	Machine Learning
ANN	Artificial Neural Networks
SVM	Support Vector Machines
GEP	Gene Expression Programming
GA	Genetic Algorithm
CNN	Convolutional Neural Networks
RNN	Recurrent Neural Networks
IoT	Internet of Things
RF	Random Forests
Bi-LSTM	Bidirectional Long Short-Term Memory Network
SIJSO	Self-Improved Jelly Search Optimization
Gmax	Maximum Gene Count
dmax	Maximum Tree Depth
RMSE	Root Mean Square Error
RMSE	Radial Basis Function
MSE	Mean Squared Error
MAE	Mean Absolute Error
MAPE	Mean Absolute Percentage Error

Table of Contents

Contents

Lists of Figures

List of Tables

Chapter 1
Introduction

1.1 General

Concrete is the world's second most commonly used material, second only to water. Traditionally, Portland cement has been utilized as the primary binding material in concrete, with India producing over 502 million tons of cement in 2018. However, cement production poses significant environmental challenges, contributing approximately 8% of global greenhouse gas emissions, primarily CO_2 (Shobeiri et al., 2021). Additionally, the process depletes natural resources and generates pollution, threatening ecological sustainability. Given the finite availability of natural resources, sustainable alternatives are imperative. Meanwhile, industrial solid wastes such as flyash rice husk ash and slag present a viable opportunity. India annually generates 200 million tonnes of fly ash from thermal power plants and 20 million tonnes of slag from steel production facilities (Imtiaz et al., 2020). These by-products, often disposed of on arable land, exacerbate environmental pollution due to their limited utilization (Qaidi et al., 2022). Traditionally, Ordinary Portland Cement (OPC) and Portland Pozzolana Cement (PPC) have been the primary binding agents in concrete, but their production significantly contributes to greenhouse gas emissions. To mitigate this, the substitution of OPC with sustainable materials is essential. The escalating demand for cement, driven by India's infrastructure growth, has intensified the need for environmentally friendly alternatives. Promising options include alkali-activated cement, calcium sulphoaluminate cement, magnesium oxy-carbonate cement (carbon-negative cement) and supersulfated cement, which offer comparable or superior performance to OPC while incorporating substantial amounts of industrial waste (Imbabi et al., 2012). As coal-based thermal power plants supplied nearly 70% of India's energy demand in the last decade, exploring these alternatives is critical for reducing the environmental footprint of the cement industry (Volaity et al., 2025).

The incremental production of Fly Ash (FA) from 1996-1997 to 2019-2020 in India is shown in Fig. 1.1, while its use across different industries is depicted in Fig. 1.2. In 2019–2020, the generated food waste amounted to around 201.8 million tons, of which only about 62% was used across different industries, while the remainder was disposed of in landfills. The treatment of a substantial volume of unutilized fly ash is a significant barrier for solid waste management. Consequently, there is significant apprehension regarding greenhouse gas emissions, particularly CO_2 emissions from the cement manufacturing industry, driven by a substantial rise in cement demand within the construction sector. Simultaneously, the increase in fly ash generation and its management presents a pressing environmental concern. In this regard, geopolymer technology offers a viable alternative binder to Portland cement for the building industry. Geopolymer technology addresses the disposal of fly ash while simultaneously decreasing CO_2 emissions from the cement industry, therefore contributing to environmental preservation. The cement production business generates around 1.35 billion tons of greenhouse gas emissions yearly, accounting for roughly 7% of total anthropogenic greenhouse gas emissions released into the atmosphere (Malhotra 2002; Central Electricity Authority (CEA) Report 2021).

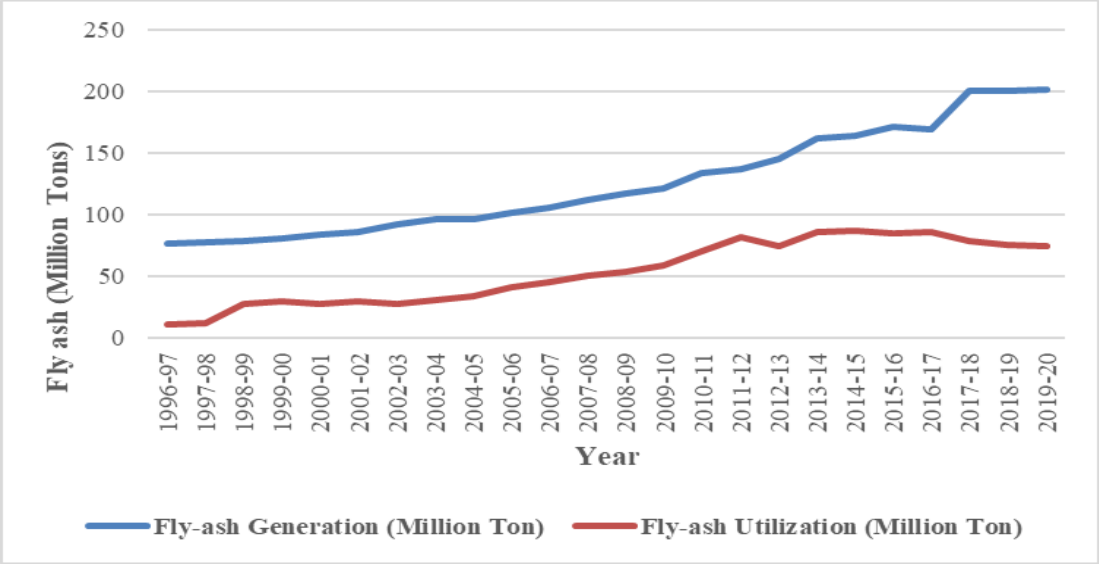

Fig. 1.1: Generation and usage of fly ash in India during the period 1996-1997 to 2019-2020 [Central Electricity Authority (CEA) Report 2021]

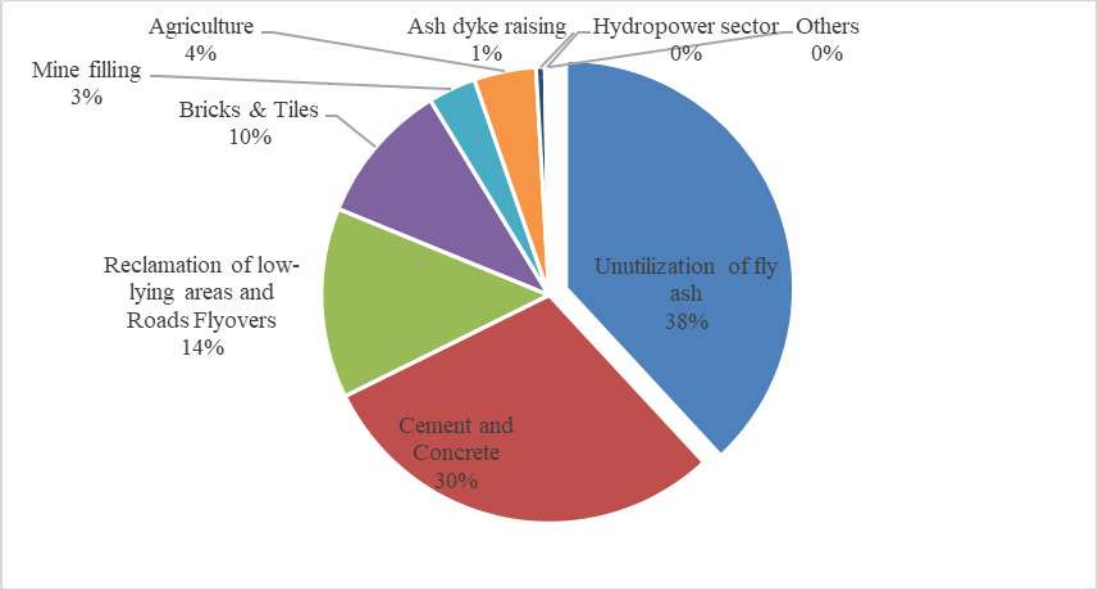

Fig. 1.2: Modes of utilization of fly ash in India during 2019–2020 [Central Electricity Authority (CEA) Report 2021]

The economic expansion in India and China has led to the establishment of new cement factories, significantly augmenting CO_2 emissions, while the enormous quantity of fly ash generated by thermal power plants is inadequately recovered (Malhotra, 2004). McCaffrey (2002) proposed three strategies to mitigate CO_2 emissions from the cement industry: (a) reducing the quantity of calcined material in cement, (b) decreasing the cement content in concrete by employing higher strength cement and (c) minimizing the use of cement in construction projects. Hardjito et al., (2004) indicated that Mehta (2002) also proposed environmentally sustainable concrete, comprising two phases: industrial ecology, which aims to minimize the utilization of natural resources, decrease energy consumption, reduce CO_2 emissions and lower material consumption rates to mitigate the impact of undesirable industrial by-products. Moreover, the reduction of Ordinary Portland Cement (OPC), the integration of additional supplementary cementitious materials, the minimization of water through the application of super-plasticizers and water reducers, the incorporation of recycled aggregates in concrete and the utilization of lightweight concrete where feasible are several strategies by which the cement and concrete industry can mitigate CO_2 emissions for sustainable construction (Malhotra, 2004).

Geopolymer concrete (GPC) is a paradigm shift in construction materials, providing a sustainable and high-performance alternative to Portland cement concrete (PCC) with its lower carbon emissions and exceptional strength properties. The growing environmental concerns surrounding CO_2 emissions associated with PCC have led to increasing research and adoption of GPC, which utilizes industrial by-products such as fly ash, slag and metakaolin as primary materials, activated by alkaline solutions like sodium hydroxide and sodium silicate (Okoye, 2017).

In ancient times, synthetic rocks were created by mixing dolomite, kaolinite, or limestone with potassium carbonate (K_2CO_3) or sodium carbonate (Na_2CO_3), which were obtained from plant waste or salt lakes, along with silica. Adding water to potassium hydroxide (KOH) and sodium hydroxide (NaOH) produced by this mixture dissolved some of the silica, which then reacted with other components to form a geopolymeric binder.

In the context of concrete and cementitious materials, the evolution of binding agents can be classified into three distinct generations: lime, considered the first-generation binder; ordinary Portland cement (OPC), regarded as the second generation; and geopolymer cement, representing the third. Geopolymer is an amorphous alkali alumina-silicate that has various names, including ‘geocements’, ‘alkali-activated cements’, ‘hydroceramics’, ‘alkali-bonded ceramics’ and ‘inorganic polymers. All these terms refer to materials synthesized through similar chemical processes. These materials undergo a process called geopolymerization, resulting in a hardened binder with enhanced durability, chemical resistance and thermal stability compared to traditional concrete (Van et al., 2012).

The geopolymerization process is a rapid chemical reaction that occurs under highly alkaline conditions. It involves aluminosilicate oxides and silicates reacting to form polymeric Si─O─Al─O bonds, resulting in a three-dimensional network (Davidovits, 1994; Van et al., 1997; Xu and Van, 2000). This network structure provides strength and durability, making geopolymers highly suitable for construction.

With growing concerns over greenhouse gas emissions, research on geopolymer concrete (GPC) has intensified in the last decade, focusing on optimizing mix design, improving durability and understanding its performance in various environmental conditions (Zhang et

al., 2014). Recent advancements have explored the addition of nano-materials and fiber reinforcements, which further enhance the mechanical properties of GPC, expanding its applications from residential buildings to large infrastructure projects (Paruthi et al., 2023).

GPC synthesis begins by activating aluminosilicate materials with highly alkaline solutions, which trigger the polymerization process. This creates a binder with a three-dimensional silico-aluminate network that often surpasses traditional Portland cement concrete (PCC) in compressive strength, chemical resistance and thermal insulation (Buchwald & Struble, 2009). The choice of precursor materials, like fly ash or slag, significantly impacts the properties of the geopolymer. For instance, low-calcium fly ash tends to produce geopolymers with greater strength and durability (Zhou et al., 2018). Since 2018, research has increasingly focused on optimizing mix proportions to achieve desired mechanical and durability characteristics while minimizing environmental impact (Xie & Liew, 2019). Curing conditions, particularly temperature and duration, are also critical for GPC strength development. Elevated temperatures accelerate geopolymerization and improve early-age strength (Girish et al., 2020). This fine-tuning of material choice, curing and mix design makes GPC a promising alternative to conventional cement in building a more sustainable.

Recent advancements in GPC have been driven by a deeper understanding of the material's microstructure and the influence of different synthesis parameters on its properties. Studies have explored the incorporation of various additives and admixtures to enhance the performance of GPC, including the use of nano-silica, graphene and other nano-materials to improve its mechanical properties and durability (Frieda & Greeshma, 2025). Furthermore, there has been a growing interest in the use of GPC in harsh environmental conditions, such as marine environments and regions with high sulfate content, where its resistance to chemical attack offers significant advantages over traditional concrete (Nazari & Sanjayan, 2020). In addition to material innovations, research has also focused on the development of new testing methods and predictive models to better understand the long-term behavior of GPC and to ensure its reliability in structural applications (Kumar et al., 2021). The integration of advanced analytical techniques, such as X-Ray Diffraction (XRD) and Scanning Electron Microscopy (SEM) has provided valuable insights into the micro

structural development of GPC and its correlation with macroscopic properties (Zhang et al., 2022).

Several case studies have demonstrated the successful application of GPC in large-scale construction projects, highlighting its economic and environmental benefits. For instance, GPC has been used in the construction of pavements, precast elements and structural components in regions with a high availability of industrial by-products, significantly reducing the overall carbon footprint of these projects (Kumar et al., 2023). In addition to its environmental benefits, GPC has been shown to offer cost savings due to its lower material costs and reduced energy consumption during production (Liew et al., 2022). The use of GPC in infrastructure projects, such as bridges and roads, has also demonstrated its durability and resistance to aggressive environments, making it a viable alternative to PCC in a wide range of applications (Rajini et al., 2022).

Despite the significant progress made in the development and application of GPC, several challenges remain. One of the primary challenges is the variability in the raw materials used for GPC production, which can lead to inconsistencies in the properties of the final product (Nazari & Sanjayan, 2023). Additionally, the long-term durability of GPC under different environmental conditions is still not fully understood and further research is needed to address these uncertainties (Zhou et al., 2024). Future research is likely to focus on the development of standardized testing methods and guidelines for the production of GPC, as well as the exploration of new precursor materials and activators that can enhance the performance of GPC while further reducing its environmental impact (Girish et al., 2023). The integration of advanced material science techniques with ML and IoT technologies is also expected to play a key role in the future development of GPC, leading to the creation of smart, sustainable construction materials that can adapt to changing environmental conditions and meet the demands of modern infrastructure (Zhang et al., 2024b).

1.2 Geopolymerization

Geopolymerization is a chemical process that converts aluminosilicate minerals into a solid, three-dimensional network of interconnected polymer chains, resulting in the formation of a geopolymer. This process involves several key stages: Initially, an activation phase combines aluminosilicate materials like fly ash, slag or metakaolin with an alkaline activator solution, typically consisting of water and an alkali metal hydroxide or silicate, which releases hydroxyl ions to begin aluminosilicate dissolution (Davidovits, 1994; Van et al., 1997). The dissolution phase then involves the breakdown of mineral structures, releasing silicon (Si) and aluminum (Al) species into solution through hydrolysis and ion exchange, leading to the formation of silicate (SiO_4) and aluminate (AlO_4) species (Provis & Van, 2009; Xu & Van, 2000).

The Polycondensation occurs as silicon and aluminum species react with hydroxyl ions, producing oligomeric and polymeric chains of alternating Si-O and Al-O bonds, rapidly creating an amorphous gel under alkaline conditions (Sofi et al., 2007; Palomo et al., 1999). Cross linking follows, wherein these chains chemically bind, forming Si-O-Al or Si-O-Si linkages that enhance the geopolymer matrix's mechanical strength (Rangan, 2010; Xu & van, 2002). As cross-linked polymeric networks condense, they form a gel-like structure of silicon and aluminum atoms within an alkaline solution, crucial for imparting structural stability (Sofi et al., 2007; Palomo et al., 1999). Finally, the setting and hardening phase, influenced by curing temperature, time and activator composition, further densifies the matrix, solidifying the material and enhancing its mechanical properties (Rangan, 2010; Xu & van, 2002). This comprehensive process as shown in Fig. 1.3 yields geopolymers with notable mechanical strength, durability, and environmental sustainability, making them suitable for various construction applications (Davidovits, 1994; Provis & Van, 2009).

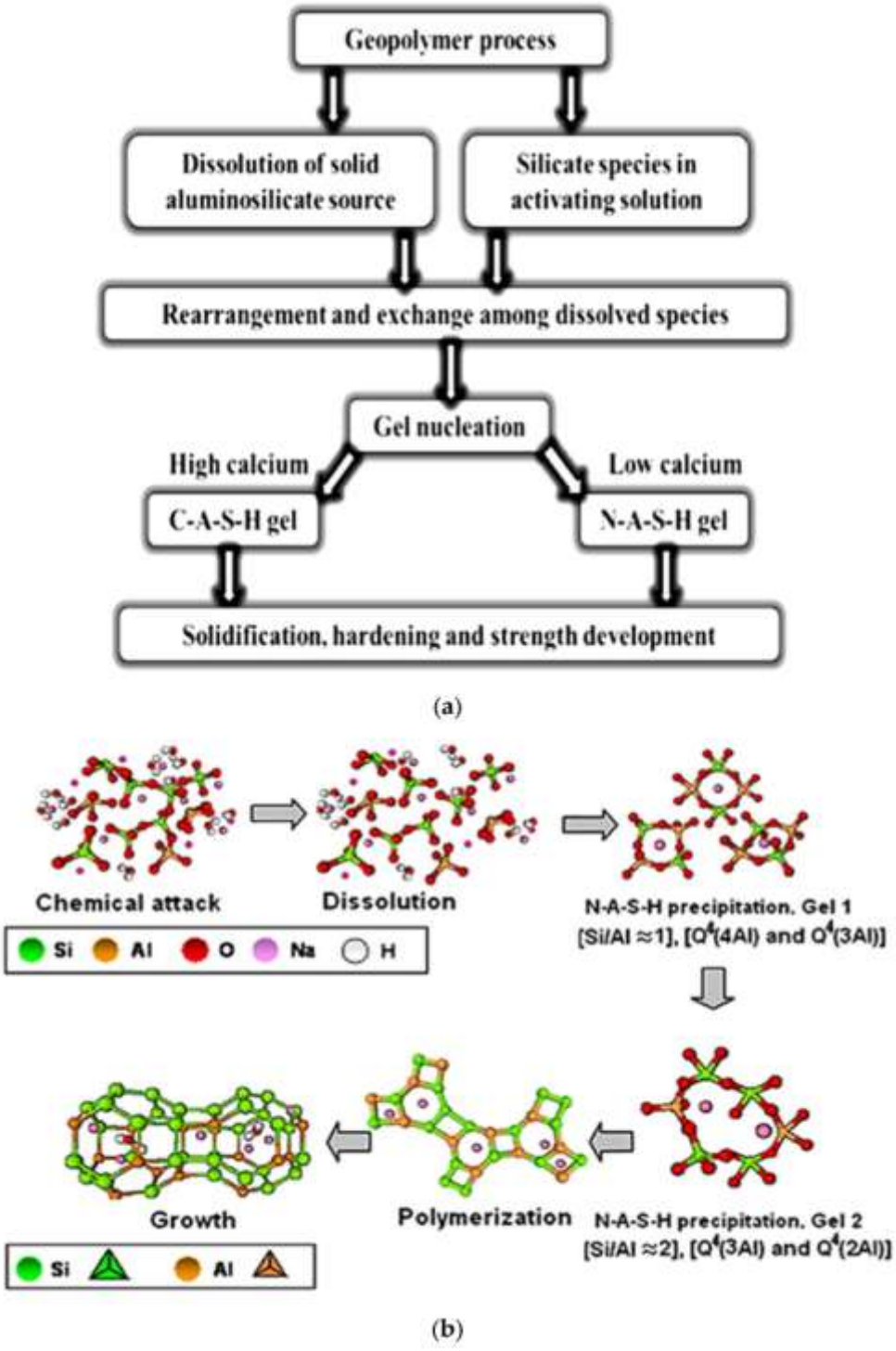

Fig. 1.3: Mechanism of Geopolymerisation (Abdila et al., 2022)

Several elements influence the geopolymerisation process, including the composition of the alkaline solution, the amount of binding material in the design mix and the curing conditions.

Pozzolanic materials, such as fly ash, GGBFS, metakaolin and rice husk ash were used as binding agents in the geopolymer because of their high silica and alumina content. According to Duxson et al., (2005), as the Si/Al ratio increases, so does the geopolymer's compressive strength.

The activation of pozzolanic material to function as a binding agent for the geopolymerization reaction was accomplished by using a solution containing sodium hydroxide and sodium silicate. Several investigations (Sung et al. 2015; Topark et al., 2015; Nagalia et al., 2016) have found a favorable correlation between the strength of the GPC mix and the molarity of NaOH. However, increasing the concentration of NaOH leads to a decrease in workability. Geopolymerization is responsible for increasing the strength of concrete, which can be affected by a variety of conditions and characteristics. The mixture's strength is affected by the alkaline ratio, which increases with the Na_2SiO_3/NaOH ratio, as described by Verma & Dev, (2021).

The utilization of GPC in concrete results in superior physical, chemical and mechanical characteristics when compared to those of OPC cement concrete. The durability characteristics of GPC exhibit superior performance in comparison to those of OPC concrete. According to several studies (Ismail et al. 2013; Bhutta et al., 2014; Gustavo et al. 2016), GPC exhibits a greater degree of resistance to sulphate attack when compared to OPC concrete.

Alccofine is an ultrafine slag-based Supplementary Cementitious Material (SCM) widely used to enhance the performance of conventional and geopolymer concrete. Its unique fineness and high calcium silicate content make it an efficient additive, promoting early strength gain, reducing permeability and improving durability in concrete structures (Sathish et al., 2020; Reddy et al., 2019). In traditional concrete applications, Alccofine acts as a pozzolanic material, reacting with calcium hydroxide to form additional calcium silicate hydrate (C-S-H), which densifies the matrix and improves both compressive and tensile strength (Sathish et al., 2020). Its ultrafine particles fill voids in the concrete mix, which reduces porosity and enhances the microstructure, leading to improved long-term durability (Kadam & Patil, 2018; Nandy et al., 2021).

In geopolymer concrete, Alccofine is beneficial as it contributes calcium, which aids in the geopolymerization process, providing a source for C-S-H gel formation alongside aluminosilicate gels. This dual-gel system enhances the mechanical properties of geopolymer concrete, especially in terms of compressive strength and durability (Reddy et al., 2019; Kadam & Patil, 2018). Alccofine also aids in reducing the setting time and enhances the early-age strength of geopolymer concrete, making it suitable for rapid construction and precast applications (Nandy et al., 2021). Overall, its inclusion improves workability, strength and durability, making Alccofine a valuable component in both conventional and geopolymer concrete mixes for infrastructure, pavements and precast elements (Sathish et al., 2020; Reddy et al., 2019).

1.3 Machine Learning Application in Geopolymer Concrete

The application of Machine Learning (ML) in Geopolymer concrete (GPC) has emerged as a focal point of interest in recent years, offering innovative methods to optimize mix design, predict mechanical properties and assess durability. Traditional empirical approaches are increasingly being supplemented or replaced by ML models due to their ability to capture complex, non-linear relationships between input variables and GPC properties (Girish et al., 2021).

1.3.1 Predictive Modelling for Compressive Strength and Durability

Artificial Neural Networks (ANNs) have proven effective in predicting the compressive strength of GPC. Factors such as fly ash content, alkaline activator concentration and curing temperature are considered as inputs in these models, which often outperform traditional regression-based techniques (Rajini et al., 2022). Similarly, Support Vector Machines (SVMs) and decision tree models have been employed to model durability metrics, including resistance to sulphate attack, carbonation and freeze-thaw cycles (Xie & Liew, 2021). These models provide accurate predictions, facilitating the development of GPC with enhanced long-term performance.

1.3.2 Advances in Deep Learning for Complex Applications

The emergence of Deep Learning has opened new possibilities in GPC research. Convolutional Neural Networks (CNNs) and Recurrent Neural Networks (RNNs) have been applied to complex tasks such as predicting the behaviour of GPC under dynamic loading and monitoring the development of micro-cracks (Liew et al., 2023). These models enable researchers to analyse intricate patterns in GPC performance, which are difficult to capture using traditional approaches.

1.3.3 Integration of ML with IoT for Smart Construction

The combination of machine learning (ML) with Internet of Things (IoT) technologies has led to the creation of smart construction systems capable of real-time monitoring of GPC structures. These systems use sensors and ML algorithms to track parameters like compressive strength, crack development and environmental exposure, providing valuable insights for maintenance and extending the lifespan of infrastructure (Zhang et al., 2023).

1.3.4 Enhanced Mix Design and Performance Optimization

Machine learning models, such as Random Forests (RF), ANN and SVM, have enabled researchers to analyse the relationships between raw material composition, curing conditions and mechanical properties, streamlining the mix design process. This minimizes trial and error, significantly improving efficiency (Nath et al., 2021; Gupta & Kumar, 2020). For instance, ML models have shown high accuracy in predicting the compressive strength and setting time of GPC, facilitating the rapid identification of optimal mixes tailored to specific performance and environmental conditions (Deepa & Gopalakrishnan, 2019).

ML also aids in optimizing the proportions of supplementary materials such as fly ash, slag and Alccofine, enhancing performance and promoting sustainable construction practices (Mishra et al., 2022; Gupta & Kumar, 2020). By leveraging historical and experimental data, ML models simulate the behaviour of GPC under various environmental and loading

conditions, enabling more reliable durability assessments and optimized designs for specific applications (Reddy & Saha, 2021).

1.3.5 Contribution to Sustainable Construction

While numerous studies have explored geopolymer concrete (GPC) mix design and the application of machine learning (ML), most focus on isolated parameters or lack experimental validation (Mishra et al., 2022; Reddy & Saha, 2021). This research offers a distinct contribution through its integrated design methodology that combines a comprehensive experimental program with machine learning-based modeling to optimize key GPC mix parameters. The study specifically examines the combined effects of Alccofine, alkaline activator concentration, and curing conditions, which remain underexplored in existing literature. Furthermore, the thesis presents a large experimental dataset and compares the experimental results with ML predictions to validate the model's accuracy and applicability. This dual approach not only strengthens the reliability of the findings but also establishes a practical and scalable framework for designing sustainable, high-performance geopolymer concrete.

1.4 Gaps Found Through Literature Review

The research gaps were systematically identified through an extensive review of the existing literature, with the aim of addressing critical limitations observed in previous studies.

- Limited research has been conducted on the influence of ambient and oven curing conditions on the properties of geopolymer concrete.
- There are few comprehensive studies exploring the various possible combinations of variables in geopolymer concrete.
- There is limited research on determining the optimum percentage of Alccofine to achieve the best balance of fresh, mechanical, and durability properties in fly ash-based geopolymer concrete.

- Limited integration of experimental studies with machine learning-based optimization frameworks for improving geopolymer concrete mix design and performance prediction.

1.5 Objectives of the Research

This study focuses on identifying and recommending optimal mix proportions for geopolymer concrete by evaluating various combinations of key variables through both experimental and data-driven approaches. Special emphasis is placed on the inclusion of Alccofine, a high-performance supplementary cementitious material, known for significantly enhancing the compressive strength, elastic modulus, and durability of geopolymer concrete. Its addition contributes to denser microstructure and improved long-term performance, making it an invaluable component in sustainable construction.

In parallel, this research leverages advanced Machine Learning (ML) techniques not only to predict the mechanical properties of geopolymer concrete but also to assist in the intelligent design and optimization of mix combinations. Models such as Artificial Neural Networks (ANN), Gene Expression Programming (GEP), and Support Vector Regression (SVR) were trained on experimental datasets to establish accurate predictive frameworks. Furthermore, optimization algorithms, including Genetic Algorithms (GA) and Jellyfish Search Optimization (JSO), were applied to fine-tune mix parameters, enabling data-informed decision-making for performance enhancement. The integration of ML with experimental validation offers a novel hybrid framework, demonstrating high predictive accuracy and offering a scalable strategy for the development of high-performance geopolymer concrete in line with modern sustainable engineering demands.

- To recommend suitable mix proportions of geopolymer concrete, considering different variable combinations.
- To determine the effect of GGBFS (alccofine) content in fresh and mechanical properties of geopolymer concrete.
- To analyse the effect of GGBFS (alccofine) content on durability properties under various conditions.

- To utilize and compare optimized machine learning models for predicting and optimizing the final mix proportions of geopolymer concrete, assessing their performance against each other and against conventional models.

1.6 Organization of Thesis

Chapter 1:

It describes the reason for choosing such field and topic. I summarize a general introduction and information required to build the knowledge required for the research topic and scope of work of the field.

Chapter 2:

This Chapter comprises of the Literature review and survey researched and analyzed so as to provide a foundation for the Research Topic. The research and information is based on the parameters affecting the strength and performance of the Geopolymer.

Chapter 3:

This chapter presents the methodology for the current study, detailing the concrete testing procedures and providing an overview of machine learning techniques used, including artificial neural networks (ANN), gene expression programming (GEP), multiple linear regression, generalized linear models, quadratic polynomial regression, support vector regression (SVR), Bi-LSTM and Self-Improved Jelly Search Optimization (SIJSO).

Chapter 4:

This chapter provides a comprehensive analysis of test results for different mix design combinations, examining the performance and properties of each variation. The goal is to evaluate the mechanical and durability characteristics of each mix to identify the most effective and balanced composition. By comparing the outcomes of various formulations, this chapter aims to determine the optimal mix design that maximizes strength and durability

Chapter 5:

This chapter examines the applications of machine learning methodologies, including artificial neural networks (ANN), gene expression programming (GEP), multiple linear regression, generalized linear models, quadratic polynomial regression and support vector regression (SVR). The approaches are used on the data acquired from Chapter 4 to assess and forecast the performance characteristics of the concrete mixes, therefore improving the comprehension of the linkages between mix design factors and their results.

Chapter 6:

This chapter concludes the study by highlighting the potential of geopolymer concrete and Alccofine as a supplementary material to enhance mechanical properties. Machine learning techniques, such as artificial neural networks (ANN) and support vector regression (SVR), Bi-LSTM and Self-Improved Jelly Search Optimization (SIJSO) effectively predicted the performance of various mix designs. The findings emphasize the importance of optimizing these mixes to improve strength and durability in sustainable construction.

Chapter 2
Literature Survey

2.1 Introductory Remarks

This chapter offers a detailed analysis of the relevant literature on the use of industrial by-products like fly ash and ground granulated blast furnace slag (GGBFS) in geopolymer concrete (GPC), highlighting their roles in enhancing sustainability and performance. It examines the effects of different additives, such as Alccofine and various parameters including alkaline solution concentration, liquid-to-binder ratios and curing conditions on the mechanical and durability properties of GPC. Furthermore, the chapter discusses the integration of machine learning (ML) techniques in GPC research, focusing on ML's ability to predict material properties, optimize mix designs and improve the overall efficiency of GPC applications. This exploration of both material components and computational methods underscores the potential of GPC as a durable, eco-friendly alternative in construction. Furthermore, advancements in machine learning (ML) have transformed GPC research by enabling more accurate prediction of material properties, optimizing mix designs and enhancing performance monitoring. ML models, including neural networks and support vector machines, help predict key characteristics such as compressive strength and durability, supporting efficient GPC formulation and broadening its practical applications in the construction industry. The relevant literature review includes: Application of Fly Ash in Geopolymer Concrete (GPC), Application of Ground Granulated Blast Furnace Slag (GGBFS) and Alccofine in Geo-Polymer Concrete (GPC), Effect of Alkaline Solution in Geo-Polymer Concrete (GPC), Effect of Aggregates in Geo-Polymer Concrete (GPC), Effect of Activator Liquid to Binder Ratio in Geopolymer Concrete (GPC), Effect of Super-plasticizers Addition in Geopolymer Concrete (GPC), Effect of Curing Conditions in Geo-Polymer Concrete (GPC), Durability of Geo-Polymer Concrete (GPC), Effect of Alkali-Silica Reaction (ASR) and Leaching on Geo-Polymer Concrete (GPC), Effect on the Bond Strength of Geo-Polymer Concrete (GPC), Application of Machine Learning in Geo-Polymer Concrete.

2.2 Application of Fly Ash in Geopolymer Concrete (GPC)

Fly ash is a by-product of coal combustion in power plants, has gained significant attention as a primary precursor material in the development of Geo-Polymer Concrete (GPC) due to its abundant availability, pozzolanic properties and its contribution to reduce the carbon footprint associated with conventional Portland cement. The utilization of fly ash in GPC offers numerous environmental and performance advantages, positioning it as a key component in the sustainable construction sector. Fly ash is rich in aluminosilicate, making it an ideal material for geopolymerization when activated by alkaline solutions such as sodium hydroxide (NaOH) and sodium silicate (Na_2SiO_3). The resulting geopolymer binder not only exhibits superior mechanical properties but also demonstrates enhanced durability, resistance to chemical attacks and lower permeability compared to traditional concrete (Altawil & Olgun, 2025).

The inclusion of fly ash in GPC formulations has been extensively studied for its influence on various mechanical and durability properties. One of the most significant benefits of using fly ash in GPC is the improvement in compressive strength. The fineness and high silica content of fly ash contribute to the formation of a denser and more homogeneous microstructure, which enhances the compressive strength of GPC over time. Studies have shown that the compressive strength of fly ash-based GPC can be further optimized by adjusting the molarity of the alkaline activator, curing temperature, and curing duration, allowing for the tailoring of concrete properties to meet specific engineering requirements (Zhou et al., 2018). Additionally, fly ash in GPC has been found to improve workability due spherical particle shape, which reduces the water requirement and enhances the flowability of the concrete mix. This property is particularly advantageous in reducing the water-to-binder ratio, thereby minimizing the potential for shrinkage and cracking in GPC structures (Xie & Liew, 2019).

Beyond mechanical properties, the durability of fly ash-based GPC is another critical area of research. Fly ash contributes to the superior durability of GPC, particularly in aggressive environments where traditional concrete may deteriorate. The lower calcium content in fly ash results in a reduced formation of calcium hydroxide, which is susceptible to leaching and chemical attack. As a result, fly ash-based GPC exhibits excellent resistance to attack, acid

corrosion and chloride penetration, making it suitable for use in marine environments, wastewater treatment plants and other chemically aggressive settings (Nazari & Sanjayan, 2020). Furthermore, the low permeability and high chemical resistance of fly ash-based GPC make it an ideal material for long-term infrastructure projects, where durability is a critical concern.

In conclusion, the application of fly ash in geopolymer concrete not only addresses the disposal challenges associated with fly ash as an industrial waste but also offers an eco-friendly substitute for conventional cement-based concrete. The use of fly ash in GPC enhances the mechanical strength, workability, and durability of the material, making it a viable option for various construction applications. As research continues to evolve, the optimization of fly ash-based GPC formulations will likely lead to even more robust and sustainable construction materials that align with global efforts to reduce the carbon footprint of the construction industry (Zhang et al., 2024a).

2.3 Application of Ground Granulated Blast Furnace Slag (GGBFS) and Alccofine in Geo-Polymer Concrete (GPC)

The incorporation of Ground Granulated Blast Furnace Slag (GGBFS) and Alccofine into geopolymer concrete (GPC) has garnered substantial interest due to the combined effects of these materials contribute to improving the mechanical strength, durability, and eco-friendliness of GPC. GGBFS, a waste product from the iron and steel industry, is recognized for its elevated calcium content and inherent hydraulic characteristics, which contribute to the formation of a dense, durable matrix when activated by alkaline solutions. Alccofine, a highly efficient ultra-fine material, is also increasingly being used in GPC formulations due to its ability to significantly improve the workability and strength of the concrete. The use of these supplementary cementitious materials not only reduces the reliance on traditional Portland cement but also addresses the disposal issues associated with industrial by-products, making GPC a more sustainable construction material (Buchwald & Struble, 2009).

The addition of GGBFS to GPC is particularly beneficial in improving the early-age strength development of the concrete. GGBFS contains reactive calcium, which, when combined with the aluminosilicate network formed during geopolymerization, enhances the overall binding

capacity and results in a higher rate of strength gain compared to fly ash-based GPC alone. This makes GGBFS an ideal component for applications requiring early strength, such as pre-cast concrete products and structural elements that need to be quickly put into service (Sujitha et al., 2025).

Additionally, the incorporation of GGBFS into GPC has been shown to improve the long-term durability of the concrete by reducing its permeability which leading to increasing its resistance to chemical attacks. The dense microstructure formed by the combination of GGBFS and the geopolymer matrix significantly limits the ingress of harmful substances, thereby extending the service life of GPC structures (Zhang et al., 2022).

Alccofine, due to its ultra-fine particle size and high reactivity, plays a crucial role in enhancing the rheological properties of GPC. The addition of Alccofine improves the workability of the concrete, allowing for easier mixing, placing and compaction without the need for excessive water or chemical admixtures. This is particularly advantageous in producing high-performance GPC with reduced water-to-binder ratios, which in turn enhances the strength and durability of the material (Kumar et al., 2021). Moreover, Alccofine's high pozzolanic activity contributes to the refinement of the pore structure and the densification of the matrix, further improving the compressive strength and reducing the permeability of GPC. Studies have shown that the combined use of GGBFS and Alccofine in GPC formulations can lead to significant improvements in both early and long-term mechanical properties, making the material suitable for a wide range of structural applications, including high-rise buildings, bridges and marine structures (Girish et al., 2021).

In conclusion, the incorporation of GGBFS and Alccofine in geopolymer concrete offers numerous benefits, including enhanced strength development, improved durability and better workability. These materials contribute to the sustainability of GPC by reducing the carbon footprint and utilizing industrial by-products that would otherwise contribute to environmental pollution. As research continues, the optimization of GGBFS and Alccofine proportions in GPC mix designs will likely lead to even more robust and durable construction materials that meet the evolving demands of the construction industry.

2.4 Effect of Alkaline Solution in Geo-Polymer Concrete (GPC)

The alkaline solution is essential in the geopolymerization process that creates the binder in geopolymer concrete (GPC). The alkaline solution, generally consisting of sodium hydroxide (NaOH) or potassium hydroxide (KOH) combined with sodium silicate or potassium silicate, activates aluminosilicate materials (such as fly ash, GGBFS, or metakaolin) in geopolymer concrete (GPC), promoting the dissolution of silica and alumina that subsequently react to establish a stable, three-dimensional polymeric network. The concentration, ratio and type of alkaline solution used significantly impact the mechanical properties, workability, setting time and durability of the resulting geopolymer concrete (Xu & Van, 2000).

The concentration of the alkaline solution, often expressed in terms of molarity, is one of the most critical factors influencing the compressive strength of GPC. Higher molarity solutions, typically ranging from 8M to 16M, provide a more aggressive alkaline environment, which enhances the dissolution of the aluminosilicate precursors, leading to a more complete polymerization process and, consequently, a denser and stronger geopolymer matrix. However, excessively high molarity can lead to rapid setting and reduced workability, making it challenging to handle and place the concrete on-site (Nath & Sarker, 2014). Therefore, optimizing the molarity is crucial to balancing strength and workability in GPC applications.

The ratio of sodium silicate to sodium hydroxide (or their potassium equivalents) is another vital parameter. A higher silicate-to-hydroxide ratio generally enhances the polymerization process, resulting in a denser and more cohesive matrix with improved compressive strength and reduced porosity. This ratio typically ranges from 1:2 to 2:1, depending on the desired properties of the GPC. For instance, a higher sodium silicate content increases the viscosity of the solution, leading to better binding between the aggregates and the paste, but it may also slow down the setting process (Temuujin et al., 2010). Adjusting this ratio allows for the tailoring of the GPC properties to meet specific engineering requirements, such as early strength development or enhanced durability in harsh environments.

The type of alkaline activator (sodium versus potassium-based) also affects the geopolymerization process. Potassium-based solutions tend to produce a more reactive

environment, leading to faster setting times and higher early-age strengths compared to sodium-based solutions. However, sodium-based activators are more commonly used due to their lower cost and availability. The choice between sodium and potassium activators often depends on the specific application and the desired balance between cost, strength and setting time (Palomo et al., 1999).

In addition to strength, the alkaline solution influences the durability of GPC, particularly its resistance to chemical attack. The denser microstructure formed with optimal alkaline activation enhances the material's resistance to aggressive environments, such as exposure to sulfates, acids and chlorides. This makes GPC an excellent material for infrastructure in marine environments, industrial settings and areas subject to deicing salts (Bakharev, 2005).

In conclusion, the alkaline solution is a key determinant of the performance characteristics of geopolymer concrete. By carefully selecting and optimizing the concentration, ratio and type of alkaline solution, it is possible to produce GPC with superior mechanical properties and durability tailored to specific construction needs. Ongoing research continues to explore the potential of different alkaline activators and formulations to further enhance the sustainability and performance of GPC in various applications.

2.5 Effect of Aggregates in Geo-Polymer Concrete (GPC)

Aggregates, which typically constitute 60-75% of the total volume of concrete, play a crucial role in determining the mechanical properties, durability and overall performance of geopolymer concrete (GPC). The type, size, shape and gradation of aggregates used in GPC significantly influence its strength, workability, density and resistance to various environmental factors. Aggregates in GPC can be categorized into two main types: fine aggregates (such as sand) and coarse aggregates (such as gravel or crushed stone), each contributing differently to the concrete's properties (Sarker et al., 2013).

The size and gradation of aggregates are vital in determining the workability and compressive strength of GPC. Properly graded aggregates, with a good balance of fine and coarse particles, help achieve a dense packing structure, which reduces the void content and enhances the strength and durability of the concrete. A well-graded mix of aggregates ensures better compaction, reducing the need for excessive binder material and contributes to

the overall economic and environmental efficiency of the GPC. Coarse aggregates, usually with a maximum size of 20 mm, contribute to the load-bearing capacity, while fine aggregates fill the voids between the coarse particles, improving the workability and surface finish of the concrete (Zhang et al., 2014).

The shape and surface texture of aggregates also affect the workability and strength of GPC. Angular and rough-textured aggregates, typically from crushed stone, provide better mechanical interlocking and bond strength with the geopolymer matrix, leading to higher compressive strength. However, they can reduce workability due to increased friction between particles. On the other hand, rounded and smooth aggregates, like natural river gravel, enhance workability but may result in lower bond strength and, consequently, reduced compressive strength. The choice of aggregate shape and texture should be balanced based on the specific requirements of the GPC application (Guo et al., 2020).

The type of aggregate used in GPC also influences its thermal and durability properties. Lightweight aggregates, such as expanded clay or fly ash aggregates, reduce the density of GPC and enhance its thermal insulation properties, making it suitable for applications where weight reduction and thermal resistance are essential. Conversely, heavy aggregates, like barite or magnetite, can be used in GPC to produce high-density concrete for radiation shielding or other specialized applications. The durability of GPC is also affected by the aggregate type, with certain aggregates providing enhanced resistance to freeze-thaw cycles, chemical attack, and abrasion (Haque et al., 2014).

Recycled aggregates, derived from construction and demolition waste, are increasingly being used in GPC as part of sustainability efforts. While recycled aggregates can lower the environmental impact and cost of GPC, they often introduce variability in properties such as water absorption, strength, and durability due to the presence of impurities and inconsistencies in the source material. Research has shown that with proper processing and quality control, recycled aggregates can be effectively utilized in GPC without significantly compromising its performance, particularly in non-structural or low-load-bearing applications (Thomas & Gupta, 2016).

In conclusion, aggregates play a critical role in the performance of geopolymer concrete, influencing its mechanical properties, workability, durability and sustainability. The selection and proportioning of aggregates must be carefully considered to optimize the balance between strength, workability, and durability in GPC, depending on the specific requirements of the construction project. As the demand for sustainable construction materials grows, the use of recycled and alternative aggregates in GPC is expected to increase, contributing to the reduction of the carbon footprint and resource consumption in the construction industry.

2.6 Effect of Activator Liquid to Binder Ratio in Geopolymer Concrete (GPC)

The activator liquid to binder ratio (L/B ratio) in geopolymer concrete (GPC) is a critical parameter that significantly influences the mechanical properties, workability, setting time and overall performance of the concrete. The activator liquid, typically a mixture of sodium or potassium hydroxide and sodium or potassium silicate, is essential for initiating the geopolymerization process by dissolving the aluminosilicate materials in the binder, which could include fly ash, slag or metakaolin. The ratio of this liquid to the binder determines the extent of the reaction, the consistency of the mix and the quality of the hardened concrete (Van et al., 2012).

The L/B ratio plays a pivotal role in determining the compressive strength of GPC. A lower L/B ratio generally leads to a higher concentration of the activator solution in relation to the binder, which can enhance the dissolution of aluminosilicate species and promote a more extensive polymerization process. This results in a denser and stronger geopolymer matrix, leading to higher compressive strength. However, if the L/B ratio is too low, it can make the mix too stiff, reducing workability and leading to difficulties in mixing, placing and compacting the concrete. Therefore, an optimal L/B ratio must be achieved to balance strength and workability (Duxson et al., 2007).

Conversely, a higher L/B ratio increases the fluidity of the mix, improving workability and ease of handling. This can be particularly advantageous in applications where complex forms or detailed finishes are required. However, an excessively high L/B ratio can dilute the concentration of the activator solution, leading to incomplete geopolymerization and a

weaker, more porous matrix. This not only reduces the compressive strength but also negatively impacts the durability of the GPC, making it more susceptible to environmental degradation such as chemical attack or freeze-thaw cycles (Lloyd & Rangan, 2010).

The L/B ratio also affects the setting time of GPC. A lower L/B ratio typically results in a faster setting time due to the higher concentration of the alkaline activator, which accelerates the geopolymerization process. This can be beneficial in situations where rapid strength gain is required, such as in pre-cast concrete production or repair works. On the other hand, a higher L/B ratio can prolong the setting time, which might be desirable in hot weather conditions or when longer workability is needed (Hardjito & Rangan, 2005).

In addition to mechanical properties, the L/B ratio influences the microstructure of the hardened GPC. A well-balanced L/B ratio Facilitates the development of a homogeneous and dense geopolymer network, reducing porosity and improving the material's resistance to permeability and chemical attack. This is crucial for applications in aggressive environments, such as marine structures or industrial floors, where durability is of paramount importance. Conversely, an inappropriate L/B ratio can lead to an inhomogeneous structure with un-reacted binder particles and micro-cracks, compromising the long-term performance of the concrete (Buchwald & Struble, 2009).

In conclusion, the activator liquid to binder ratio is a key factor in determining the success of geopolymer concrete applications. It must be carefully optimized to achieve a balance between workability, strength, setting time and durability, depending on the specific requirements of the project. As the development of GPC continues to advance, understanding the effects of the L/B ratio will be crucial for tailoring the material to meet the diverse needs of modern construction.

2.7 Effect of Superplasticizers Addition in Geopolymer Concrete (GPC)

Superplasticizers, often referred to as high-range water reducers, are chemical additives employed in concrete to improve workability while maintaining a low water content. In the context of geopolymer concrete (GPC), the addition of super-plasticizers is particularly important due to the inherently low workability of GPC mixtures, which are typically more viscous than conventional Portland cement concrete. Super-plasticizers help to improve the

fluidity and ease of placement of GPC, thereby addressing challenges related to mixing, compaction and finishing, while also maintaining or even enhancing the mechanical properties of the hardened concrete (Nath & Sarker, 2014; Xie & Kayali, 2016).

The primary function of super-plasticizers in GPC is to disperse the particles of the geopolymer binder, reducing the friction between them and thus lowering the viscosity of the mix. This leads to an increase in the slump value, indicating better workability, which is essential for producing complex shapes, achieving high-quality surface finishes and ensuring uniformity in the final product. The use of super-plasticizers is particularly beneficial when producing self-compacting geopolymer concrete (SCGPC), which requires high flowability without segregation or bleeding (Ghafoor & Fujiyama, 2023).

In addition to improving workability, super-plasticizers can influence the compressive strength of GPC. By reducing the water content while maintaining workability, super-plasticizers contribute to the formation of a denser geopolymer matrix, which enhances the compressive strength of the concrete. However, the effect of super-plasticizers on strength can vary depending on the type and dosage used. Some studies have reported that excessive use of super-plasticizers can lead to a delay in the setting time and a reduction in early-age strength, particularly when using certain types of fly ash or slag as binders. Therefore, optimizing the type and dosage of super-plasticizers is crucial for achieving the desired balance between workability and strength (Ribeiro et al., 2025).

The compatibility of super-plasticizers with the alkaline environment of GPC is another important consideration. Unlike traditional Portland cement concrete, GPC requires super-plasticizers that can function effectively in high pH conditions. Polycarboxylate ether (PCE)-based super-plasticizers are commonly used in GPC because of their high efficiency in dispersing particles and maintaining fluidity in alkaline conditions. These super-plasticizers also have a lower impact on the setting time of GPC compared to other types, such as naphthalene-based super-plasticizers, making them a preferred choice for many GPC applications (Li et al., 2025).

The addition of super-plasticizers also affects the durability of GPC. By improving the workability and reducing the water content, super-plasticizers help to produce a more

homogeneous and compact concrete, which is less permeable to water and aggressive chemicals. This enhances the durability of GPC in harsh environments, such as marine or industrial settings, where exposure to chlorides and other corrosive agents is common. Moreover, the reduced water content helps to minimize shrinkage and the risk of cracking, further contributing to the longevity of GPC structures (Kanagaraj et al., 2024).

In conclusion, the addition of super-plasticizers in geopolymer concrete is essential for enhancing workability, maintaining or improving strength and ensuring durability. The choice of superplasticizer type and dosage must be carefully optimized to achieve the best results, considering the specific binder materials and the alkaline environment of GPC. As the use of GPC continues to grow in sustainable construction, super-plasticizers will play a crucial role in overcoming the practical challenges associated with its production and application.

2.8 Effect of Curing Conditions in Geo-Polymer Concrete (GPC)

Curing conditions play a vital role in determining the mechanical properties, durability and overall performance of geopolymer concrete (GPC). Unlike traditional Portland cement concrete, where hydration is the primary chemical reaction during curing, GPC undergoes geopolymerization, a process heavily influenced by temperature and moisture conditions during the curing phase. The choice of curing method and environment significantly impacts the strength development, microstructure, and long-term durability of GPC, making it a critical factor in the production of high-quality geopolymer concrete (Hardjito & Rangan, 2005).

One of the most significant differences between GPC and conventional concrete is the effect of curing temperature. Elevated curing temperatures, typically ranging from 60°C to 90°C, are often used to accelerate the geopolymerization process, leading to rapid strength gain and improved early-age properties. This is particularly true for GPC mixtures based on fly ash or other aluminosilicate materials that require thermal activation. Heat curing helps to enhance the dissolution of silica and alumina from the precursor materials, facilitating a more complete polymerization and resulting in a denser and stronger geopolymer matrix (Duxson

et al., 2007). As a result, GPC cured at elevated temperatures often exhibits higher compressive strength compared to those cured at ambient temperatures.

However, the benefits of elevated temperature curing come with some trade-offs. Heat curing can lead to the formation of micro cracks due to thermal shrinkage, especially if the temperature is too high or if the concrete is subjected to rapid temperature changes. These micro cracks can compromise the durability of GPC, making it more susceptible to environmental degradation, such as freeze-thaw cycles or chemical attack. Therefore, careful control of the curing temperature and duration is essential to maximize the benefits of heat curing while minimizing potential drawbacks (Nath & Sarker, 2014).

Ambient temperature curing, on the other hand, is more practical for in-situ construction and is increasingly being explored for GPC formulations that do not require heat activation. Ambient curing conditions, typically around 20°C to 30°C, can still produce high-strength GPC, especially when blended with slag or other calcium-rich materials that contribute to early strength development. However, the rate of strength gain is generally slower compared to heat-cured GPC and the final strength may be lower unless the mix design is optimized for ambient curing. Moisture retention during ambient curing is also critical to prevent drying shrinkage and to ensure the complete geopolymerization of the binder materials (Alameri et al., 2025).

Curing duration is another key factor influencing the properties of GPC. Longer curing times generally allow for more complete geopolymerization, resulting in higher ultimate strength and better durability. However, the optimal curing duration depends on the curing temperature and the specific mix design. For heat-cured GPC, shorter durations may be sufficient to achieve high strength, whereas ambient-cured GPC may require extended curing periods to reach its full potential. Post-curing conditions, such as exposure to drying or wetting cycles, can also affect the long-term performance of GPC, particularly its resistance to cracking and chemical attack (Olivia & Nikraz, 2011).

In conclusion, curing conditions are critical to the success of geopolymer concrete, affecting everything from strength development to durability. Elevated temperature curing is highly effective for rapid strength gain but requires careful control to avoid thermal damage.

Ambient curing is more practical for many applications but may require optimized mix designs and extended curing periods. Understanding and controlling the curing conditions is essential for producing high-performance GPC that meets the specific demands of modern construction.

2.9 Durability of Geo-Polymer Concrete (GPC)

The durability trials demonstrate that the long-term strength of the GPC declines with time when subjected to various severe environmental conditions that lead to concrete degradation. The durability tests included acid exposure, maritime environments, sulphate attack, concrete carbonation, chloride ingress, alkali-aggregate reactions, and freeze-thaw cycles.

2.9.1 Effect of Sulfate Attack on Geo-Polymer Concrete (GPC)

Sulfate attack is a significant durability concern for concrete structures exposed to environments containing sulfates, such as soils or water with high content. In traditional Portland cement concrete, sulfates react with the hydration products, leading to expansive reactions that cause cracking, spalling and ultimately, structural failure. Geopolymer concrete (GPC), however, exhibits a higher resistance to sulfate attack due to its unique chemistry, which lacks the calcium hydroxide found in Portland cement and is thus less prone to forming expansive products like ettringite (Bakharev, 2005).

The primary reason for GPC's superior sulfate resistance is its aluminosilicate-based binder, which is more chemically stable in the presence of sulfates compared to the calcium silicate hydrates (C-S-H) found in traditional cement. Studies have shown that GPC, especially those based on fly ash and slag, can withstand prolonged exposure to sulfate-rich environments with minimal degradation. The absence of calcium phases in GPC means that there are no sulfate-reactive phases that would typically lead to expansion and cracking. As a result, GPC maintains its mechanical stability and mechanical properties even after prolonged exposure to sulfates (Songpiriyakij et al., 2010: Xie et al., 2019).

However, the sulfate resistance of GPC can vary depending on its composition, particularly the type and proportion of aluminosilicate precursors used. For instance, GPCs with higher slag content may show different behavior due to the presence of calcium in the slag, which

could introduce minor vulnerability to sulfate attack. Nevertheless, even in these cases, GPC generally outperforms conventional concrete in sulfate environments, making it an excellent choice for infrastructure in aggressive conditions (Olivia & Nikraz, 2011).

In conclusion, geopolymer concrete has enhanced resilience to degradation relative to conventional Portland cement concrete, principally owing to its distinctive aluminosilicate binder chemistry. This resistance renders GPC a viable material for use in demanding situations, where long-term durability is essential.

2.9.2 Effect of Acid Attack on Geo-Polymer Concrete (GPC)

Acid attack is a critical concern for concrete structures exposed to aggressive acidic environments, such as industrial effluents, sewage systems or acid rain. Traditional Portland cement concrete is particularly vulnerable to acid attack because the calcium hydroxide present in the cement matrix reacts with acids, leading to leaching, softening and loss of mechanical stability. Geopolymer concrete (GPC), on the other hand, has shown superior resistance to acid attack due to its low calcium content and dense aluminosilicate matrix, which is less reactive with acids (Bakharev, 2005).

The enhanced acid resistance of GPC is primarily attributed to the absence of calcium hydroxide and the presence of a stable aluminosilicate gel, which does not easily degrade in acidic environments. When exposed to acids, GPC undergoes less mass loss and retains more of its mechanical properties compared to Portland cement concrete. This resistance makes GPC particularly suitable for applications where long-term exposure to acidic conditions is expected, such as in chemical plants or wastewater treatment facilities (Zuhua et al., 2009).

However, the degree of acid resistance in GPC can vary depending on the type and concentration of the acid, as well as the specific composition of the geopolymer. For instance, GPC made with higher proportions of fly ash has been found to perform better against acid attack than those with slag, as the latter may contain some calcium that could react with acids. Additionally, the curing conditions and the mix design, including the type and ratio of activators used, also influence the acid resistance of GPC (Rangan, 2008).

In conclusion, geopolymer concrete exhibits significantly better resistance to acid attack compared to traditional Portland cement concrete, makingit a viable option for structures exposed to harsh acidic environments. This resistance is primarily due to its low calcium content and chemically stable aluminosilicate matrix.

2.9.3 Effect of Sea Water on Geo-Polymer Concrete (GPC)

Exposure to seawater presents significant challenges for concrete structures due to the combined effects of chloride-induced corrosion, sulfate attack and continuous wetting and drying cycles. Traditional Portland cement concrete is particularly vulnerable to these conditions, as the chlorides in seawater can penetrate the concrete, leading to the corrosion of embedded steel reinforcement, while sulfates can cause expansive reactions, resulting in cracking and deterioration. Geopolymer concrete (GPC), however, has demonstrated superior resistance to seawater due to its unique chemical composition, which lacks the calcium hydroxide and calcium silicate hydrates that are susceptible to these forms of degradation (Palomo et al., 1999).

GPC's high resistance to chloride penetration is one of its most significant advantages in marine environments. The dense, low-permeability microstructure of GPC, formed through the geopolymerization process, acts as a barrier against chloride ions, significantly reducing the risk of corrosion of steel reinforcement. This characteristic makes GPC a promising material for marine structures, such as coastal defenses, bridges, and piers, where long-term durability is crucial (Hussein et al., 2017).

In addition to chloride resistance, GPC exhibits excellent resistance to sulfate attack, which is a common problem in seawater environments due to the presence of magnesium and sulfate ions. Unlike Portland cement concrete, GPC does not form ettringite or other expansive products when exposed to sulfates, thereby maintaining its mechanical stability, and preventing cracking. Studies have shown that GPC can withstand prolonged exposure to seawater with minimal degradation, making it an ideal material for use in aggressive coastal conditions (Sarker et al., 2013).

Overall, geopolymer concrete offers significant advantages over traditional concrete in seawater environments, particularly in terms of resistance to chloride-induced corrosion and

attack. Its durability and longevity in such harsh conditions make it a sustainable and reliable choice for marine and coastal infrastructure.

2.10 Effect of Alkali-Aggregate Reaction and Leaching on Geo-Polymer Concrete (GPC)

The Alkali-Aggregate Reaction is a critical durability concern in conventional Portland cement concrete, whereby reactive silica in aggregates interacts with alkalis from the cement, resulting in the creation of expanding gel, cracking, and structural deterioration. Geopolymer concrete (GPC) has reduced vulnerability to Alkali-Aggregate Reaction owing to its low calcium content and the stable aluminosilicate gel matrix, which limits the availability of alkalis that initiate Alkali-Aggregate Reaction (Rangan, 2008). The absence of calcium hydroxide in GPC reduces the potential for expansive gel formation, contributing to its enhanced durability in environments prone to Alkali- Aggregate Reaction.

Leaching, on the other hand, involves the dissolution of components from the concrete matrix when exposed to water, leading to a loss of material and a decrease in strength. GPC shows resistance to leaching due to its dense microstructure and stable geopolymer network, which limits the dissolution of its components in aggressive environments (Sun & Vollpracht, 2020). This resistance to leaching further enhances the longevity and durability of GPC, especially in applications where exposure to water or aggressive chemicals is a concern.

2.11 Effect on the Bond Strength of Geo-Polymer Concrete (GPC)

Bond strength between concrete and reinforcing steel is a critical factor in the mechanical stability of reinforced concrete structures. In traditional Portland cement concrete, the bond is achieved through a combination of mechanical interlocking and chemical adhesion, primarily influenced by the hydration products. Geopolymer concrete (GPC), with its unique aluminosilicate binder, exhibits different bonding characteristics, which can be both advantageous and challenging depending on the specific mix design and application (Almutairi et al., 2021).

The bond strength in GPC is generally influenced by several factors, including the type of aluminosilicate source material (e.g., fly ash, slag), the molarity and composition of the alkaline activators and the curing conditions. Studies have shown that GPC can achieve bond strengths comparable to or even exceeding that of traditional concrete, particularly when using high-quality materials and optimized curing processes. The dense microstructure of GPC, which results from the geopolymerization process, contributes to strong mechanical interlocking between the steel and the concrete matrix (Benli et al., 2025).

However, the chemical adhesion in GPC is somewhat different due to the absence of calcium hydroxide and the presence of a geopolymeric gel, which may alter the nature of the bond at the interface. While this can result in high initial bond strength, it also means that the bond performance can vary more with changes in mix composition and curing methods. For example, elevated temperature curing, often used in GPC production, can enhance early-age bond strength but may also lead to shrinkage issues that affect the long-term bond (Sarker et al., 2013).

In conclusion, GPC can achieve excellent bond strength with reinforcing steel, provided the mix design and curing conditions are carefully controlled. Its unique bonding mechanism, driven by mechanical interlocking and influenced by the geopolymeric matrix, offers potential advantages in specific structural applications, though it requires careful consideration of the specific materials and methods used.

2.12 Application of Machine Learning in Geo-Polymer Concrete

The application of Machine Learning (ML) in the domain of Geopolymer Concrete (GPC) has significantly advanced since 2018, transforming how researchers and engineers approach the design, optimization, and performance prediction of this sustainable construction material. As GPC gains traction as a low-carbon alternative to traditional Portland cement concrete, the inherent complexity of its chemical composition and the variability in the properties of its constituent materials such as flyash, rice husk ash, slag, and other industrial by-products - have necessitated the use of advanced computational methods to model and predict its behavior under various conditions. Traditional empirical methods, while useful, have often struggled to capture the non-linear relationships between the numerous factors

that influence GPC's performance. This has led to a surge in the adoption of machine learning techniques, which excel in identifying patterns within large datasets and can provide more accurate predictions of material properties, thereby improving the reliability and efficiency of GPC in practical applications (Nguyen et al., 2025).

One of the primary areas where ML has made a substantial impact is in the prediction of the compressive strength of GPC. Compressive strength is a critical parameter for concrete materials and its accurate prediction is essential for ensuring the mechanical stability and safety of constructions. Researchers have employed various machine learning models, such as Artificial Neural Networks (ANNs), Support Vector Machines (SVMs), decision trees and ensemble learning methods, to predict the compressive strength of GPC based on input variables such as the type and proportion of raw materials, the concentration of alkaline activators, curing conditions and the addition of supplementary materials like nano-silica or fibers (Xie & Liew, 2019). ANNs, in particular, have shown considerable success in this domain due to their ability to model complex, non-linear relationships between input features and output properties. Studies have demonstrated that ANN models can outperform traditional regression-based methods in predicting compressive strength, offering higher accuracy and generalization across different mix designs (Girish et al., 2020). Additionally, the use of ensemble learning methods, which combine the predictions of multiple models to improve overall accuracy, has further enhanced the reliability of strength predictions in GPC, making these models valuable tools in both research and industrial applications (Liew et al., 2022).

Beyond compressive strength, ML has been instrumental in predicting other key properties of GPC, such as workability, durability against to environmental factors like sulfate attack, carbonation and freeze-thaw cycles. For instance, SVMs and random forest models have been used to predict the workability of GPC mixes by analyzing the influence of water-to-binder ratio, aggregate gradation and the specific surface area of precursors. Accurate predictions of workability are crucial for ensuring that GPC can be efficiently mixed, transported and placed on-site without compromising its performance (Rajini et al., 2022). Furthermore, machine learning has facilitated the development of predictive models for the long-term durability of GPC, which is particularly important for its use in infrastructure

exposed to harsh environmental conditions. Researchers have employed ML models to assess the potential for sulfate attack, chloride penetration and carbonation in GPC, providing valuable insights into how different mix compositions and curing regimes affect the material's resistance to these forms of degradation (Nazari & Sanjayan, 2020). These models not only enhance the understanding of GPC's behavior over time but also guide the formulation of more durable GPC mixes tailored to specific environmental challenges.

In addition to property prediction, ML has also been applied to optimize the mix design of GPC, a task traditionally performed through trial and error or based on empirical relationships derived from limited experimental data. Machine learning algorithms such as Genetic Algorithms (GAs) and Particle Swarm Optimization (PSO) have been integrated with predictive models to identify optimal mix proportions that meet specific performance criteria, such as maximizing strength while minimizing the environmental impact or cost (Xie & Liew, 2021). These optimization techniques allow for the exploration of a vast design space, enabling the identification of mix designs that might not be evident through conventional approaches. The result is a more efficient and targeted development process that reduces the need for extensive laboratory testing and accelerates the implementation of GPC in real-world projects (Wang & Zhang, 2025).

Moreover, the integration of Machine Learning with the Internet of Things (IoT) has opened new dimensions for the real-time monitoring and management of GPC structures. Smart sensors embedded within GPC elements can continuously collect data on parameters such as temperature, humidity, and strain, which are then analyzed by machine learning algorithms to assess the structural health and predict potential failure points before they occur (Zhang et al., 2023). This capability is particularly valuable for critical infrastructure, where early detection of potential issues can prevent catastrophic failures and extend the service life of structures. The combination of ML and IoT thus represents a significant step towards the development of smart construction materials that can adapt to their environment and provide continuous feedback on their condition, enhancing both safety and sustainability in construction practices (Liew et al., 2023).

Despite the significant advancements in applying ML to GPC, challenges remain in fully realizing it’s potential. One of the primary challenges is the availability of high-quality,

standardized datasets, which are essential for training accurate and generalizable machine learning models. The variability in raw materials, experimental setups and testing methods used across different studies can lead to inconsistencies in the data, complicating the development of robust models (Nazari & Sanjayan, 2023). To address this, there is a growing emphasis on creating comprehensive, open-access databases that aggregate data from multiple sources, providing a more reliable foundation for model development. Additionally, the interpretability of machine learning models, particularly more complex ones like deep neural networks, remains a concern, as it can be challenging to understand the decision-making process of these models and ensure they are making accurate predictions based on relevant features (Girish et al., 2023). Ongoing research is focused on developing interpretable ML models that balance accuracy with transparency, making them more accessible and trustworthy for use in critical applications like construction. The application of machine learning in geopolymer concrete has revolutionized the field by providing powerful tools for predicting material properties, optimizing mix designs, and enhancing the monitoring and management of GPC structures. These advancements have the potential to accelerate the adoption of GPC in the construction industry, contributing to more sustainable and resilient infrastructure. As research continues to evolve, it is likely that ML will play an increasingly central role in the development and application of GPC, paving the way for new innovations and broader adoption of this environmentally friendly material (Zhang et al., 2024b).

2.13 Concluding Remarks

In conclusion, this chapter provides a comprehensive review of the use of industrial by-products like fly ash and GGBFS in geopolymer concrete (GPC), focusing on their roles in promoting sustainability and improving material performance. The effects of various parameters including alkaline solution concentration, liquid-to-binder ratios and curing conditions are discussed, showing how they significantly influence GPC's mechanical and durability properties. Additionally, this chapter highlights the transformative role of machine learning (ML) in GPC research, particularly in predicting material properties, optimizing mix designs, and enhancing durability assessments. ML techniques, such as neural networks, support vector regression and soon, enable more accurate predictions for key characteristics

like compressive strength, workability, and environmental resistance. This integration of ML not only streamlines the GPC design process but also supports its use as a durable, eco-friendly alternative in construction, contributing to more resilient and sustainable infrastructure.

Chapter 3
Materials and Methodology

3.1 Introduction

This chapter outlines the methodology adopted in the current study, focusing on the procedures for testing concrete properties and the application of various machine learning techniques. It begins with a detailed description of the concrete testing methods used to evaluate the material's performance. The chapter then provides an overview of the machine learning models employed, including Artificial Neural Networks (ANN), Gene Expression Programming (GEP), multiple linear regression, generalized linear models, quadratic polynomial regression, and Support Vector Regression (SVR), Bi-LSTM and Self-Improved Jelly Search Optimization (SIJSO). These techniques were selected to analyze and predict concrete behavior, leveraging their unique strengths in handling complex, nonlinear relationships within the data. The methodologies presented here lay the foundation for developing robust predictive models in concrete research.

3.2 Materials

The section provides a comprehensive analysis of materials used in geopolymer concrete, including fly ash, Alccofine, sodium hydroxide, sodium silicate, aggregates, and superplasticizers. It highlights their chemical and physical properties, sourcing, and significance in concrete applications.

3.2.1 Fly-Ash

Fly ash, a byproduct of coal combustion in thermal power plants, is an industrial solid waste that is commonly collected through electrostatic precipitation of coal ash fumes (Ahmaruzzaman, 2010). The particle size of fly ash is similar to or slightly smaller than ordinary Portland cement (OPC), and its composition is notably rich in silica and alumina, making it a valuable pozzolanic material in various construction applications (Ahmaruzzaman, 2010; Malhotra, 2002). For this study, the fly ash was sourced from the National Thermal Power Plant in Dadri, Gautam Budh Nagar, Uttar Pradesh, and is classified

as Class F fly ash.

The physical characteristics of Class F fly ash are distinct, as the particles are predominantly spherical and porous, which improves workability and bonding in concrete mixes. (Gougazeh & Buhl, 2014). The properties of the fly ash used, Tables 3.1 and 3.2 detail the chemical and physical compositions, respectively. Table 3.1 lists the main oxides such as silica (SiO_2), alumina (Al_2O_3), iron oxide (Fe_2O_3), and calcium oxide (CaO) that influence the reactivity and pozzolanic behavior of the fly ash (Chindaprasirt et al., 2005).

Table 3.1: Mineral Composition of Fly Ash

Chemical Analysis	**Mass %**
SiO_2	55
Al_2O_3	26
Fe_2O_3	7
CaO	9
MgO	2
SO_3	1

Table 3.2 presents physical properties like specific gravity, fineness, and particle size distribution, which are essential parameters for assessing fly ash's performance in geopolymer concrete mixes. The data support the suitability of this Class F fly ash for use in geopolymer concrete, leveraging its reactivity and particle structure for improved durability and performance.

Table 3.2: Physical Properties of Fly Ash

Physical analysis	Range
Specific gravity (G)	2.5
Surface Area (Blaine air permeability method)	360 cm^2/g
Particle Shape	Spherical particles

3.2.2 Alccofine

Alccofine, obtained from Ambuja Cements, Gurugram, is an advanced supplementary cementitious material (SCM) increasingly used in construction for enhancing concrete properties. Made as a fine-grained powder primarily derived from rice husk combustion, Alccofine demonstrates high reactivity, allowing it to act as a pozzolanic material that reacts with calcium hydroxide in the presence of water to form additional cementitious compounds, thus improving concrete strength and durability (Singh et al., 2023; Patel et al., 2024).

Due to its ultra-fine particle size and high pozzolanic activity, Alccofine effectively fills micro-pores within the concrete matrix, enhancing density, durability, and resistance to permeation (Patel et al., 2024). Fig. 3.1 illustrates the Scanning Electron Microscopy (SEM) analysis of Alccofine, showing a fine particle structure conducive to efficient chemical reactions. The elemental composition of Alccofine is detailed in Fig. 3.2 using Energy Dispersive X-ray Spectroscopy (EDS), indicating the presence of essential components like silicon (Si), calcium (Ca), and aluminum (Al), which contribute to its cementitious capabilities.

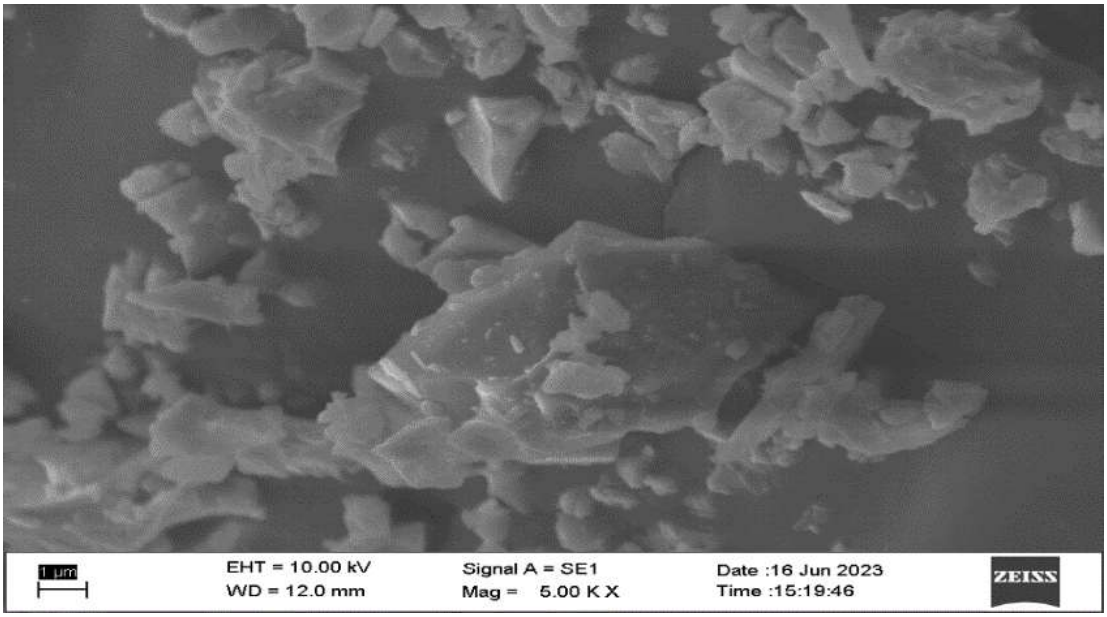

Fig. 3.1: SEM Image of Alccofine

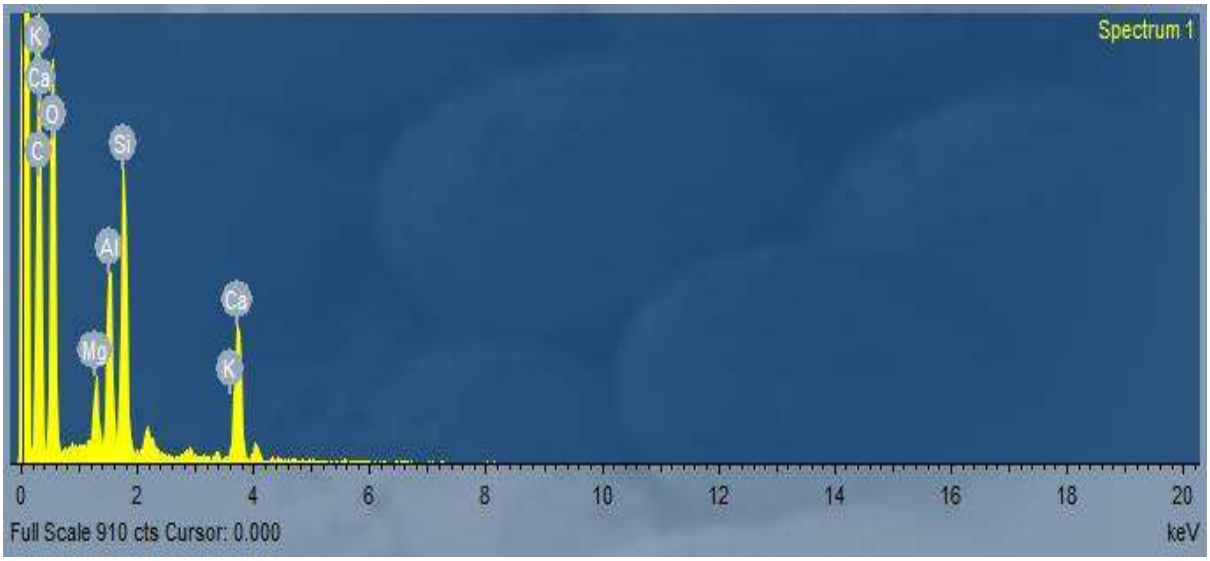

Fig. 3.2: EDS Graph of Alccofine

Tables 3.3 and 3.4 present the chemical and physical properties of Alccofine. Table 3.3 includes the key chemical components, such as SiO_2, Al_2O_3, Fe_2O_3, and CaO, which play a pivotal role in enhancing concrete performance (Sharma & Gupta, 2024).

Table 3.3: Mineral Composition of Alccofine

Chemical Analysis	**Mass %**
CaO	30- 34
Al_2O_3	18 -25
Fe_2O_3	18 -25
SO_3	0.1-0.4
MgO	6 to 10
SiO_2	30-36

Table 3.4 provides physical characteristics such as fineness, specific surface area, and particle size distribution, essential for optimizing Alccofine's effectiveness in concrete applications. Collectively, these properties make Alccofine a promising SCM for producing high-performance, durable concrete (Sharma et al., 2016).

Table 3.4: Physical Properties of Alccofine

Physical Analysis	**Range**
Specific Gravity	2.86
Surface Area (Blaine Air Permeability Method)	1200 cm^2 /gm
Particle Shape	Irregular/Angular

3.2.3 Sodium Hydroxide

For activating the fly ash, a blend of sodium hydroxide (NaOH) and sodium silicate solution was selected as the alkaline activator, as sodium-based activators are more cost-effective compared to potassium-based alternatives (Kryvenko et al., 2024). The NaOH solution was prepared by dissolving flakes or pellets in water, with its concentration specified in molarity (M). For instance, an 8M NaOH solution was made by dissolving 320 grams of NaOH solids (in flake or pellet form) per litre of solution, where 40 represents the molecular weight of NaOH (Oti et al., 2024).

The amount of NaOH solids per kilogram of solution varies based on the concentration: 262 grams for 8M, 314 grams for 10M, 361 grams for 12M, 404 grams for 14M, and 444 grams for 16M. In these solutions, water constitutes the majority of the mass, while NaOH solids make up a smaller portion (Kumar et al., 2023). This precise formulation is crucial for ensuring consistent geopolymerization and achieving optimal binding properties in the resultant concrete.

The NaOH and sodium silicate solutions were combined to prepare the alkaline activator, which was left to stabilize for 20–24 hours before use. Sodium hydroxide was procured from Qualigens Scientific, a company based in Powai, Mumbai, Maharashtra, India, as depicted in Fig. 3.3. The stability period prior to application ensures that the mixture reaches a homogenous state conducive to effective fly ash activation (Jin et al., 2023)

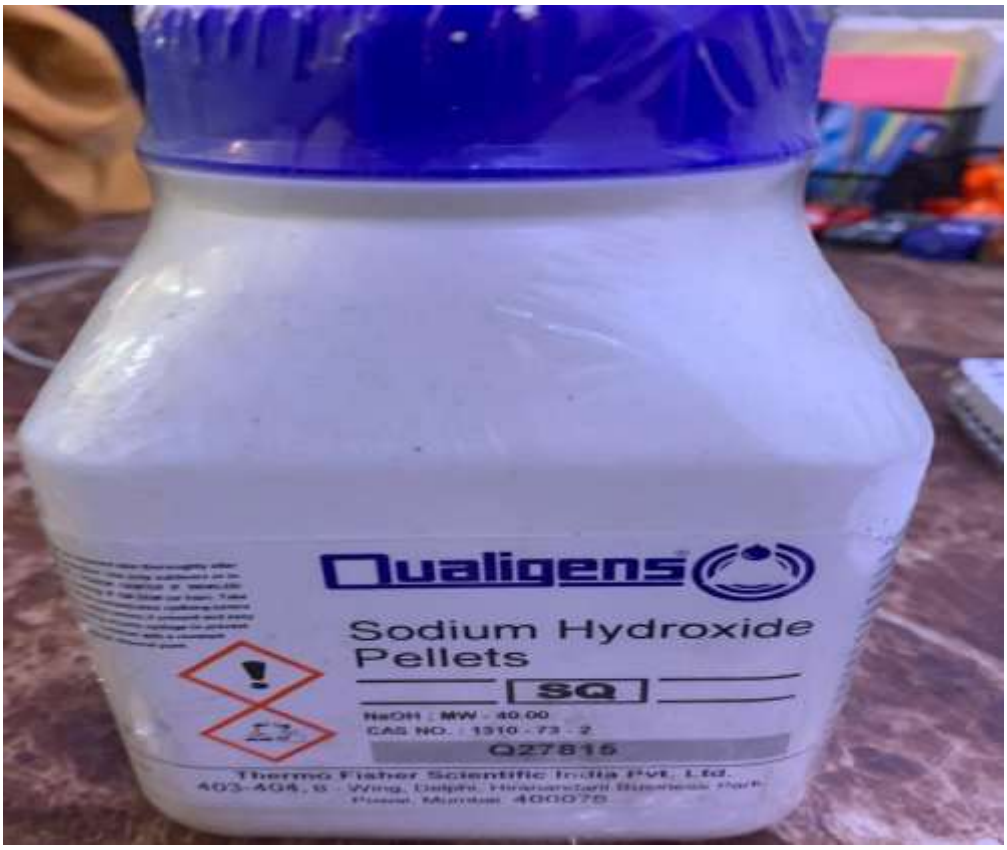

Fig. 3.3: Sodium Hydroxide Pellets

3.2.4 Sodium Silicate Solution

Sodium silicate, often referred to as water glass, plays a crucial role in the activation of pozzolanic materials, enhancing their binding properties through the formation of a gel matrix. This gelation process is pivotal in the geopolymerization of materials, wherein the alkaline solution facilitates the dissolution of aluminosilicate compounds, leading to the crosslinking and setting of the material. Sodium silicate is typically supplied as a slightly cloudy or tacky liquid, containing high concentrations of sodium oxide (Na_2O), which is essential for the activation of pozzolans. In the case of the sodium silicate solution Shown in Fig. 3.4 purchased from Loba Chemie Pvt. Ltd. in New Delhi (India), the product contains a minimum Na_2O assay of 10.0%, with a silicon dioxide (SiO_2) content ranging between 25.5% and 28.5% (gravimetric). This formulation ensures the solution's effectiveness in the

geopolymerization process, promoting the formation of strong and durable binders.

Recent studies have highlighted the significance of sodium silicate in optimizing the properties of geopolymer concrete, with improvements in mechanical strength, durability, and environmental sustainability (Dadsetan et al., 2022; Wu et al., 2022). Sodium silicate's role in enhancing the reactivity of aluminosilicate materials has been extensively explored, with particular attention given to its interactions with various alkaline activators, which influence the final material performance (Adeleke et al., 2023). Furthermore, the precise formulation and concentration of Na_2O and SiO_2 in the solution are critical to achieving the desired setting times and strength development in geopolymer materials, as noted in recent studies on geopolymer concrete (Castillo et al., 2021).

Fig. 3.4: Sodium Silicate Solution

3.2.5 Fine Aggregates

Aggregate forms the structural framework of concrete, making up 75-85% of its total volume. It is broadly divided into two main types: fine aggregates and coarse aggregates. Fine aggregates include particles smaller than 4.75 mm, whereas coarse aggregates consist of particles larger than 4.75 mm. Commonly used coarse aggregates in mix design are 10 mm and 20 mm in size, while fine aggregates typically comprise crushed stone dust. Before

incorporating aggregates into the mix design, their quality must be verified according to Indian Standard codes. Preliminary testing should include assessments of the aggregate's gradation, zone classification, fineness modulus, specific gravity, water absorption, silt content, and bulk density of the fine aggregates or stone dust (Patel & Yadav, 2023). Fig.3.5 shows a sample of the stone dust used for testing in various mix designs.

Fig. 3.5: Stone-Dust or Fine Aggregate

Table 3.5 provides the particle size distribution, detailing the percentage of material retained on each sieve and the corresponding percentage passing through each sieve size. The analysis highlights the characteristics of the particles in the samples. The results indicate that the stone dust sample falls within Zone II, classified as medium and well-graded based on its particle size distribution.

Table 3.5: Sieve Analysis of Sand / Stone Dust (IS 383:2016)

Sieve Size	Weight Retained (g)	Cumulated Weight Retained	Cumulated % Weight Retained	Cumulated % Passing	Remarks
4.75mm	0	0	0	100	Sand falls in zone II
2.36mm	105	105	10.5	89.5	
1.18mm	294	399	39.9	60.1	
600µ	216	615	61.5	38.5	
300µ	133	748	74.8	25.2	
150µ	128	876	87.6	12.4	
75 µ	38	914	91.4	8.6	
Pan	86	1000	100	0	

Table 3.6 outlines all the properties of the dust samples, based on the tests conducted on the sample materials. As per the code IS 383:2016 standards, the sand belongs to gradation II. From the gradation curve, we find the sand is well graded sand.

Table 3.6: Properties of Fine Aggregate/Stone Dust (m-sand)

S. No.	Test	Results
1	Zone & Grade	Zone – II & well graded
2	Fineness Modulus	2.743(Medium Sand)
3	Specific Gravity (G)	2.55
4	Water Absorption	1.13%
5	Silt Content	6%
6	Bulk Density (ρ)	1587 kg/m^3

3.2.6 Coarse Aggregate

Coarse aggregate, consisting of crushed stone or gravel retained on a 4.75 mm sieve, is a crucial component in concrete, providing strength and durability. Proper grading ensures optimal packing, reducing voids and enhancing the mix's performance. Fig.3.6 illustrates that locally available coarse aggregate samples were utilized in various mix designs, emphasizing their relevance to the study.

Fig. 3.6: Coarse Aggregate Sample

Table 3.7 provides a detailed analysis of the particle size distribution of the coarse aggregate samples, presenting the percentage of material retained on each sieve and the corresponding percentages passing through. This comprehensive distribution helps in understanding the gradation and uniformity of the aggregates. Additionally, the Table 3.7 includes the calculation of the fineness modulus, a critical parameter indicating the aggregate's coarseness and its suitability for use in concrete mix designs.

Table 3.7: Sieve Analysis of Coarse aggregate (IS 383:2016)

Sieve size	Weight retained (g)	Cumulative weight retained	Cumulative % weight retained	% Cumulative passing	% Passing of nominal size IS383:2016
80 mm	0	0	0	100	85-100
40 mm	0	0	0	100	-
20 mm	266	266	13.3	86.7	-
16 mm	571	837	41.85	58.15	-
12.5 mm	730	1567	78.35	21.65	-
10 mm	336	1903	95.15	4.85	0-20
4.75 mm	87	1990	99.5	0.5	0-5
PAN	10	2000	100	0	-

Fineness modulus: (0+0+13.3+41.85+78.35+95.15+99.5+5X100)/100 = 7.28

Table 3.8 describes their properties. Preliminary tests were conducted to assess the quality of the raw materials before their use, ensuring that the materials met the necessary standards for the mix design (Etxeberria et al., 2007; Kore & Vyas, 2015).

Table 3.8: Properties of Coarse Aggregate

Sl. No.	Test	Results
1	Fineness Modulus	7.28
2	Specific Gravity (G)	2.77
3	Water Absorption	20%
4	Crushing Value	23%
5	Impact Value	24%
6	Flakiness Index	23%
7	Elongation Index	20%
8	Abrasion Value	9%

3.2.7 Superplasticizer

Superplasticizers are used to enhance concrete performance by reducing the water content in the mix design while increasing the workability of the fresh mixture. The SNF-based superplasticizer used in the concrete mix design is SP Sikaplast-5061, produced by Sika India Pvt. Ltd, as per IS 9103:1999 (April 1999). Table 3.9 delineates the characteristics of the superplasticizer sample. Fig. 3.7 illustrates the superplasticizer used in the mix designs.

Table 3.9: Superplasticizer Properties

Sl. No.	Test	Results
1.	Visual Aspect	Brown Color Liquid
2.	Specific Gravity	1.19 @ 25°C
3.	Chloride Content	Nil to BS5076 / BS: EN936
4.	Air Entrainment	< 2% (Additional Air Entrained at Usual Dosages)

Fig. 3.7: Superplasticizer Sample Picture

3.3 Mix Proportion

The mix design calculation for geopolymer concrete (GPC) was performed after conducting thorough testing on the material samples to ensure the appropriate properties for the desired mix. Table 3.10 outlines the model mix designs used for the various tests conducted throughout the study. These mix designs were developed using empirical relations derived from extensive research in the field of geopolymer concrete, along with established reference journals and guidelines on mix proportions. The design process took into account several key factors, including the ratio of alkaline activator to pozzolanic material, the specific type of binder used, and the moisture content of the mix. Additionally, adjustments were made based on the workability, setting time, and strength development characteristics observed in the preliminary tests. The formulation of the mix was guided by the principles outlined in current literature on GPC, which suggests the optimization of the SiO_2/Na_2O ratio, the use of fly ash or other industrial by-products as supplementary cementitious materials, and the careful selection of alkaline activators like sodium hydroxide and sodium silicate. Several studies have highlighted that these ratios significantly influence the mechanical properties and durability of GPC, particularly in terms of compressive strength, shrinkage, and resistance to chemical attacks (Patel & Yadav, 2023; Sharma et al., 2024). The reference mix designs were derived and adjusted according to the local material properties, ensuring the mix was both cost-effective and sustainable, while still achieving the targeted performance standards for the geopolymer concrete used in the study.

Table 3.10: Summary of Material Quantities for M30 Mix (for 1 m^3)

Material	**Quantity (kg/m^3)/ Range**
Fly Ash	405 kg/m^3
Coarse Aggregate	1273 kg/m^3
Fine Aggregate	672 kg/m^3
NaOH Solution	8 M -14 M
Na_2SiO_3/ NaOH	0.5 - 2.5
Liquid/Binder (NaOH + Na_2SiO_3)	0.35-0.65
Superplasticizer	0.5 - 2.5 %

3.4 Mixing, Casting and Curing

The mix designs for geopolymer concrete (GPC) were implemented by combining all constituents in specified proportions using a pan mixer, following the mixing procedure outlined in Indian Standard IS 12119-1987. For GPC, the alkaline solution was prepared 20-24 hours before the main mixing to ensure full activation of the pozzolanic materials. During the mixing process, the alkaline solution was added to the dry materials, and the mixture was subsequently poured into moulds with proper compaction to achieve optimal density in the cast samples. The GPC specimens, including cubical, cylindrical, and beam-shaped forms, were then cured in an oven at 60°C for 24 hours to enhance the polymerization process and improve the final strength of the concrete (Paruthi et al., 2024; Davidovits, 2002).

The fresh produced GPC from fly ash was black in hue because to the intrinsic coloration of the fly ash and had cohesive characteristics. The water content in the mix played a crucial role in determining the behaviour of the fresh concrete, affecting both workability and cohesiveness. Observations revealed that extended mixing times with high water content led to bleeding and segregation of the aggregate and paste, negatively impacting the compressive strength of the hardened concrete. Davidovits (2002) emphasized the importance of pre-mixing the sodium silicate and sodium hydroxide solutions before their incorporation into the solid constituents to prevent these issues. Based on preliminary findings, water content and mixing duration were identified as essential parameters in the detailed study (Smith & Patel, 2023). The following standardized mixing process was adopted for all further tests to ensure consistent quality in the GPC preparation:

1. **Pre-mix the Alkaline Solutions**: Sodium hydroxide and sodium silicate solutions were mixed together 20-24 hours before combining with the solid materials to maximize the reactivity of the alkaline solution.

2. **Dry Mixing of Materials**: All dry components (e.g., fly ash, sand, aggregates) were mixed in the pan mixer for approximately three minutes to achieve uniform distribution.

3. **Addition of Liquid Component**: The pre-mixed alkaline solution was added to the

dry materials, followed by an additional four minutes of mixing to ensure even distribution and activation.

Fig. 3.8: Pan Mixture in the Laboratory

3.4.1 Slump Cone Test

The slump cone test is a widely used method for assessing the workability and consistency of fresh concrete, providing a quick and reliable measure of its physical properties. This test is commonly employed on construction sites and in laboratories due to its simplicity and effectiveness (Neville & Brooks, 2023). The main instrument for the slump test is a conical metal mold, Referred to as a slump cone, it is open at both ends and generally has a height of 300 mm, a base diameter of 200 mm, and a top diameter of 100 mm.

To perform the slump test, fresh concrete is placed in the cone in three layers, with each layer compacted by tamping with a rod to eliminate air voids and ensure uniform density (Mindess et al., 2023). Once filled, the cone is gently lifted in a vertical motion, enabling the concrete to settle under its own weight. The difference in height between the filled cone and the slumped concrete indicates the workability. High slump values correspond to more fluid, workable concrete, while lower slump values suggest a stiffer, less workable mix, critical for

applications requiring specific workability characteristics (Mehta & Monteiro, 2024). This test ensures that the concrete mix meets necessary requirements for placement and compaction, especially for structural and foundational applications where consistency is essential.

Fig. 3.9: Slump Apparatus

3.4.2 Curing of Specimens

In this study, two curing methods were utilized to enhance the strength of the geopolymer concrete (GPC) specimens: ambient curing and oven curing. Curing plays a critical role in the polymerization process, which is essential for developing the strength and durability of GPC. In ambient curing, specimens are left to cure at room temperature, typically for a specified period depending on the mix design and the requirements of the study (Patel & Yadav, 2023). This method is often preferred when minimal energy input is desired, as it allows the specimens to harden naturally, which is particularly beneficial in moderate climates. Ambient curing is advantageous for GPC applications where extended curing times are feasible and where thermal energy for curing is either unavailable or cost-prohibitive.

In contrast, oven curing involves placing the specimens in a controlled environment,

typically set to a temperature of 60°C, for a defined period often around 24 hours (Mehta et al., 2024). Oven curing accelerates the geopolymerization reaction by providing additional heat, which enhances the bonding of aluminosilicate materials within the GPC matrix. This method is particularly effective in increasing early-age strength, as the elevated temperature expedites the chemical reactions necessary for hardening (Tayeh et al., 2023). Fig. 3.10 and Fig. 3.11 illustrate the specimens during the ambient and oven curing processes, respectively, demonstrating the setup used for each method.

Both curing methods have been extensively studied, with research indicating that oven curing generally leads to higher compressive strength in GPC compared to ambient curing, particularly within the early stages (Sharma & Singh, 2023). However, ambient curing remains a viable alternative for structural applications where strength development can occur over a more extended period.

Fig. 3.10: Specimens During Ambient Curing

Fig. 3.11: Oven for Heat Curing

3.4.3 Density

The weight of the specimens is a critical parameter used to identify the density of the geopolymer concrete (GPC) mixes before undergoing destructive testing. Density is calculated to assess the material's compactness, which correlates directly with strength and durability characteristics. In this study, density measurements were taken 28 days after casting, aligning with standard practices for evaluating concrete properties at a significant curing age (Neville & Brooks, 2023). By recording the weight of each specimen, the mass-to-volume ratio is calculated to determine density, which is fundamental for understanding the quality and performance of the GPC. To obtain these measurements, each specimen was weighed using a digital scale. The digital weighing process provides high precision, reducing any potential errors that may affect the density calculation. This density measurement serves as a non-destructive preliminary test that indicates how well the materials are compacted in the mix, indirectly affecting the porosity and strength development within the GPC (Patel & Yadav, 2023). The 28-day density values are particularly important because they help evaluate the stability of the hardened matrix, offering insights into the GPC's overall mechanical stability and its suitability for load-bearing applications. This assessment aligns

with current practices in concrete evaluation, where density is considered an indicator of material performance under various environmental and mechanical stresses (Mehta et al., 2024).

3.4.4 Compressive Strength

The compressive strength of geopolymer concrete mixes was evaluated using the cube sample test, conducted under a Compression Testing Machine (CTM) at a steady loading rate of 5.25 kN/sec. This gradual, statically applied load is essential for obtaining accurate compressive strength values, as specified by standard testing procedures (Patel et al., 2023). The 100 mm × 100 mm × 100 mm cube specimens were prepared according to Indian Standard (IS) code specifications, ensuring consistency in results.

In the case of geopolymer concrete (GPC), most of the strength development occurred by 14 days under ambient curing conditions and by 7 days with oven curing, which accelerates the geopolymerization process and produces high early-age strength (Raja & Sujatha, 2024).

This difference in curing times is significant for GPC, as oven curing promotes a rapid chemical reaction between the alkaline activators and pozzolanic materials, achieving structural strength within a short period. For GPC, testing intervals of 7, 14, 28 and 56 days were observed to monitor the standard strength gain curve and GPC's strength gain at earlier stages highlights its potential for applications requiring faster readiness (Neville & Brooks, 2023).

Fig. 3.12 illustrates a cube specimen under compressive strength testing on a Compression Testing Machine (CTM). This setup provides a controlled environment for assessing the material's load-bearing capacity, which is critical for GPC mixes. By testing at these specified intervals, the compressive strength results for each mix design contribute to an understanding of how these materials perform under load, guiding their use in structural applications that demand rapid strength development or conventional strength progression (Mehta et al., 2024).

Fig. 3.12: Compressive Strength Test of GPC Cube in the CTM

3.4.5 Splitting Tensile Strength

The splitting tensile test evaluates the indirect tensile strength of concrete using cylindrical specimens with dimensions of 150 mm in diameter and 300 mm in length, conducted in accordance with Indian Standard codes. A loading rate of 4.5 kN/sec is applied transversely to these cylindrical specimens, allowing measurement of their splitting tensile strength, which generally exceeds direct tensile strength but is lower than the flexural strength for the same mix design.

3.4.6 Flexural Strength

Flexural strength, also referred to as the modulus of rupture, evaluates the bending capacity of concrete specimens and serves as a critical measure of a concrete mix's resistance to bending stress. For specimens with a maximum aggregate size of 20 mm or less, standard beam dimensions of 100 mm × 100 mm × 500 mm are used for casting. The flexural strength test involves applying a two-point load along the specimen's transverse axis, using a flexural testing machine. This setup helps to simulate the bending forces that concrete may encounter in structural applications. Fig. 3.13 shows a beam specimen positioned during the flexural strength test.

Fig. 3.13: The Flexural Strength Test Setup

3.4.7 Elastic Modulus

The elastic modulus of the concrete mix is measured by applying a uniaxial static load in the vertical direction to cylindrical specimens. This test setup enables the assessment of both vertical and horizontal displacements, as well as the compressive strength of the specimens.

To determine the elastic modulus, the test involves incrementally loading the specimens up to approximately one-third of their ultimate strength, then releasing and repeating this loading cycle multiple times. A stress-strain curve is plotted and the elastic modulus is obtained from the chord modulus according to ASTM standards.

3.4.8 Rebound Strength

A rebound hammer equipment is a non-destructive testing device used to evaluate the strength of geopolymer concrete samples by assessing the surface indentation. This method is widely applied to both cube and cylindrical specimens to estimate their compressive strength. The device works by striking the concrete surface with a spring-loaded hammer, and the rebound distance is measured to infer the material's strength. The rebound number obtained from this test correlates with the compressive strength, providing a quick and efficient estimate without causing damage to the sample (Brencich et al., 2020; Kumavat et al., 2021). Fig. 3.14 illustrates the rebound hammer strength test being conducted on a concrete sample.

Fig. 3.14: Picture During Rebound Hammer Strength Test

3.4.9 Seawater Condition

The seawater condition is created by using salt to simulate a saline environment in compliance with ASTM standards. A 5% concentration of salt is dissolved in 40 liters of tap water. Following the preparation of the saline solution, the GPC cube specimens were submerged in it for durability assessment. The specimens' weight measurements and compressive strength evaluations after 6, 12, 18, and 24 weeks were conducted in the saline solution. Fig. 3.15 illustrates the seawater conditions established in a water tub containing concrete sample.

Fig. 3.15: Picture of Seawater Solution with the Cube Specimens

3.4.10 Sulphate Attack

A sulfate solution was prepared in the laboratory by dissolving 5% magnesium sulfate in tap water and storing it in a 40-liter tub. The sulfate attack test involved submerging the GPC cube specimens in this solution for a period of 18 weeks. Fig. 3.16 depicts the sulfate attack setup, showing the water tubs containing the concrete cube specimens. The GPC specimens were analyzed for weight and compressive strength at intervals of 6 weeks, 12 weeks, and 18 weeks, respectively.

Fig. 3.16: Picture of Sulphate Solutions with the Cube Specimens

3.4.11 Acid Attack

The acid attack resistance of the concrete specimens was evaluated by immersing them in an acidic solution for durations ranging from 6 weeks to 18 weeks. The solution, prepared in accordance with ASTM standards, consisted of 5% sulfuric acid dissolved in tap water and stored in a tub. The specimens were analyzed for weight and compressive strength after 6 weeks of exposure to the solution.

3.4.12 Wetting-Drying Condition

The wetting-drying condition was assessed on GPC specimens by submerging them in water at room temperature for 24 hours, followed by repeated cycles of wetting and drying. After completing 30, 45, 60, 75, and 90 cycles, the specimens were assessed for weight and compressive strength.

3.5 Machine Learning

3.5.1 Genetic Programming (GP)

Genetic techniques (GA) are adaptive heuristic search techniques categorized under evolutionary algorithms. Genetic algorithms are based on the ideas of natural selection and genetics. These strategies include using historical data to direct a random search toward regions of the solution space that are probable to provide superior performance. They are often used to provide enhanced solutions for optimization and search problems. Genetic algorithms emulate the process of natural selection, wherein organisms capable of adapting to environmental changes may live, reproduce, and pass their traits to subsequent generations. These simulations use the notion of "survival of the fittest" to identify the most successful individuals in each generation as they endeavour to resolve a difficulty. Each generation has people that signify points inside the search space and potential solutions. Each person is denoted by a sequence of characters, numbers, floats, or bits. This sequence has resemblance to the chromosome.

Genetic Programming (GP) is a methodology for pattern recognition that involves developing a model via adaptive learning using many occurrences of input data. The innovation may be credited to Koza in 1992. It utilizes genetic algorithms (GA) to simulate the natural evolution of living organisms for the purpose of analysing their behaviour. In classical regression analysis, the user must explicitly specify the model structure. In Genetic Programming (GP) regression, the model's structure and parameters are autonomously established. The answer is presented in either a hierarchical structure or a concise mathematical statement, depending upon the provided information. The GP model, distinguished by its hierarchical tree structure of nodes, is sometimes termed a GP tree. A functional set, sometimes termed a terminal set, has nodes that serve as its primary elements. The expression can incorporate mathematical operators (-, +, ×, ÷), mathematical functions (e.g., sin, cos, tanh, ln), Boolean operators (e.g., AND, OR, NOT), logical statements (e.g., IF, THEN), or any other user-defined functions. The comprehensive collection comprises variables (e.g., x1, x2, x3, etc.) or numerical values (e.g., 3, 5, 6, 9, etc.), or a synthesis of both. A GP tree is generated by the stochastic selection of functions and terminals, culminating in a total of 44 terminals. Fig. 3.17 depicts the hierarchical configuration of the

tree, with a central node and subordinate nodes that branch from each functional node to terminal nodes. The equation (3*x + 8/2) may be simplified for enhanced clarity. The variable x denotes the terminal nodes. This topic includes the mathematical function and the operations of addition (+), subtraction (-), multiplication (×), and division (/).

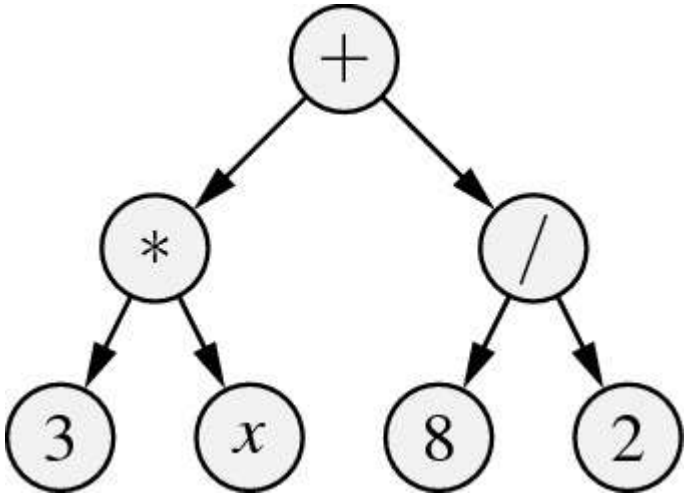

Fig. 3.17: A Typical GP Tree Encoding a Mathematical Equation: 3*x + 8/2 (Kruse et al., 2022)

A collection of GP trees is created based on the user-specified population size. The growth of these trees is arbitrary, with the user supplying several functions and terminals. The fitness criteria are defined by the objective function and are used to assess the relative quality of each individual within a population. Successive generations are created by selectively breeding individuals from the initial population based on their level of adaptation. Evolutionary techniques such as reproduction, crossover, and mutation are then applied to the functions and terminals of the selected GP trees. The new population replaces the existing one, and this process continues until termination criteria are met, which may involve achieving a specified fitness value or reaching the maximum number of generations. The result of genetic programming is determined by selecting the GP model with the highest fitness value across all generations. This document provides a concise overview of the evolutionary techniques employed in genetic programming (GP).

Space Search in Genetic Programming

The genetic programming starts by generating a population, which comprises a collective of individuals. Every individual function as a resolution to the provided issue. An individual is characterized by a set of elements referred to as Genes. Genes are linked together to create a sequence and generate chromosomes, which function as the solution to the problem. An extensively used technique for initialization involves the utilization of randomly generated binary strings.

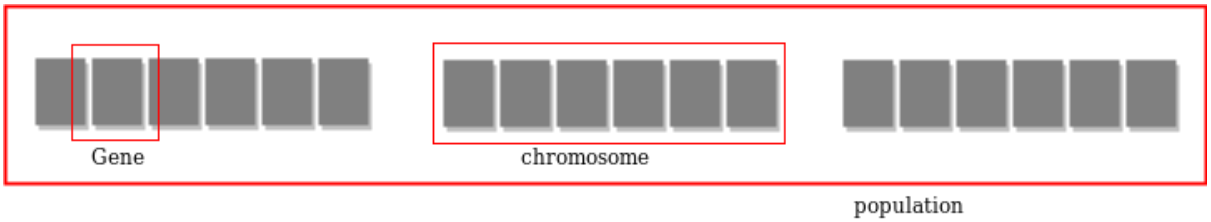

Fig. 3.18: Search Space in Genetic Programming (https://www.geeksforgeeks.org/genetic-algorithms/)

Fitness Assignment in Genetic Programming

A fitness function is implemented to evaluate an individual's degree of physical fitness. Competitiveness is the ability of a person to successfully compete with others. During each iteration, people are assessed according to their fitness function. The fitness function allocates a fitness score to each individual. This score further influences the probability of selection for reproduction. A higher fitness score increases the probability of selection for reproduction.

Selection in Genetic Programming

The selection phase entails the process of choosing people to produce children. Subsequently, the chosen people are paired together to enhance the process of reproduction. Subsequently, these people pass on their genetic material to the next generation.

Three types of selection methods are available, namely:

- Tournament selection

- Roulette wheel selection
- Rank-based selection

Tournament Selection

Throughout this procedure of selection, a certain quantity of GP trees engage in tournaments. The tournament size is determined by the number of GP trees that participate in the competition. The winner persists and obtains a larger number of reproductions, while the loser is prevented from advancing to the subsequent offspring.

Roulette Wheel Selection

Parent selection is based on their fitness levels, with higher-quality chromosomes having a greater likelihood of being chosen. This process is illustrated through the example of a Roulette wheel, where the chromosomes in the population are arranged. The size of each segment on the Roulette wheel is directly proportional to the fitness function value of the corresponding chromosome. In simple terms, chromosomes with higher fitness values occupy larger segments on the wheel, as depicted in Fig. 3.19. A marble is then spun on the wheel, and the chromosome where it lands is selected. Consequently, chromosomes with superior fitness values are more likely to be selected frequently.

The procedure may be delineated by the following phases.

Phase 1: Determine the total fitness of all chromosomes in the population; sum =S.

Phase 2: Generate a random number, denoted as r, from a given interval (0, S)

Phase 3: Iterate across the population and calculate the total fitness by summing the values from 0 to the sum of Si. Terminate and output the ith chromosome when the total Si exceeds r.

Phase 4: Perform steps 2 and 3 again

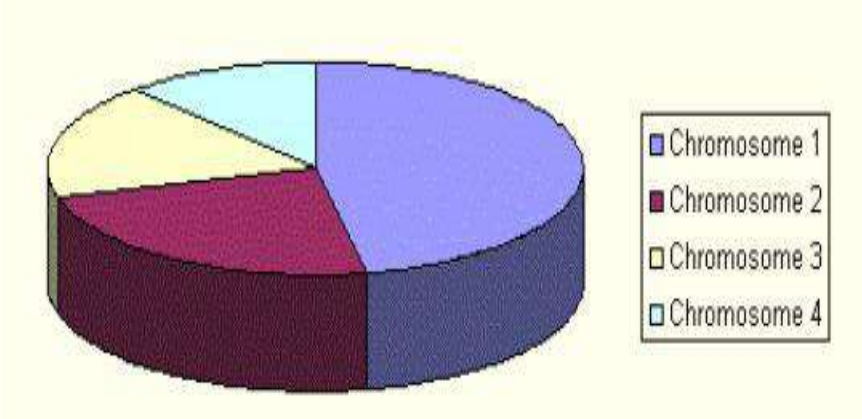

Fig. 3.19: Roulette Wheel Selection in Genetic Programming
(https://www.obitko.com/tutorials/genetic-algorithms/selection.php)

Rank-Based Selection

The traditional selection process faces challenges when there is a significant variation in fitness levels among chromosomes. For example, if a single chromosome possesses a fitness level exceeding half the total value of the roulette wheel, other chromosomes will have a reduced chance of selection. To address this, rank selection is employed, where the population is first sorted by fitness levels, and each chromosome is assigned a fitness value based on its rank. The chromosome with the lowest fitness is assigned a value of 1, the next lowest a value of 2, and so forth, with the fittest chromosome receiving a value equal to the total number of chromosomes in the population. This ensures that all chromosomes have an opportunity for selection. The probability of selecting a chromosome is determined by its rank in the sorted list rather than its actual fitness value. However, this method may lead to slower convergence due to the minimal difference between the best-performing chromosomes and the rest.

Reproduction in Genetic Programming

Following the selection process, the reproduction stage focuses on generating offspring. During this phase, the genetic algorithm employs two variation operators to modify the parent population. These two operators play a crucial role in the reproduction process.

Crossover

The crossover operation is a key component of the reproductive phase in the genetic algorithm. In this process, a random point is chosen within the genetic material. The crossover operator enables the exchange of genetic information between two parent chromosomes, resulting in the generation of a new individual representing the offspring.

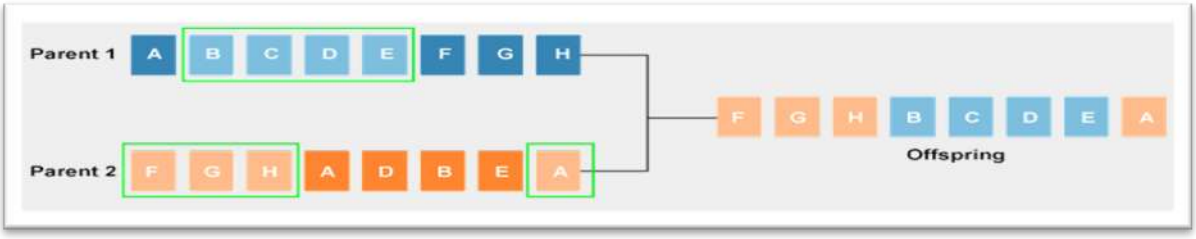

Fig. 3.20: A Typical Crossover Operation in Genetic Programming
(https://www.javatpoint.com/genetic-algorithm-in-machine-learning)

Mutation

The mutation operator introduces random genetic variations into the offspring to preserve diversity within the population. This process is achieved by altering specific segments within the chromosomes. Mutation helps prevent premature convergence and promotes the inclusion of a broad range of variations. Fig. 3.21 illustrates the mutation process.

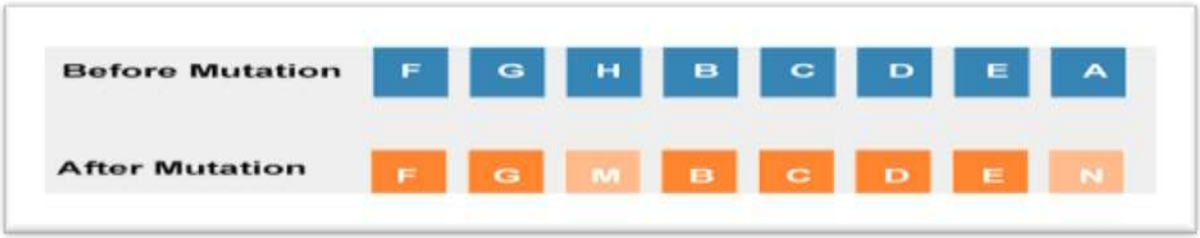

Fig. 3.21: The Mutation Process in Genetic Programming
(https://www.javatpoint.com/genetic-algorithm-in-machine-learning)

Termination in Genetic Programming

Following the reproduction phase, a termination criterion is applied to decide when the process should end. The algorithm terminates once it reaches a fitness value that meets the predefined threshold. The final selection is identified as the optimal solution among the population. The GP predictive algorithm incorporates several control parameters, including the function set, population size, number of generations, maximum gene count per individual (Gmax), maximum tree depth (dmax), tournament size, probability of crossover events, major crossover, minor crossover, mutation events, subtree mutation, replacement of input terminals with random terminals, Gaussian perturbation of randomly selected constants, reproduction, and ephemeral random constants.

These parameters are essential for determining the algorithm's outcomes. The selection of these control parameters significantly influences the model's generalization capabilities, as generated by GP. The parameters are selected through a trial-and-error method, tailored to the specific problem and guided by values previously recommended by Searson et al. (2010). The user has flexibility in choosing the function set, which may include arithmetic operators, mathematical functions, and other relevant operations based on their understanding of the physical system being analysed.

Population size determines the number of individuals within the population, while the number of generations refers to how frequently the algorithm iterates during the run. The complexity of the problem typically influences the ideal population size and the required number of generations. Various generations and populations are thoroughly tested to identify the most efficient model. As overfitting occurs, the fitness value for training data decreases, while the fitness value for testing data increases due to higher Gmax and dmax values. This overfitting results in reduced generalization capability for the previously generated model.

Therefore, when constructing the MGGP model, it is essential to achieve a balance between accuracy and complexity, particularly concerning Gmax and dmax. Research indicates that optimal values for Gmax and dmax exist, leading to the creation of highly efficient models (Searson et al., 2010). Using optimal parameter values often enhances the GP algorithm's

effectiveness, but exceeding these values can further improve the algorithm's performance when appropriately managed.

In the Genetic Programming (GP) process, a diverse range of potential models is generated randomly. Each model is subsequently trained and evaluated using the respective training and testing datasets. The fitness of each model is assessed by minimizing the root mean square error (RMSE) between the predicted and actual values of the output variable, Compressive Strength (C), through the objective function (f).

$$RMSE = \sqrt{\frac{\sum_{i=1}^{n}(LI - LI_{Pre})^2}{n}} \quad (3.1)$$

Let n denote the total number of instances within the fitness group. If the errors calculated using Eq. (3.1) for all models in the current population do not satisfy the termination criteria, the iterative process of generating a new population continues until the desired optimal model is obtained, as previously described.

3.5.2 Support Vector Machines (SVM)

The Support Vector Machine (SVM) technique is a versatile machine learning method used for both classification and regression tasks, where the goal is to predict continuous output variables from given inputs. SVM achieves this by mapping input data into a higher-dimensional feature space using kernel functions, enabling the identification of a regression line that minimizes error and maximizes the margin within defined tolerance levels (Drucker et al., 1999). One of the key advantages of SVM is its ability to handle complex, non-linear relationships between input and output variables. By employing kernels such as polynomial, radial basis function (RBF), and sigmoid, SVM can effectively model intricate variable interactions (Chalimourda et al., 2004).

SVM has been successfully applied across various industries, including banking, transportation, and healthcare. Selecting and optimizing the kernel function and its associated parameters is crucial for achieving optimal performance. To transform a linear classifier into a non-linear one, a non-linear function can be used to map the input space x into a higher-dimensional feature space F. Alternatively, a non-linear mapping function can be employed to achieve the desired transformation.

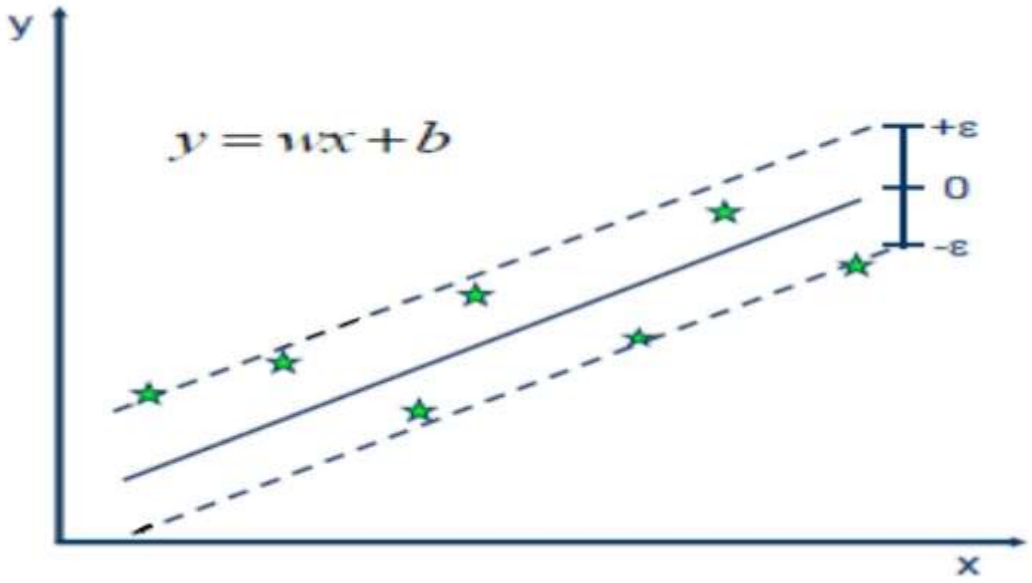

Fig. 3.22: Support vector machine (SVM) hyper plane (Reddy et al., 2024)

The separating function in space F may be defined as: (Reddy et al., 2024)

$$f(x) = w^T \varphi(x) + b \quad (3.2)$$

The function f(x) serves as the decision function in the feature space F. It calculates the output for a given input xx by performing the dot product of the weight vector W and the feature vector ϕ(x), followed by the addition of a bias term b. The decision function classifies new data points by determining their position relative to the hyperplane within the feature space.

The statistical techniques within the subspace are expressed through the algebraic function f(x, w).

$$w = \sum_{i=1}^{n} \alpha_i x_i \quad (3.3)$$

$$f(x, w) = \sum_{j=1}^{n} \alpha_i x_i \varphi_i(x) + b \quad (3.4)$$

$$f(x) = \sum_{i=1}^{n} \alpha_i x_i^T x + b \quad (3.5)$$

The weight vector w is represented as a linear combination of the support vectors xi, with the coefficients αi determined during the optimization process of solving the SVM problem. These coefficients signify the importance or contribution of each support vector in defining the orientation of the separating hyperplane. The function f(x, w) is expressed as a summation over all support vectors xi, where each support vector is mapped to a higher-dimensional space using the feature mapping function ϕi(x). The decision function is then computed by taking the dot product of each mapped support vector with its corresponding coefficient αi, adding a bias term b, and summing the results across all support vectors.

This statement is represented in the feature space F.

$$f(x) = \sum_{i=1}^{n} \alpha_i \varphi(x_i)^T \varphi(x) + b0 \leq \alpha_i \leq C \quad (3.6)$$

$$k(x, x') = \varphi(x)^T \varphi(x') \quad (3.7)$$

$$f(x) = \sum_{i=1}^{n} \alpha_i k(x, x_i) + b \quad (3.9)$$

3.5.3 ANN Model

The ANN is a noteworthy computational methodology that is currently experiencing rapid advancements in its development. An ANN is a system comprised of interconnected components referred to as neurons or nodes, which are organized in a layered structure for ease of manipulation. The diagram depicted in Fig. 3.23 illustrates the structural composition of an ANN that adheres to the back-propagation neural network (BPNN) model and features a feed forward design comprising three layers. The three layers are comprised of I input neurons, m hidden neurons and n output neurons. The input layer serves as the point of entry for the data into the network. The intermediate layer, commonly referred to as the hidden layer, acquires input data from the preceding layer, namely the input layer, which is primarily responsible for data processing. The subsequent layer, namely the output layer, receives the processed data from the network. The information derived from the output is transmitted to external receptors. ANNs are structured in layers that are linked to subsequent layers through interconnections established among them. The connections are commonly denoted as weights and weighted values, correspondingly. Increasing the weights of interconnections as a means

of constraining the behavior of designated cost functions within an ANN (Upreti et al., 2022).

In this investigation, an Artificial Neural Network (ANN) was employed to forecast the compressive strength of geopolymer concrete incorporating alccofine. The feed-forward network, implemented in Python, utilized a backpropagation training algorithm for effective prediction. The network must first undergo a training phase, during which the weights and biases of the neurons are fine-tuned to minimize the error and align with the desired outputs. The ANN training process relies on three fundamental components: inter-neuron weights to signify the relevance of input variables, a sigmoid activation function to regulate neuron outputs, and learning rules that iteratively adjust the weights for optimal performance. In the process of training, a non-linear function, typically a sigmoid function, is employed by Upreti et al., (2022):

$$F(a) = \frac{1}{1+e^{-a}} \tag{3.8}$$

Where a represents the sum of the weighted input values plus the bias. The resulting value is passed to the next layer of nodes for further processing. The feed-forward back-propagation neural network method consists of four key stages, outlined as follows:

Sum the weighted input:

$$Nod_z = \sum_{i=1}^{n}(W_{xz}k_x) + \epsilon_z \tag{3.9}$$

Where Nod_z represents the sum for the zth hidden node, n is the total number of input nodes, W_{xz} denotes the connection weight between the xth input and the zth hidden node, kz is the normalized input at the xth input node, and $\in_z$ is the bias value associated with the zth hidden node.

Transform the weighted input:

$$Out_z = \frac{1}{1+e^{-Nod_z}} \tag{3.10}$$

where Out_z = output from the zth hidden node.

Sum the hidden node output:

$$Nod_y = \sum_{j=1}^{m}(W_{zy} Out_y) + \in_y \quad (3.11)$$

Where Nod_y = sum of yth output node, m = total number of hidden nodes, W_{zy} = connection weights between the zth hidden node and the yth output node and $\in_y$ = bias value at the yth output node.

Transform the weighted sum:

$$Out_y = \frac{1}{1+e^{-Nod_y}} \quad (3.12)$$

Where Out_y = output at the yth output node.

The neural network's architecture was established by utilizing eleven neurons for the input layer, varying neurons for the hidden layers and one neuron for the output layer

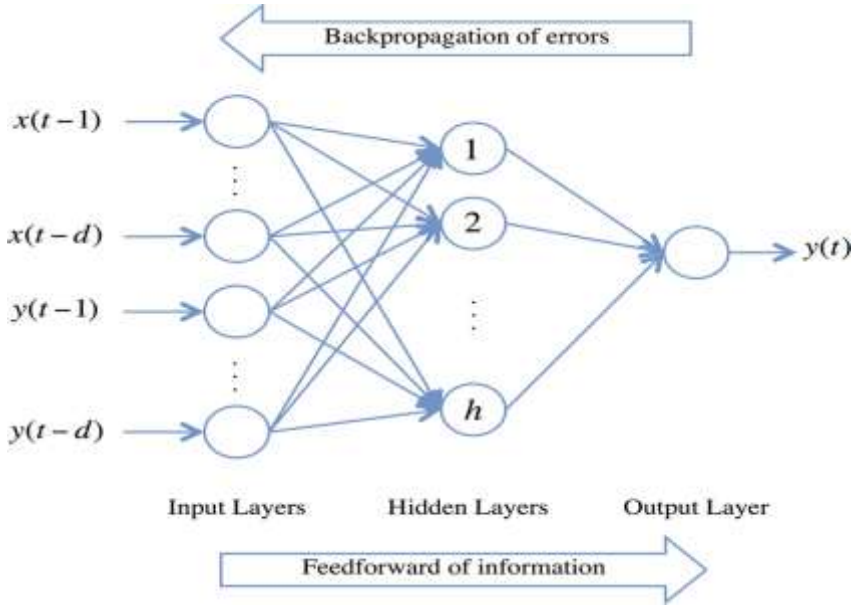

Fig. 3.23: Artificial Neural Networks (ANN) Architecture (https://www.analyticsvidhya.com/blog/2021/09/introduction-to-artificial-neural-networks/)

3.5.4 Bi-LSTM Structure Formation

The Bi-LSTM model consists of two different layers named as forward hidden layers and backward hidden layers (Rahman et al., 2021). Let h_i^f be the forward hidden layer, which receives input in incremental order i.e. $i = 1,2,3,4,\cdots I$, whereas h_i^b be the backward hidden layer, which receives input in decrement order i.e. $i = I,\cdots 3,2,1$. The combination of h_i^f and h_i^b produces outputy^i. The implementation of Bi-LSTM is represented in Eq. (3.13), to Eq. (3.15), where V is the weight parameter (V_{hy} points out the weight, which is linked the input to hidden layer), $a$indicates bias vector, $tan\,h$represent the hidden layer activation function,

$$h_i^f = tan\,h\,(V_{xh}^f x_i + V_{hh}^f h_{i-1}^f + a_h^f) \quad (3.13)$$

$$h_i^b = tan\,h\,(V_{xh}^b x_i + V_{hh}^b h_{i+1}^b + a_h^f) \quad (3.14)$$

$$y^i = V_{hy}^f h_i^f + V_{hy}^b h_i^b + a_y \quad (3.15)$$

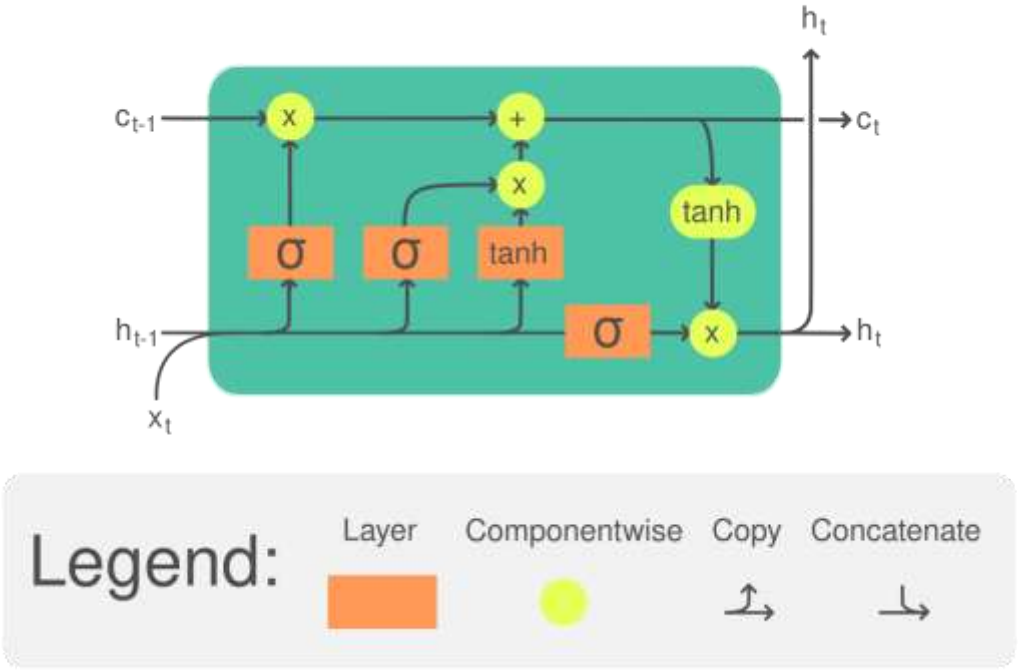

Fig. 3.24: The Architecture of Bi-LSTM Model

(https://en.wikipedia.org/wiki/Long_short-term_memory)

Conventionally, the sigmoid activation function is employed in Bi-LSTM, which has some drawbacks like gradient vanishing problem, challenging in weight updation. To tackle this issue, we utilize an improved tangent activation function using ICMIC map.

Hyperbolic Tangent Activation Function: Conventional

The hyperbolic activation function is also known as Tanh function, which is almost same as sigmoid activation function, but it is equal around the origin (Sharma et al., 2017). It receives the input value and generates output between -1 and 1. The expression of tan H activation function is indicated in Eq. (3.16), here σ is the sigmoid activation function. The gradient of hyperbolic tangent activation function is steeper, which is not limited to change in any direction and self-centered.

$$tanh(z) = 2\sigma(2z) - 1 \tag{3.16}$$

Improved Hyperbolic Tangent Activation Function Using ICMIC Map

Let the sigmoid function σ in the tanH activation function is computed using ICMIC map. The ICMIC map is one of the 1-D chaotic map (Rani et al., 2023). The expression of ICMIC map is shown in Eq. (3.17), where the selection of value $c$is achieved based on Lyapunov exponent, the ICMIC map exhibits chaotic behavior.

$$ICMICmap = sin(\frac{c}{k_n}), c \in (0, \infty), k_n \in (-1,1) \tag{3.17}$$

3.5.5 Self-Improved Jelly Search Optimization (SIJSO):

The SIJSO approach is a met heuristic optimization algorithm supports to find the optimal hyper parameterized the weight parameter V of Bi-LSTM. This algorithm developed by the behavior of jellyfish. The food searching procedure of jelly fish involves the following process (Alam et al., 2021).

- The movement of jelly fish within the swarm.
- For the creation of jelly fish proliferation, which means the sudden upgrading of jelly fish population is done by following the ocean currents.

- According to the time control mechanism, passive and active movements within the jelly fish swarms that are switched to each other.
- Jelly fish are move towards the area with higher concentration of available food.
- Measuring the amount of food is influenced by the specific position and its respective objective function.

Primarily, the SIJSO approach includes random initialization for distributing solutions (weight) within the searching process. The fitness value is evaluated as per Eq. (3.20). The motion of jelly fish is either pursuing ocean current or towards the improvement within the swarm based on time control mechanism.

Ocean Current: Jelly fish are drawn to ocean currents because these oceans current contains abundant nutrients. The ocean current is depending on the average vectors of individual jelly fish present in the ocean to the jelly fish, which possess current optimal position. The ocean current vector is determined using Eq. (3.18) and Eq. (3.19), where j^* indicates jelly fish occurs at a present best position in the entire population, Mindicates total number of jelly fish, η'points out the average position of jelly fish swarm and a^c represent attraction coefficient.

$$\bar{O}_c = j^* - a^c \frac{\sum j_q}{M} \tag{3.18}$$

$$\bar{O}_c = j^* - a^c \eta' \tag{3.19}$$

The mathematical representation of ocean current is shown in Eq. (3.20), the computation of updated location of each jelly fish in ocean current is indicated in Eq. (3.21), here $j_q(k)$ indicates location of q^{th} jelly fish at instance k. The instance of time k equals to the algorithm iteration.

$$\bar{O}_c = j^* - \gamma \times ran(0,1) \times \eta' \tag{3.20}$$

$$j_q(k+1) = j_q(k) + ran(0,1) \times j^* - \gamma \times ran(0,1) \times \eta' \tag{3.21}$$

Jelly Fish Swarm: The movement of jelly fish is classified into active and passive. During the creation of swarm, jelly fish pursues active motion, which moves around their self-position and updating the location of every jelly fish. The mathematical representation of

updated position of each jelly fish is indicated in Eq. (3.22), where χ represent movement co-efficient appropriate to the distance of motion across the position of jelly fish, $U^b$and L^b indicated upper and lower bounds in the search zone.

$$j_q(k+1) = j_q(k) + \chi \times ran(0,1) \times (U^b - L^b) \tag{3.22}$$

Proposed Position Update Formation: According to the proposed SIJSO, the position update formation is evaluated by combining the updated location of each jelly fish in ocean current and the updated position of each jelly fish within the swarm. The computation of updated position in self-improved JSO is expressed in Eq. (3.25), Eq. (3.26), Eq. (3.25)

$$j_q(k+1) + j_q(k+1) = j_q(k) + ran(0,1) \times j^* - \gamma \times ran(0,1) \times \eta' + j_q(k) + \chi \times ran(0,1) \times (U^b - L^b) \tag{3.23}$$

$$2(j_q(k+1)) = 2(j_q(k) \times ran(0,1)) + ran(0,1) \times j^* - \gamma \times \eta' + \chi \times (U^b - L^b) \tag{3.24}$$

$$Imp = \frac{2(j_q(k) \times ran(0,1)) + ran(0,1) \times j^* - \gamma \times \eta' + \chi \times (U^b - L^b)}{2(j_q(k+1))} \tag{3.25}$$

In Eq. (3.23), the computation of random value $ran(0,1)$ is done by using tent map. The tent map is group of functions. Its iteration forms a discrete dynamical system. The evaluation of tent map is expressed in Eq. (3.26), where x^n points out data, ω indicates real valued function. When $\omega = 2$, the system mapping interval $[0,1]$ on itself. The density of periodic points contributes to the chaotic nature of the map.

$$tentmap = \omega(1 - x^n) \tag{3.26}$$

3.6 Conclusion

The study conducted in this chapter established a comprehensive methodology for evaluating the properties of geopolymer concrete using various material tests and advanced predictive modeling techniques. Non-destructive methods, like the rebound hammer and ultrasonic pulse velocity tests, proved effective in estimating the compressive strength without damaging samples. The use of high-reactivity materials like Class F fly ash and Alccofine, combined with optimized alkaline activator solutions, significantly enhanced the mechanical properties of the concrete. Machine learning models, including genetic programming and support vector machines, ANN, Bi-LSTM and Self-Improved Jelly Search Optimization were developed to predict concrete behavior with high accuracy. The integration of both empirical and computational methods ensures reliable performance assessments, providing a robust framework for future research and applications in concrete technology.

Chapter 4

Results and Discussions

4.1 Introduction

This chapter presents a comprehensive analysis of the experimental investigations carried out to evaluate the mechanical performance, durability, and microstructural behaviour of geopolymer concrete (GPC) under various influencing parameters. A series of experiments were designed and executed to assess the impact of critical factors such as liquid-to-binder (L/B) ratio, superplasticizer dosage, sodium hydroxide (NaOH) molarity, and the sodium silicate to sodium hydroxide (SS/SH) ratio. Each of these parameters was varied systematically to study their influence on workability, density, compressive strength, and other mechanical properties. The role of curing temperature was also explored, ranging from 60°C to 120°C, to understand its effect on the geopolymerization process and subsequent strength development. Furthermore, the inclusion of Alccofine, an ultra-fine pozzolanic material, was investigated as a partial replacement for fly ash in proportions ranging from 0% to 25%. Its influence on strength development, density, and durability was thoroughly evaluated.

In addition to evaluating the basic mechanical properties, a series of advanced experiments was conducted on the optimized geopolymer concrete (GPC) mix incorporating 15% Alccofine to assess its durability under aggressive environmental conditions, including seawater exposure, sulfate and acid attacks and cyclic wetting-drying regimes. These tests provided critical insights into the long-term durability performance of the mix. Furthermore, microstructural characterization techniques such as Fourier Transform Infrared Spectroscopy (FTIR), Scanning Electron Microscopy (SEM), and Energy Dispersive X-ray Spectroscopy (EDX) were employed to analyze the internal morphology and elemental composition of the hardened matrix. Complementary mechanical assessments, including splitting tensile strength, flexural strength and rebound hammer tests, were also performed to validate and support the observed results. The experimental findings offer a comprehensive understanding of the synergistic effects of key mix parameters on both fresh and hardened properties of

GPC, serving as a robust foundation for optimizing geopolymer concrete formulations aimed at improved strength, durability, and sustainability.

4.2 Effect of Liquid to Binder Ratio:

The liquid-to-binder (L/B) ratio is a critical parameter in geopolymer concrete, governing the interaction between the liquid activator and the binder, which directly influences properties such as workability, compressive strength, density, and durability. Optimizing the L/B ratio is essential to achieving the desired balance between workability and mechanical properties, ensuring the material's long-term mechanical stability and suitability for various applications.

4.2.1 Workability

The liquid-to-binder (L/B) ratio is a critical factor influencing the properties of geopolymer concrete, particularly its workability, strength, and durability. Increasing the L/B ratio enhances workability, as shown by the Fig.4.1, rise in slump values from 15 mm at an L/B ratio of 0.35 to 150 mm at 0.65, due to the greater availability of liquid reducing the viscosity of the geopolymer paste and facilitating easier handling and placement. However, while higher L/B ratios improve workability, they often lead to reduced compressive strength and durability as the increased porosity weakens the microstructure of the geopolymer matrix. Conversely, lower L/B ratios, such as 0.35 or 0.40, result in reduced workability due to limited water availability, making the mix challenging to compact, which can also hinder the geopolymerization process. The optimal L/B ratio of 0.55 and a slump of 89 mm, strikes a practical balance between workability. Striking this balance is crucial, as an inappropriate L/B ratio can compromise either the workability or the strength of the material.

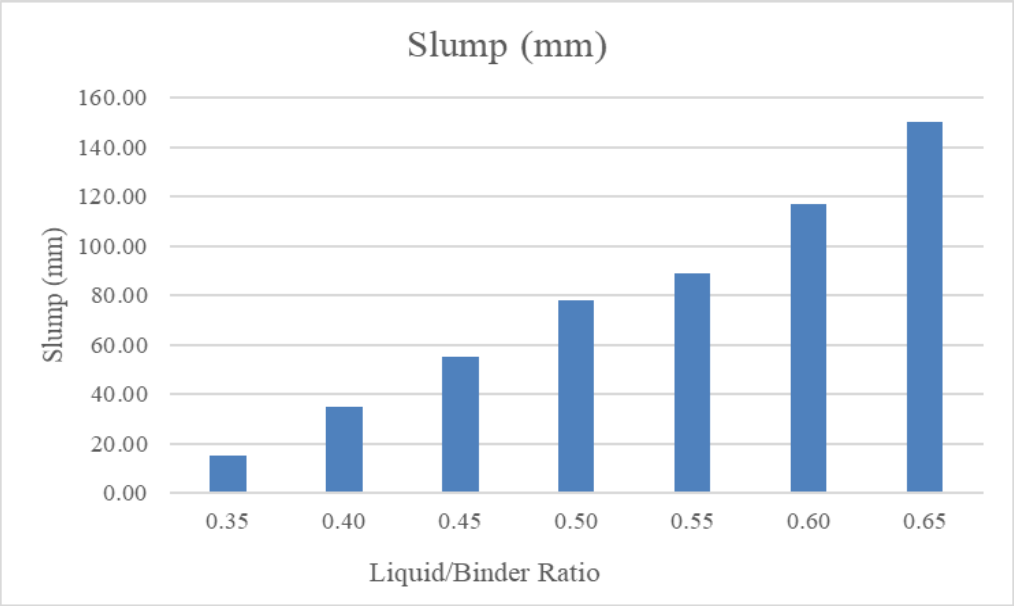

Fig. 4.1: Workability of Geopolymer Concrete with Varying Liquid/Binder Ratio

4.2.2 Density

The liquid-to-binder (L/B) ratio significantly influences the workability and density of geopolymer concrete, with curing methods playing a critical role. At lower L/B ratios (e.g., 0.35 or 0.40), density decreases (2400 kg/m³ for ambient curing and 2421 kg/m³ for oven curing) due to insufficient liquid, resulting in incomplete geopolymerization, poor mixing, and higher porosity. Optimal density and workability are achieved at an L/B ratio of 0.50 (2465 kg/m³ for ambient curing and 2480 kg/m³ for oven curing), while higher ratios (e.g., 0.65) reduce density (2412 kg/m³ for ambient curing and 2423 kg/m³ for oven curing) due to excess liquid causing porosity. Oven curing enhances density by accelerating geopolymerization and improving the bond between components. Balancing the L/B ratio and employing effective curing methods are crucial for achieving the desired properties.

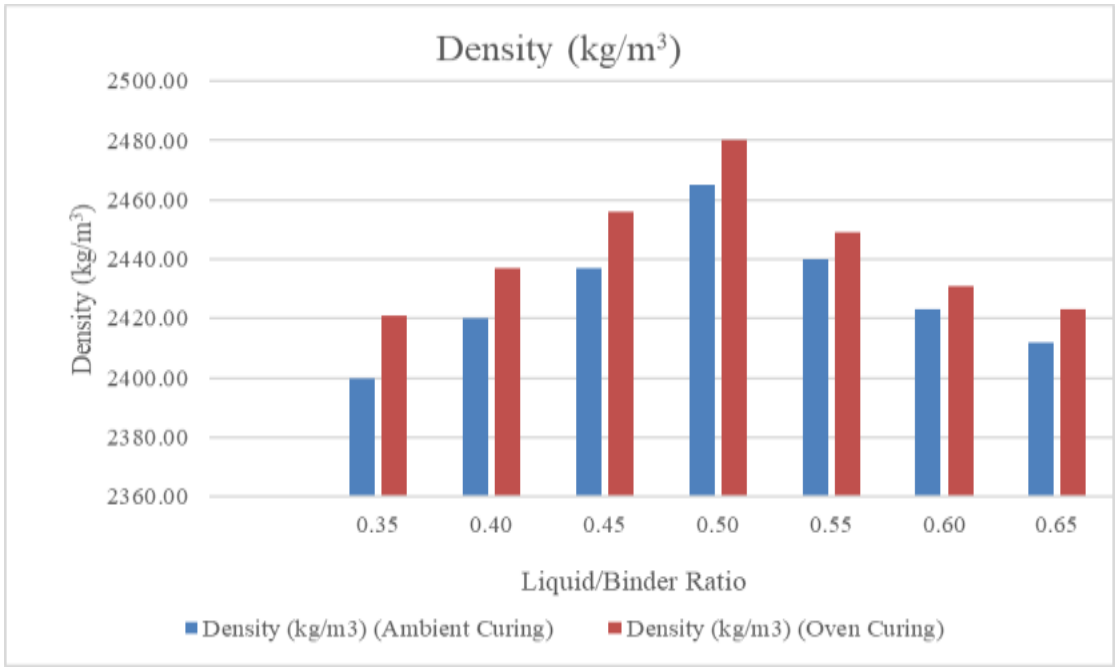

Fig. 4.2: Density of Geopolymer Concrete with Varying Liquid/Binder Ratio

4.2.3 Compressive Strength

The compressive strength of geopolymer concrete (GPC) was evaluated using cube specimens in a Compression Testing Machine (CTM) at 7, 14, 28, and 56 days. As illustrated in Fig. 4.3, the maximum compressive strength under ambient curing was recorded as 30.07 MPa at a liquid-to-binder (L/B) ratio of 0.55, while oven curing yielded 32.87 MPa at the same ratio. Beyond this optimal L/B ratio, the strength decreased due to higher porosity resulting from excess liquid. Fig.4.4 highlights that oven curing consistently produces higher compressive strength than ambient curing, attributed to accelerated geopolymerization at higher temperatures. While higher L/B ratios increase porosity and micro-cracks, reducing strength, overly low L/B ratios can hinder workability and compaction, also affecting strength. Maintaining a balanced L/B ratio around 0.55 is essential for optimal workability and mechanical performance of GPC.

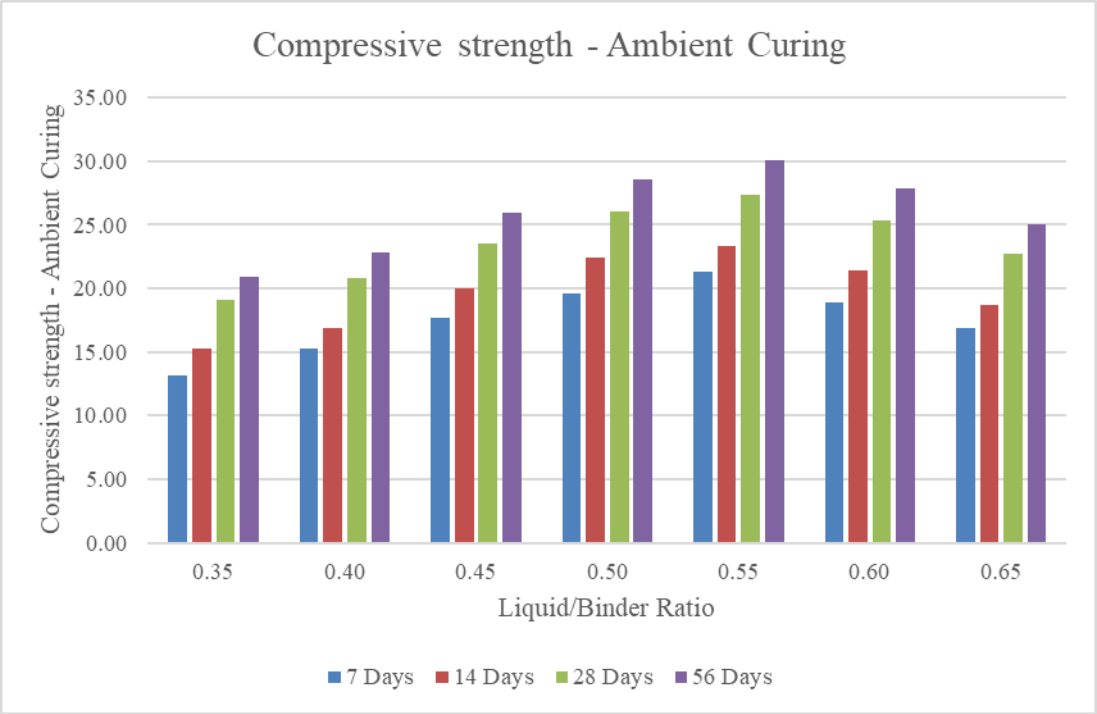

Fig. 4.3: Compressive Strength of Ambient Cured Geopolymer Concrete with Varying

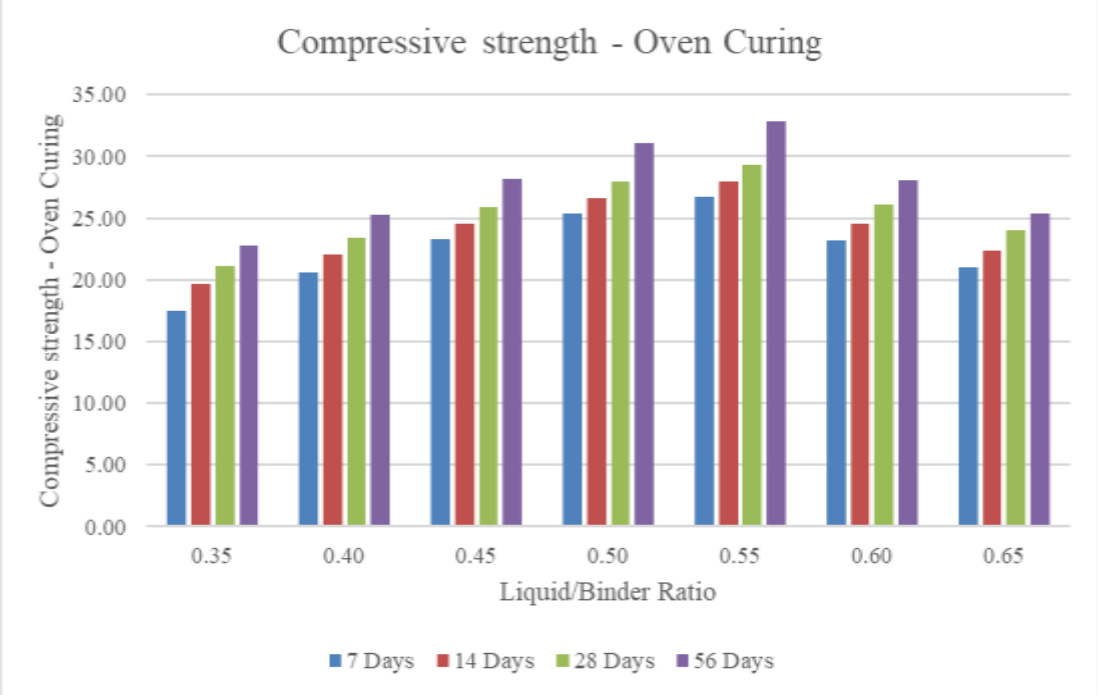

liquid/binder ratio

Fig. 4.4: Compressive Strength of Oven-Cured Geopolymer Concrete with Varying Liquid/Binder Ratio

4.3 Effect of Superplasticizer Dosage Percentage

The dosage of superplasticizer in geopolymer concrete plays a significant role in enhancing its workability, as reflected by variations in slump values. The recommended dosage typically ranges between 0.5% and 2% of the binder content, ensuring optimal flowability and ease of placement without compromising the mix's mechanical stability. In addition to workability, the compressive strength is critical parameters that influence the overall properties of geopolymer concrete, particularly its strength, density, and durability. These factors collectively determine the concrete's ability to perform under various loading and environmental conditions, making their optimization essential for achieving the desired balance between mechanical performance and durability.

4.3.1 Workability

The dosage of superplasticizer in geopolymer concrete plays a critical role in determining workability, as reflected in changes to slump values. Recommended dosages range between 0.5% and 2% of the binder content, with increasing dosage improving flowability by reducing water demand and enhancing particle mobility within the concrete matrix. As shown in Table 4.1 and Fig. 4.5, a 1.5% dosage with an L/B ratio of 0.45 resulted in a slump value of 90 mm, indicating sufficient workability for typical structural applications. Higher dosages, such as 2% with an L/B ratio of 0.65, increased the slump value to 210 mm, offering exceptional workability but introducing risks of segregation and bleeding. Conversely, lower dosages, like 0.5% with an L/B ratio of 0.40, yielded a slump value of only 42 mm, creating a stiff and less workable mix unsuitable for practical applications. These findings underscore the importance of optimizing superplasticizer dosage to strike a balance between fluidity and stability, ensuring adequate workability while maintaining the integrity and quality of the concrete.

Table 4.1: Slump Values of Geopolymer Concrete with Varying Superplasticizer Dosage

Super plasticiser Dosage	Liquid/Binder Ratio	Slump (mm)
0.5	0.4	42.00
	0.45	67.00
	0.50	88.00
	0.55	110.00
	0.60	127.00
	0.65	164.00
1	0.40	52.00
	0.45	75.00
	0.50	97.00
	0.55	110.00
	0.60	135.00
	0.65	175.00
1.5	0.40	70.00
	0.45	90.00
	0.50	107.00
	0.55	135.00
	0.60	148.00
	0.65	195.00
2	0.40	89.00
	0.45	110.00
	0.50	130.00
	0.55	156.00
	0.60	175.00
	0.65	210.00

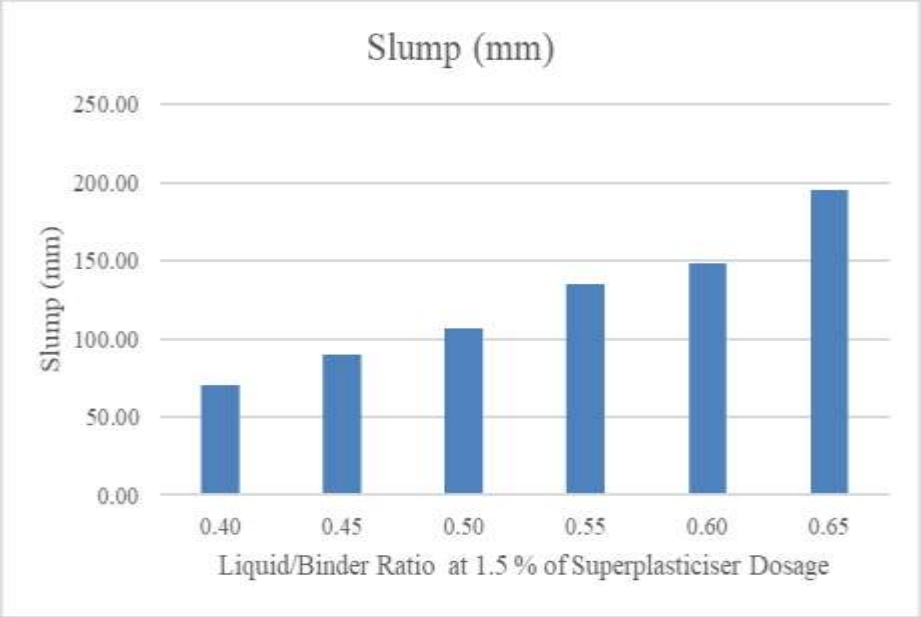

Fig. 4.5: Slump Values of Geopolymer Concrete with 1.5 % Superplasticizer Dosage

4.3.2 Density

The dosage of superplasticizer significantly affects the density of geopolymer concrete by enhancing flowability, reducing water content, and improving particle packing, which minimizes voids. Appropriate dosages facilitate proper compaction, reducing air entrapment and increasing density. However, excessive dosages can cause segregation or bleeding, leading to density variations and reduced uniformity. As shown in Table 4.2 and Fig. 4.6, density consistently increased with superplasticizer dosages up to 1.5%, achieving a maximum of 2538 kg/m³ (oven curing) and 2524 kg/m³ (ambient curing) at an L/B ratio of 0.45. Lower superplasticizer dosages, such as 0.5%, resulted in reduced density, with 2497 kg/m³ (oven curing) and 2486 kg/m³ (ambient curing) at an L/B ratio of 0.4 due to low availability of water. At 2% of superplasticizer dosage, density began to decline due to segregation and bleeding. These findings emphasize the importance of optimizing superplasticizer dosage to achieve a dense, uniform, and cohesive geopolymer concrete mix.

Table 4.2: Density of Geopolymer Concrete with Varying Superplasticizer Dosage

Superplasticizer Dosage	Liquid/Binder Ratio	Density(kg/m^3) (Ambient Curing)	Density (kg/m^3) (Oven Curing)
0.5	0.4	2486	2497
	0.45	2497	2505
	0.50	2500	2515
	0.55	2523	2528
	0.60	2520	2529
	0.65	2503	2514
1	0.40	2496	2502
	0.45	2506	2514
	0.50	2510	2521
	0.55	2515	2524
	0.60	2513	2520
	0.65	2510	2518
1.5	0.40	2513	2517
	0.45	2524	2538
	0.50	2518	2524
	0.55	2515	2520
	0.60	2513	2518
	0.65	2508	2513
2	0.40	2522	2534
	0.45	2515	2524
	0.50	2507	2516
	0.55	2500	2506
	0.60	2496	2501
	0.65	2487	2493

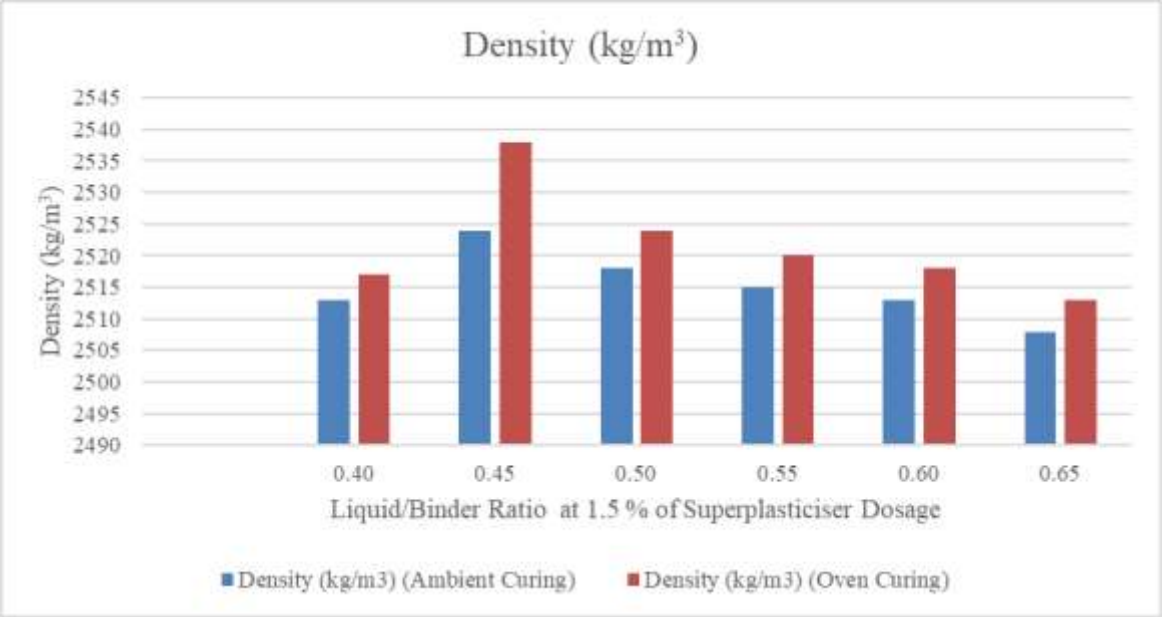

Fig. 4.6: Density of Geopolymer Concrete with 1.5 % Superplasticizer Dosage

4.3.3 Compressive Strength

The compressive strength of geopolymer concrete (GPC) is evaluated by testing cube samples using a Compression Testing Machine (CTM) at 7, 14, 28 and 56 days after casting. As shown in Fig. 4.7 (ambient-cured samples) and Fig. 4.8 (oven-cured samples), oven-cured samples consistently exhibit higher compressive strength than ambient-cured samples due to the accelerated geopolymerization process under heat. The dosage of superplasticizer plays a critical role in compressive strength by enhancing workability, improving particle dispersion and reducing water content, which leads to a denser and more compact concrete matrix, thus improving strength. However, excessive superplasticizer can cause segregation or bleeding, reducing the homogeneity and strength. As indicated in Fig. 4.7, for ambient-cured GPC, the maximum compressive strength of 35.99 MPa was achieved with a 1.5% superplasticizer dosage and an L/B ratio of 0.45 after 56 days. Similarly, Fig. 4.8 shows that oven-cured samples reached a maximum compressive strength of 40.99 MPa under the same conditions.

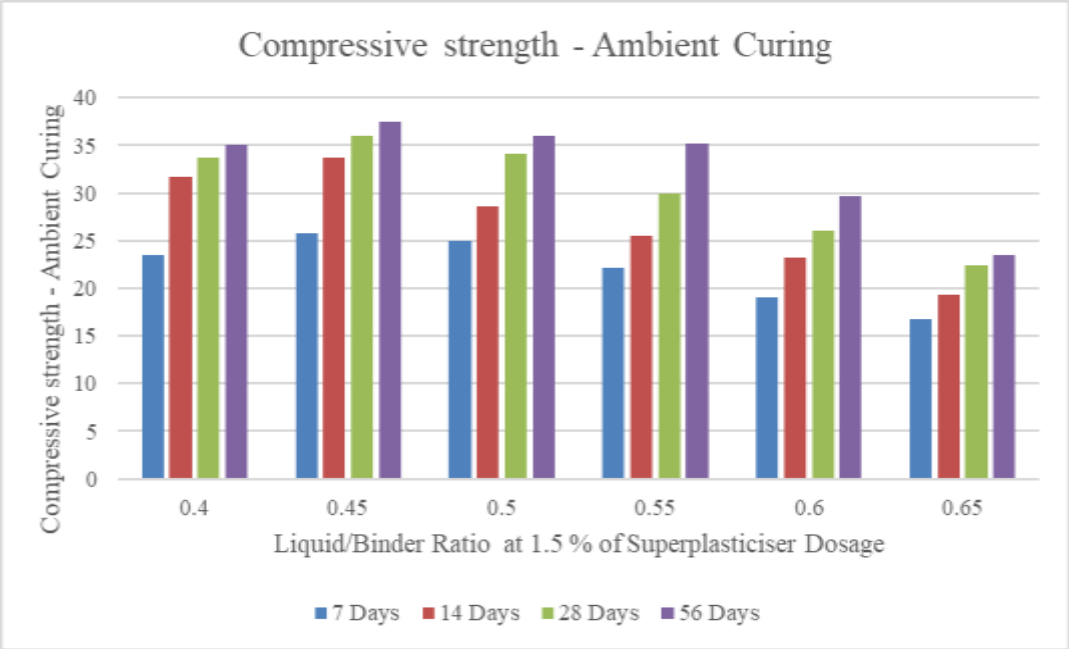

Fig. 4.7: Compressive Strength of Ambient-Cured Geopolymer Concrete At 1.5 % of Superplasticizer

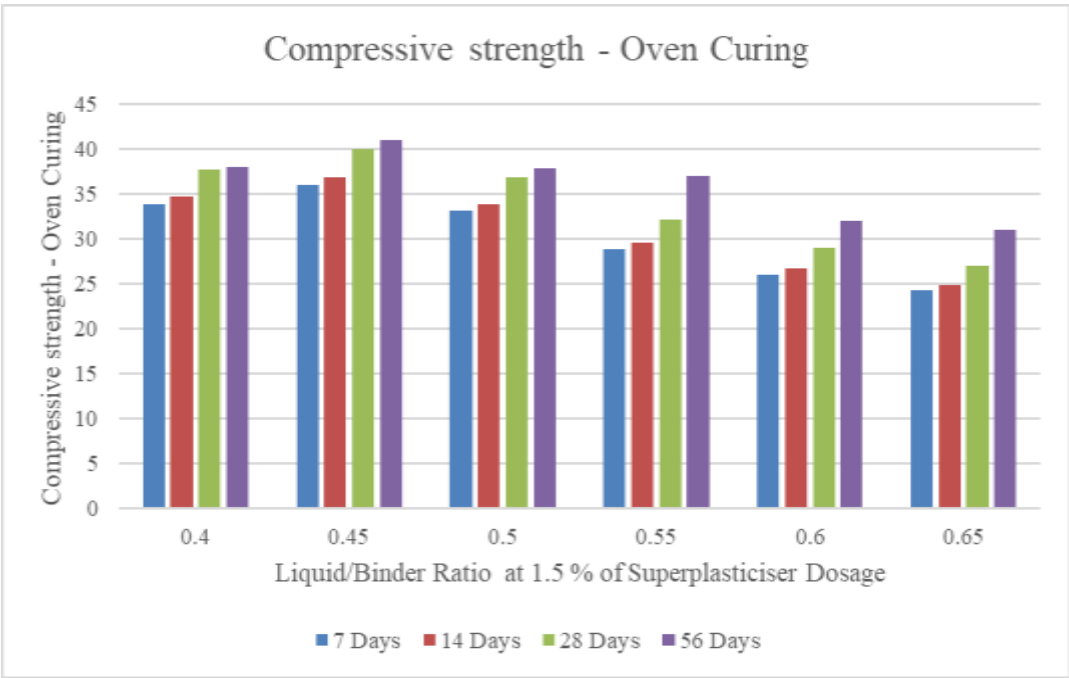

Fig. 4.8: Compressive strength of Oven-Cured Geopolymer Concrete At 1.5 % of Superplasticizer

4.4 Effect of Molarity of Sodium Hydroxide

Sodium hydroxide (NaOH) serves as an activator for binders like fly ash and GGBFS in geopolymer concrete (GPC) mix designs. The molar concentration of NaOH plays a critical role in influencing the mix design and the properties of GPC. Variations in NaOH molarity, ranging from 8M to 14M, directly impact key characteristics such as workability, strength, and durability. Specimens prepared with different molarities were tested using destructive strength tests to evaluate their performance. These tests revealed how the molar concentration of NaOH affects critical properties like compressive strength and density. Optimizing NaOH concentration is essential to achieving a balanced mix design that meets the desired performance criteria for geopolymer concrete.

4.4.1 Workability

In geopolymer concrete (GPC) mix designs, the molarity of sodium hydroxide (NaOH) plays a crucial role in determining both workability and compressive strength. As the molarity of NaOH increases from 8M to 14M, the slump value decreases significantly, as shown in Fig. 4.9, where the slump value drops from 193 mm at 8M to 60 mm at 14M. Higher NaOH molarity improves compressive strength, making it suitable for structural applications, while lower molarities, such as 8M, enhance workability but result in reduced strength. Thus, balancing NaOH molarity is essential for optimizing both workability and strength based on project-specific requirements.

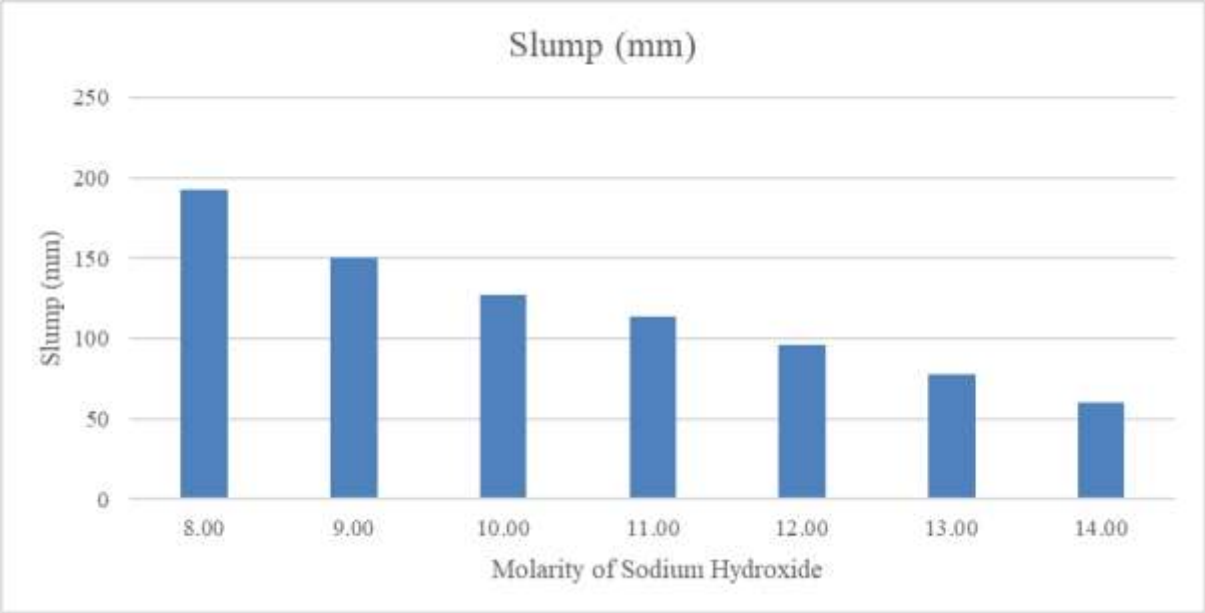

Fig. 4.9: Slump Values of Geopolymer Concrete with Varying NaOH Molarity

4.4.2 Density

The molarity of sodium hydroxide (NaOH) in geopolymer concrete (GPC) significantly influences its density. Higher molarity NaOH solutions, such as 12M, result in a denser microstructure. As shown in Fig. 4.10, the maximum density was achieved at 12M, with ambient-cured and oven-cured specimens recording densities of 2537 kg/m³ and 2545 kg/m³, respectively. Beyond this point, densities began to decline, with 14M ambient and oven-cured specimens having densities of 2447 kg/m³ and 2462 kg/m³, respectively. Lower molarity levels, such as 8M, yielded ambient- and oven-cured densities of 2410 kg/m³ and 2432 kg/m³, respectively. These findings highlight the importance of optimizing NaOH molarity to achieve balance in density and mechanical strength.

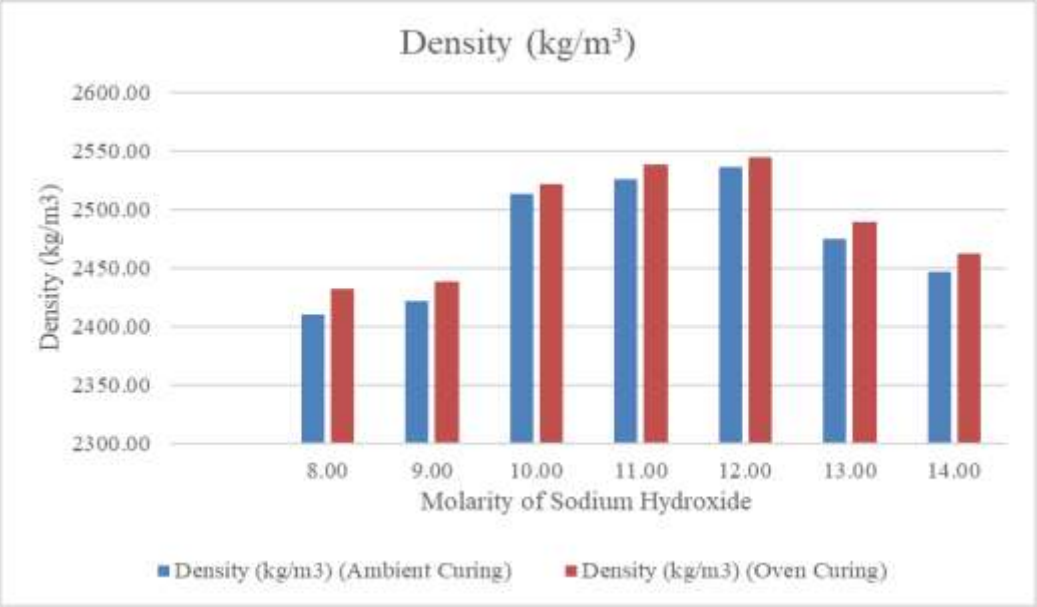

Fig. 4.10: Density of Geopolymer Concrete with Varying NaOH Molarity

4.4.3 Compressive Strength

The molarity of sodium hydroxide (NaOH) in geopolymer concrete (GPC) significantly affects its compressive strength. As the molarity of NaOH increases up to 10M, compressive strength improves due to enhanced dissolution of aluminosilicates, resulting in a denser and more robust geopolymer matrix. As shown in Fig. 4.11 and Fig. 4.12, the maximum compressive strength for ambient-cured specimens reached 38.46 MPa at 10M after 56 days, while oven-cured samples achieved peak strength of 41.16 MPa at the same molarity. Beyond 10M, compressive strength declines, with ambient-cured samples decreasing to 14.77 MPa and oven-cured samples dropping to 20.86 MPa at 14M. These findings highlight the importance of optimizing NaOH molarity to achieve maximum compressive strength while minimizing micro structural defects caused by excess alkali concentration.

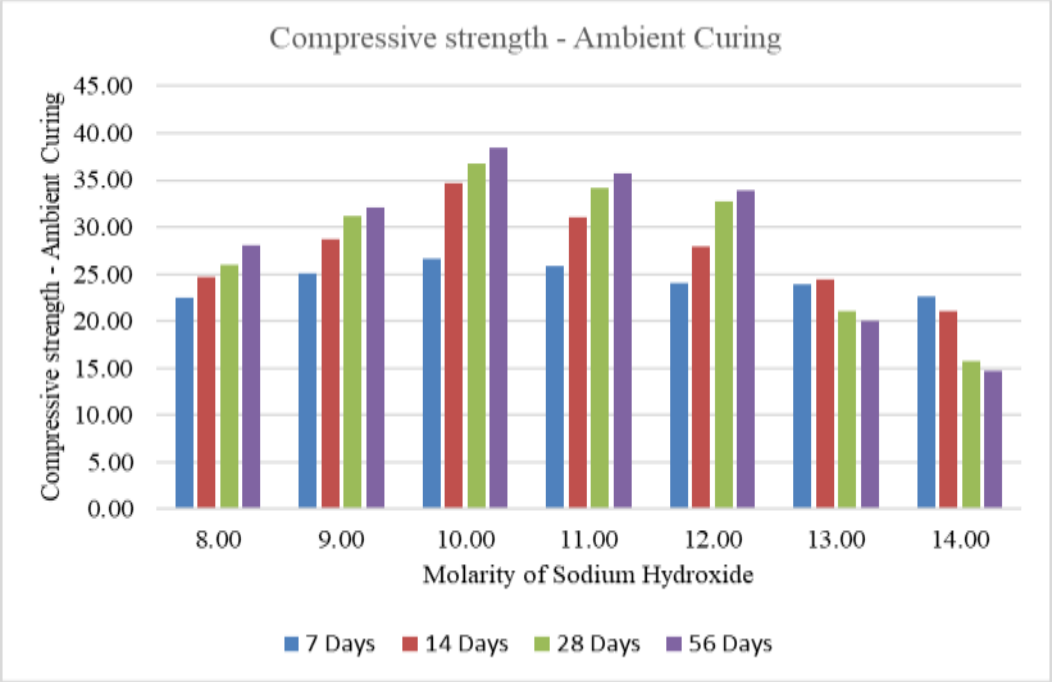

Fig. 4.11: Compressive Strength Ambient Cured Geopolymer Concrete with Varying Percentage of NaOH Molarity

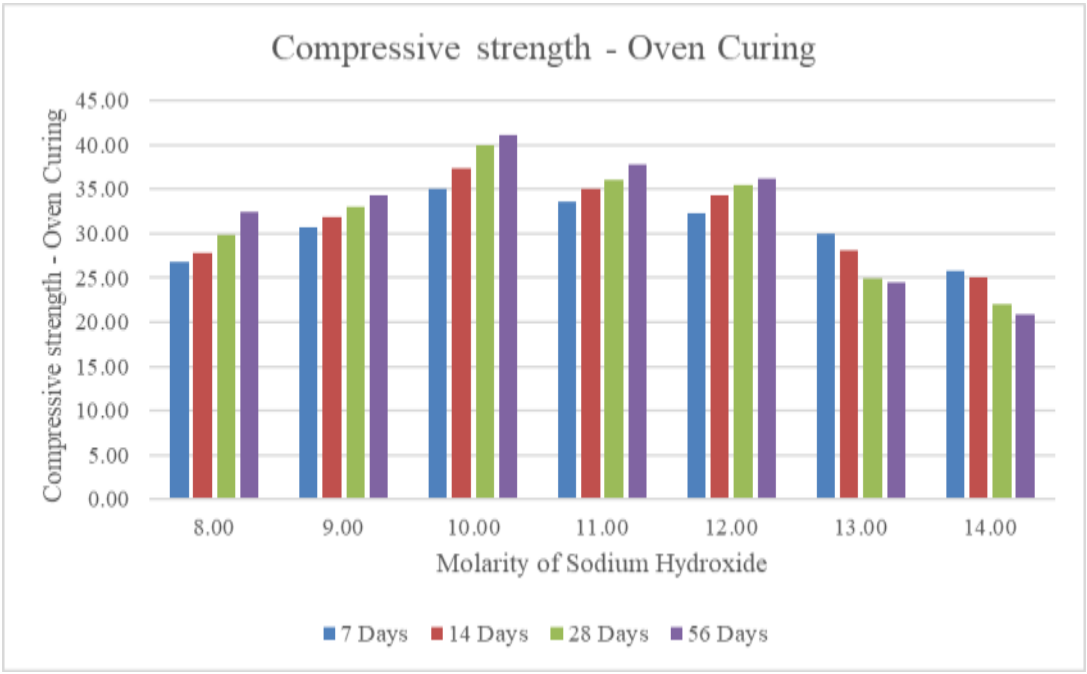

Fig. 4.12: Compressive Strength Oven Cured Geopolymer Concrete with Varying Percentage of NaOH Molarity

4.5 Effect of Sodium Silicate to Sodium Hydroxide Ratio (SS/SH)

The sodium silicate to sodium hydroxide (SS/SH) ratio is a critical factor influencing the workability, density, compressive strength, and durability of geopolymer concrete. A higher SS/SH ratio increases the liquid content, enhancing flowability and resulting in higher slump values, which improve workability and compaction. However, excessively high ratios may lead to segregation and bleeding, adversely affecting mix quality. This ratio also impacts density by ensuring proper consolidation and uniformity, while an optimal balance strengthens the activation of aluminosilicate materials, contributing to higher compressive strength and durability. Careful adjustment of the SS/SH ratio is essential for achieving the desired performance of geopolymer concrete.

4.5.1 Workability

The Sodium Silicate to Sodium Hydroxide (SS/SH) ratio significantly affects the workability of geopolymer concrete (GPC). As the SS/SH ratio increases, slump values decrease, indicating reduced workability due to higher viscosity in the activator solution. As shown in Fig. 4.13, the highest slump value of 143 mm was observed at an SS/SH ratio of 0.50, indicating superior workability. However, as the ratio increased to 2.00, the slump value dropped to 91 mm and at higher ratios of 2.50 and 3.00, the slump values further decreased to 79 mm and 67 mm, respectively. These results emphasize the importance of selecting an optimal SS/SH ratio to balance workability and mechanical performance, ensuring proper compaction and superior long-term durability in structural applications.

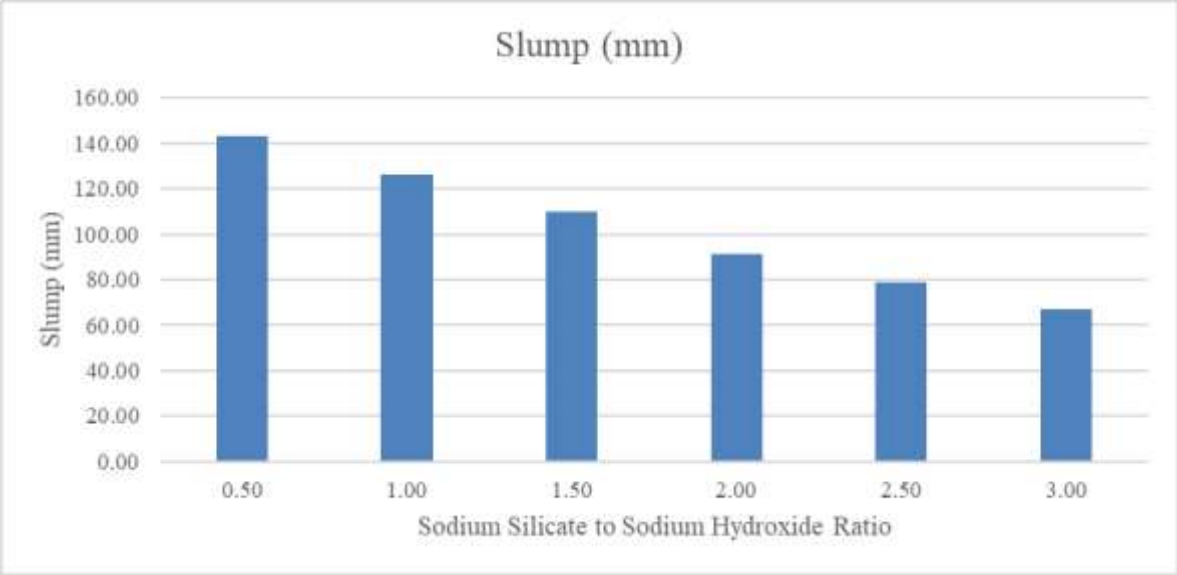

Fig. 4.13: Workability of Geopolymer Concrete with Varying Sodium Silicate to Sodium Hydroxide (SS/SH) Ratio

4.5.2 Density

The sodium silicate to sodium hydroxide (SS/SH) ratio significantly influences the density of geopolymer concrete (GPC) by affecting its polymerization and compaction properties. A higher SS/SH ratio enhances geopolymerization, resulting in a denser microstructure with improved binding and reduced porosity. As shown in Fig. 4.14, the maximum densities were recorded at an SS/SH ratio of 2.00, with ambient-cured specimens reaching 2510 kg/m³ and oven-cured specimens achieving 2520 kg/m³. However, further increases in the ratio led to a slight reduction in density, with ambient-cured and oven-cured densities dropping to 2443 kg/m³ and 2469 kg/m³, respectively, at a ratio of 2.50. These findings highlight the importance of selecting an optimal SS/SH ratio to achieve maximum density while maintaining proper workability and compaction, ensuring the suitability of GPC for structural applications requiring high-density and durable materials applications.

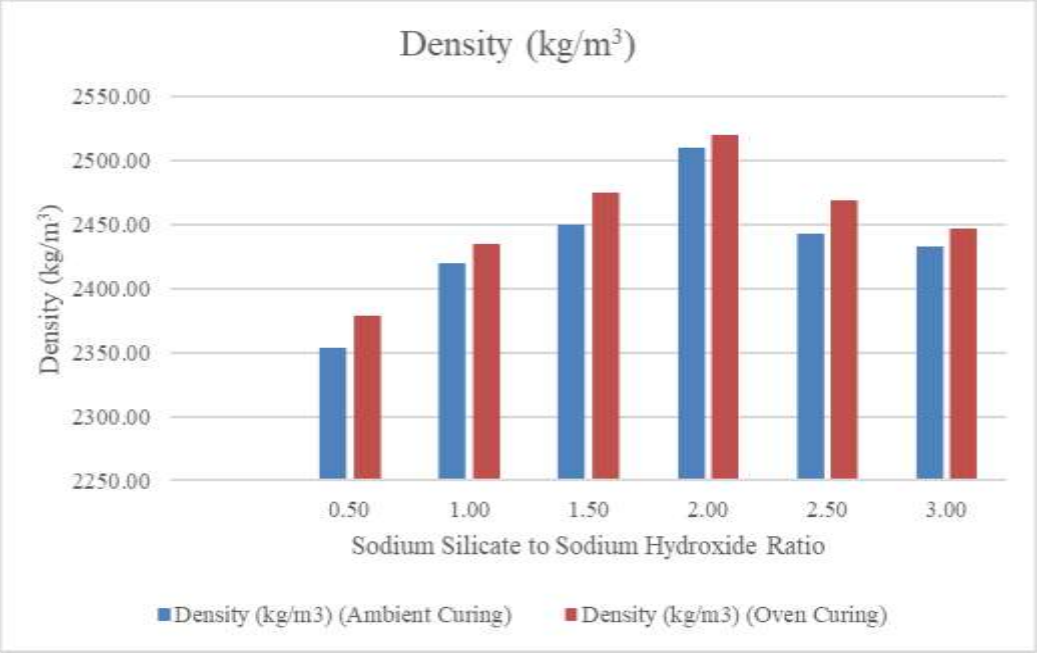

Fig. 4.14: Density of Geopolymer Concrete with Varying Sodium Silicate to Sodium Hydroxide (SS/SH) Ratio

4.5.3 Compressive Strength

The sodium silicate to sodium hydroxide (SS/SH) ratio significantly affects the compressive strength of geopolymer concrete (GPC) by controlling the degree of geopolymerization. A higher SS/SH ratio enhances the formation of aluminosilicate gels, resulting in a denser and more cohesive matrix capable of withstanding greater compressive loads. As shown in Fig. 4.15 and Fig. 4.16, the maximum compressive strength for ambient-cured GPC was 37.50 MPa at an SS/SH ratio of 2.00 after 56 days, while oven-cured specimens achieved 41.76 MPa at the same ratio. Beyond this point, compressive strength declined, with ambient-cured specimens dropping to 34.32 MPa at a ratio of 2.50 and 27.66 MPa at 3.00, while oven-cured specimens fell to 40.00 MPa and 30.66 MPa, respectively. These results emphasize the importance of selecting the optimal SS/SH ratio to achieve maximum compressive strength while maintaining workability and ease of compaction, ensuring GPC's suitability for high-strength structural applications.

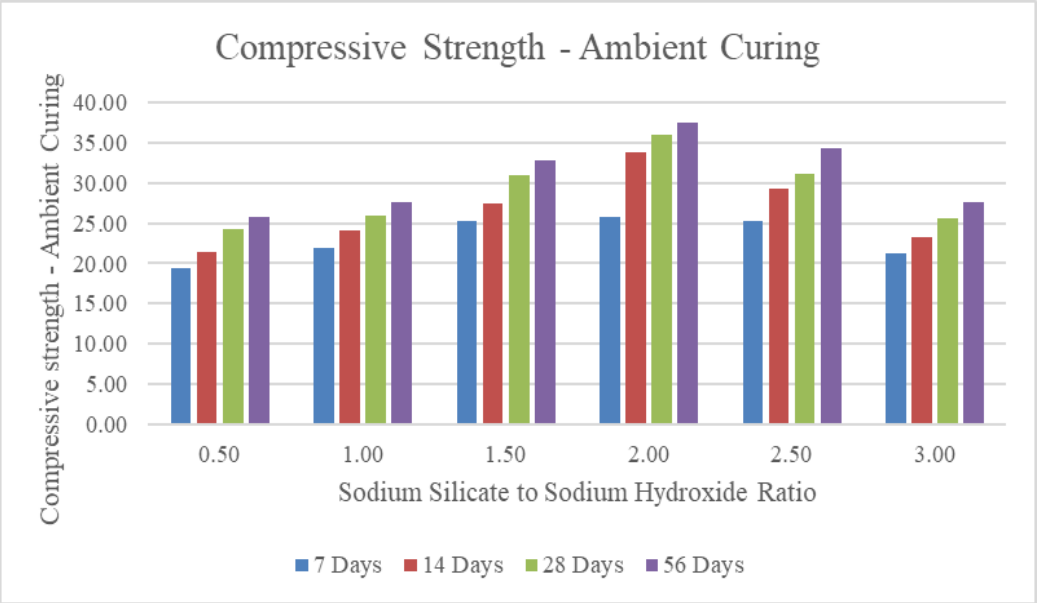

Fig. 4.15: Compressive Strength Ambient Cured Geopolymer Concrete with Varying Sodium Silicate to Sodium Hydroxide (SS/SH) Ratio

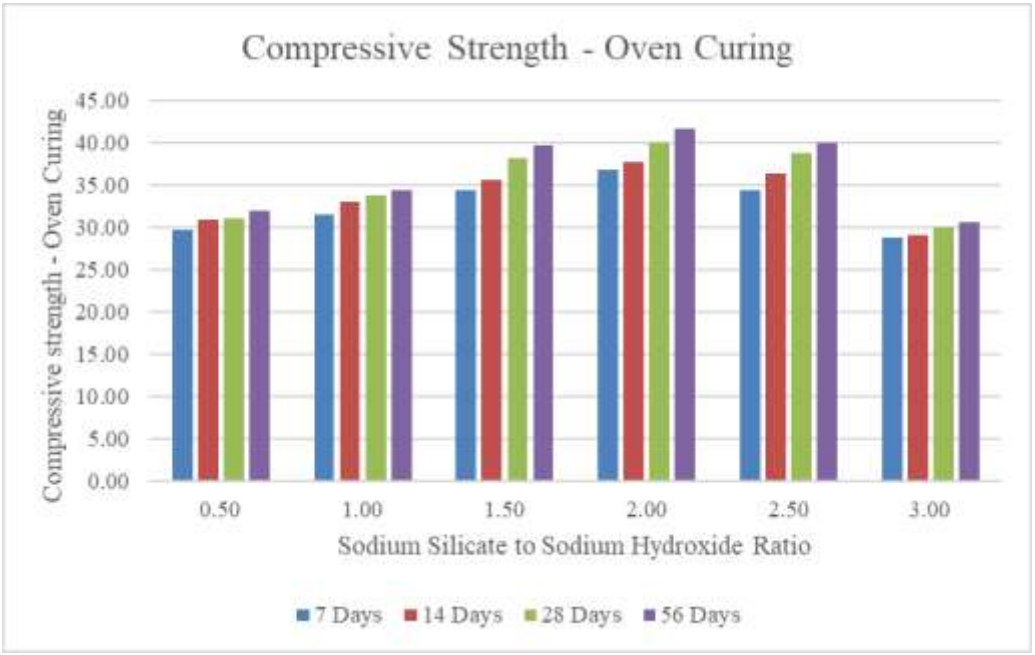

Fig. 4.16: Compressive Strength Oven Cured with Varying Sodium Silicate to Sodium Hydroxide (SS/SH) Ratio

4.6 Effect of Curing Temperature

The curing temperature for the optimal geopolymer concrete (GPC) mix design varies within the range of 60°C to 120°C. Variations in curing temperature significantly influence the chemical and mechanical properties of the GPC specimens, as these temperatures affect the geopolymerization process. To assess the impact of curing temperature, an experimental analysis was conducted. This analysis focused on examining how changes in temperature during the curing phase alter properties such as the density and compressive strength. The study systematically evaluated GPC specimens cured at different temperature levels to identify the optimum curing conditions for achieving the best balance of strength in the mix design.

4.6.1 Density

The density of geopolymer concrete (GPC) specimens is influenced by curing temperature, which affects water evaporation and the formation of micro-voids in the concrete matrix. As curing temperature increases, more water evaporates, reducing density and potentially weakening the geopolymer structure. As shown in Fig. 4.17, the maximum density of 2523 kg/m³ was recorded at a curing temperature of 100°C, reflecting optimal geopolymerization where water loss was effectively balanced with structural formation. At 120°C, the density decreased slightly to 2513 kg/m³ due to excessive water evaporation. Lower curing temperatures, such as 60°C and 80°C, produced densities of 2520 kg/m³ and 2522 kg/m³, respectively, indicating that moderate water loss supports matrix consolidation.

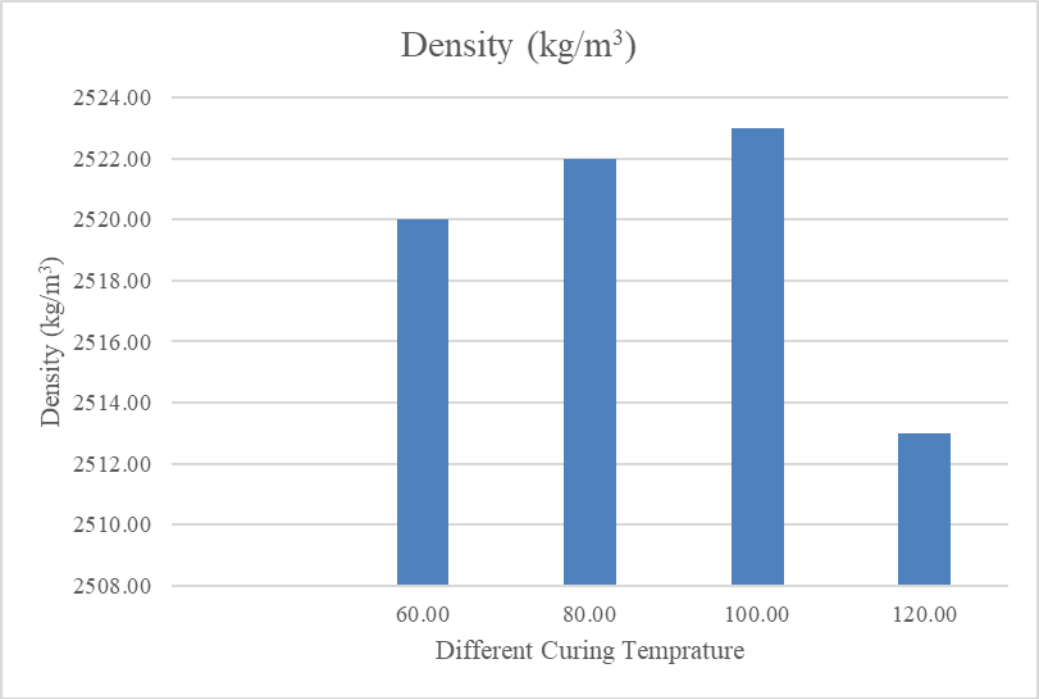

Fig. 4.17: Density of Geopolymer Concrete with Varying Curing Temperatures

4.6.2 Compressive Strength

The compressive strength of geopolymer concrete (GPC) increases with rising curing temperatures due to the acceleration of the geopolymerization process. Higher temperatures enhance the chemical reaction between aluminosilicate particles and the alkaline activator, resulting in a denser and stronger matrix (Rajput et al., 2024). As shown in Fig. 4.18, the maximum compressive strength of 43.65 MPa was achieved at 100°C after 28 days of curing, indicating optimal geopolymerization. At a temperature of 120°C, compressive strength decreased slightly to 42.02 MPa after 28 days due to excessive water loss, micro-cracking, and reduced cohesion. At lower curing temperatures of 60°C and 80°C, compressive strengths of 40.00 MPa and 42.11 MPa, respectively, were recorded after 28 days, showing that moderate temperatures support adequate geopolymerization but are less effective than curing at 100°C.

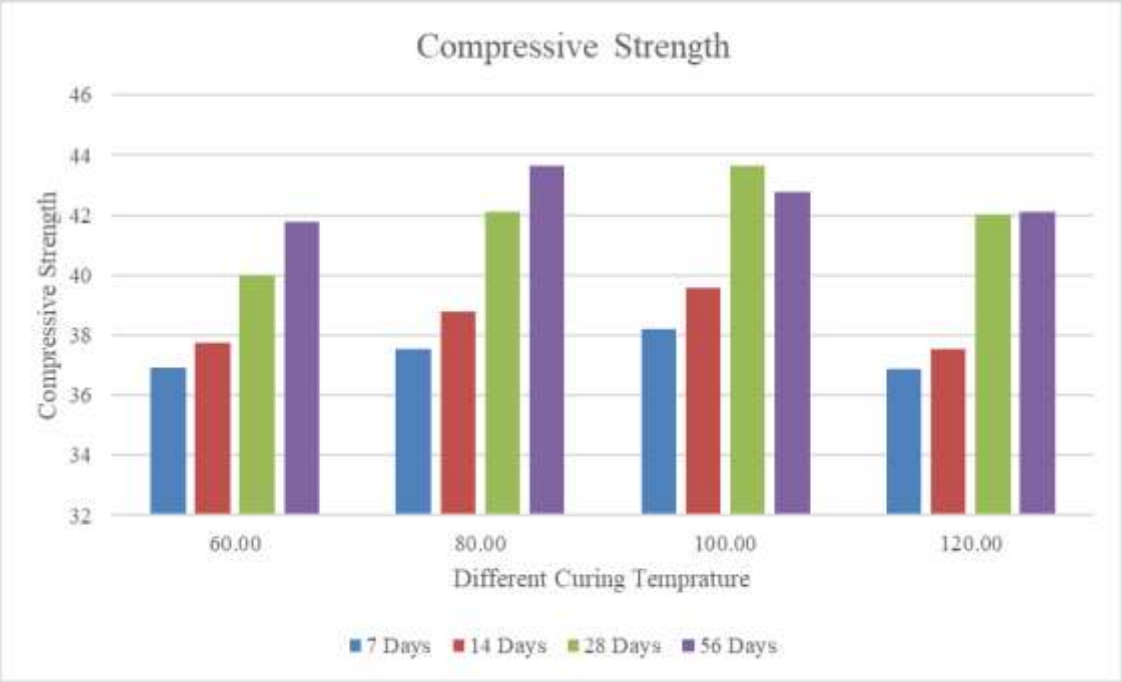

Fig. 4.18: Compressive Strength of Geopolymer Concrete with Varying Curing Temperatures

4.7 Effect of Alccofine/Fly-Ash Ratio

The effect of the Alccofine/Fly Ash ratio in concrete and geopolymer composites has garnered significant attention due to its influence on mechanical properties and durability. Alccofine, an ultra-fine slag-based material and early strength, while fly ash contributes to long-term strength development and sustainability. In this study inclusion of Alccofine in the range of 0% to 25% has shown significant improvements in compressive strength, and enhanced durability, particularly at early stages. Optimizing their ratio within this range can improve the microstructure, making it a critical factor in achieving desired performance characteristics while promoting eco-friendly construction practices.

4.7.1 Workability

The inclusion of Alccofine in fly ash-based geopolymer concrete (GPC) significantly affects workability due to their fine particle size. As the percentage of Alccofine increases, the slump value decreases, indicating reduced workability. As shown in Fig. 4.19, the slump value dropped from 98 mm at 0% Alccofine dosage to 30 mm at a 25% dosage, highlighting the inverse relationship between Alccofine dosage and workability. This reduction in workability is attributed to the increased surface area of finer particles, which reduces the free water available for lubrication within the mix. While decreased workability may require additional water or super-plasticizers to ensure proper mixing and placement. Balancing the dosage of Alccofine with appropriate water content or chemical admixtures is crucial to optimizing both workability and mechanical properties for practical applications.

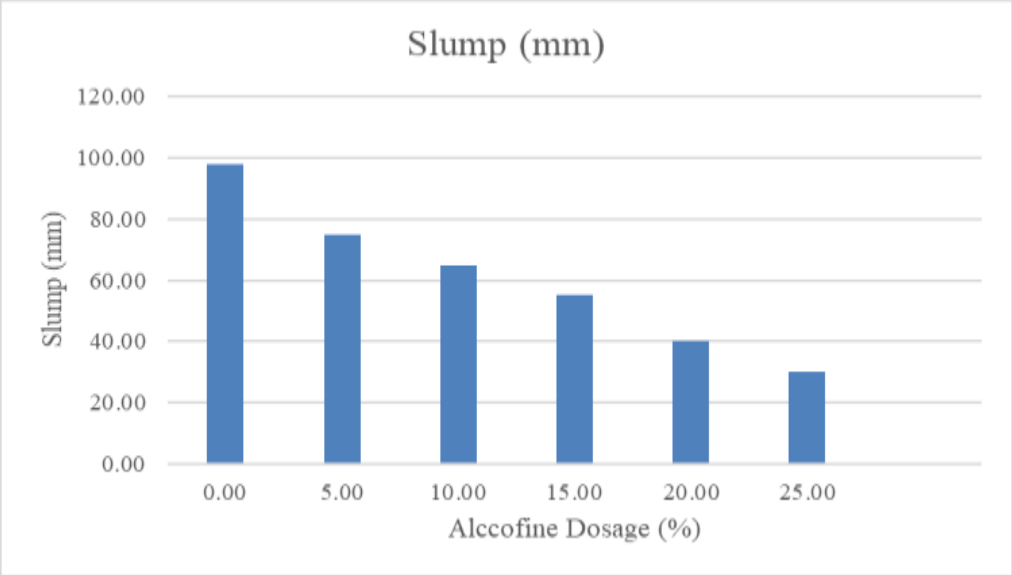

Fig. 4.19: Workability of Geopolymer Concrete with Varying Percentages of Alccofine Replacement

4.7.2 Density

The density of geopolymer concrete (GPC) evolves with curing time and temperature due to the progressive polymerization of aluminosilicate materials. During curing, the chemical reaction between fly ash and alkaline activators densifies the matrix by consuming un-reacted

materials and reducing porosity, with heat curing further accelerating this process. Additionally, the inclusion of Alccofine enhances density by promoting calcium silicate hydrate (C-S-H) formation alongside geopolymer gels, refining the pore structure. As shown in Fig. 4.20, the density increased from 2510 kg/m³ at 0% Alccofine dosage to 2549 kg/m³ for ambient-cured specimens and 2552 kg/m³ for oven-cured specimens at 25% Alccofine dosage. This improvement is attributed to enhanced particle packing and a denser microstructure. Higher Alccofine content accelerates the reaction rate, promoting more complete geopolymerization and better compaction. Optimizing curing conditions and supplementary cementitious material dosage is essential to maximize density and overall mechanical performance while maintaining workability.

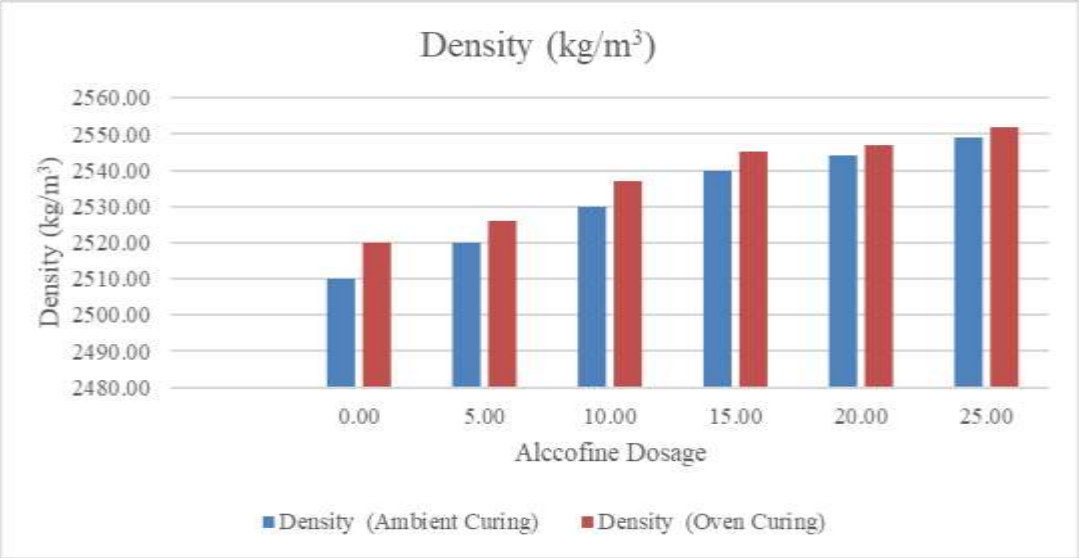

Fig. 4.20: Density of Geopolymer Concrete with Varying Percentages of Alccofine Replacement

4.7.3 Extra Water

The inclusion of Alccofine in geopolymer concrete (GPC) significantly affects water demand due to its finer particle size, angular in shape, and higher reactivity compared to fly ash. Alccofine's increased surface area requires more water for adequate dispersion and hydration, raising the water-to-binder ratio necessary to maintain workability. In contrast, fly

ash's spherical particles enhance workability by reducing water demand and improving particle flow within the mix. As shown in Table 4.3, slump values decreased with increased Alccofine dosage unless additional water was added. For instance, at a 5% alccofine dosage with 50 ml of extra water, the slump reached 145 mm, indicating high workability. However, at a 25% dosage with the same water content, the slump dropped to 72 mm, demonstrating reduced flowability due to increased water absorption by Alccofine particles. These findings highlight the importance of adjusting the water-to-binder ratio with higher Alccofine dosages to maintain a balance between workability and mechanical properties, ensuring proper mixing, placement and compaction.

Table 4.3: Additional water applied in geopolymer concrete with varying percentages of alccofine replacement

Alccofine Dosage	**Extra water (ml)**	**Slump (mm)**
0.05	10	84
	20	107
	30	112
	40	133
	50	145
0.1	10	78
	20	86
	30	96
	40	118
	50	127
0.15	10	65
	20	77
	30	81
	40	92
	50	112
0.2	10	45
	20	58

	30	71
	40	85
	50	100
0.25	10	37
	20	44
	30	56
	40	61
	50	72
	60	87

4.7.4 Compressive Strength

The inclusion of Alccofine in geopolymer concrete (GPC) significantly enhances compressive strength due to its ultra-fine particles and high pozzolanic activity. Its increased surface area improves particle packing, creating a denser and more cohesive matrix. Additionally, Alccofine's chemical composition facilitates the formation of calcium silicate hydrate (C-S-H) gels, complementing the aluminosilicate network of geopolymer matrices and boosting compressive strength. As shown in Fig. 4.21 and Fig. 4.22, the maximum compressive strength for ambient-cured GPC reached 50.98 MPa after 56 days at a 15% Alccofine dosage, while oven-cured specimens achieved 53.10 MPa at the same dosage, showcasing the benefits of heat curing in enhancing geopolymerization. Lower dosages, such as 5% and 10%, also improved strength compared to fly ash-only mixes, driven by enhanced matrix binding and flowability. However, exceeding the 15% Alccofine dosage resulted in diminished strength, emphasizing the importance of balancing Alccofine content to optimize both strength and workability in GPC.

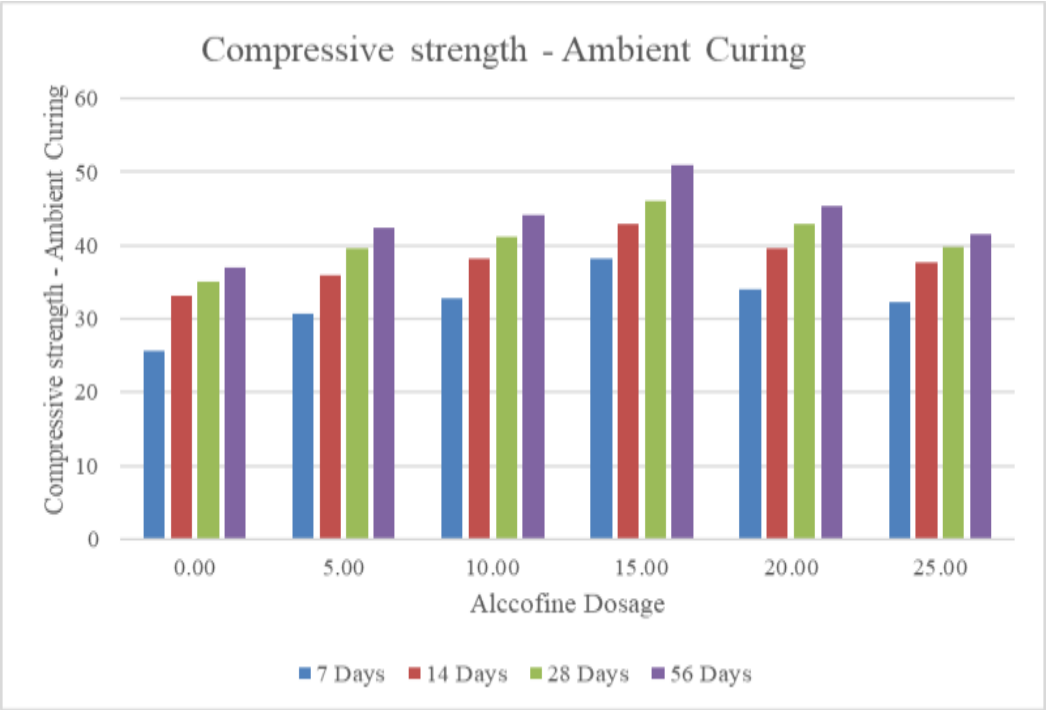

Fig. 4.21: Compressive Strength of Ambient Cured Geopolymer Concrete with Varying Percentages of Alccofine Replacement

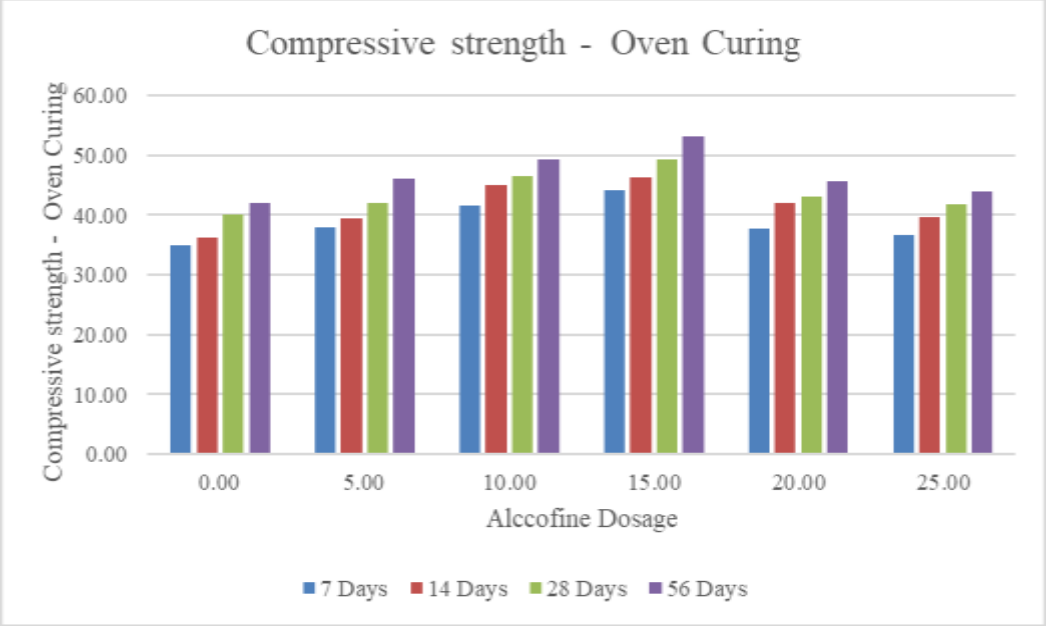

Fig. 4.22: Compressive Strength of Oven Cured Geopolymer Concrete with Varying Percentages of Alccofine Replacement

4.7.5 Splitting Tensile Strength

The Alccofine-to-fly ash ratio significantly influences the splitting tensile strength of geopolymer concrete (GPC). As shown in Fig. 4.23 and Fig. 4.24, the maximum splitting tensile strength for ambient-cured GPC was 6.16 MPa at a 15% Alccofine dosage after 56 days, while oven-cured specimens achieved 6.95 MPa at the same dosage, reflecting enhanced matrix bonding and reduced porosity. Beyond 15%, tensile strength decreased slightly, with ambient-cured specimens dropping to 5.02 MPa and oven-cured samples to 5.76 MPa at a 25% dosage. This reduction is attributed to reduced workability, compaction challenges and micro-crack formation due to excessive Alccofine content.

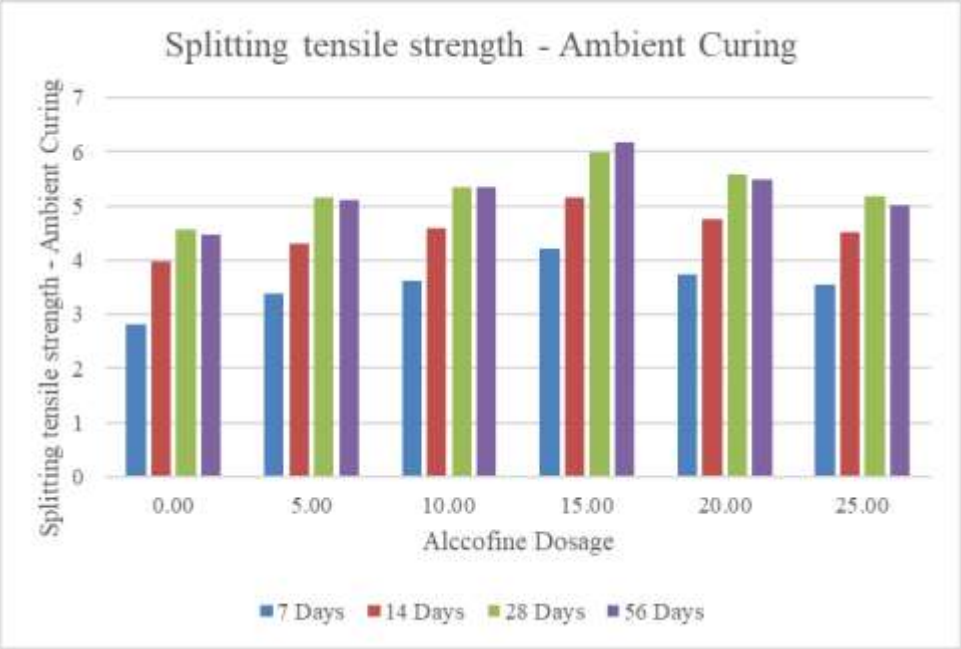

Fig. 4.23: Split Tensile Strength of Ambient Cured Geopolymer Concrete with Varying Percentages of Alccofine Replacement

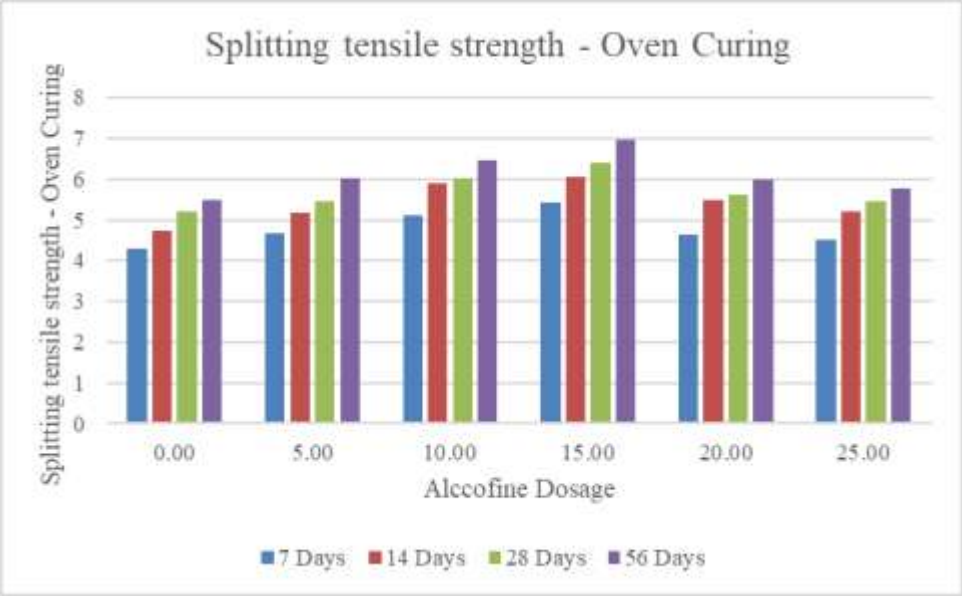

Fig. 4.24: Split Tensile Strength of Oven Cured Geopolymer Concrete with Varying Percentages of Alccofine Replacement

4.7.6 Flexural Tensile Strength

The Alccofine-to-fly ash ratio significantly affects the flexural strength of geopolymer concrete (GPC). Increasing Alccofine dosage enhances flexural strength. As shown in Fig. 4.25 and Fig. 4.26, the maximum flexural strength for ambient-cured GPC was 8.15 MPa after 56 days at a 15% Alccofine dosage, while oven-cured specimens achieved 9.45 MPa at the same dosage, demonstrating enhanced geopolymerization under heat. Beyond 15%, flexural strength slightly decreased due to reduced workability and potential compaction challenges, which are critical considerations in field applications.

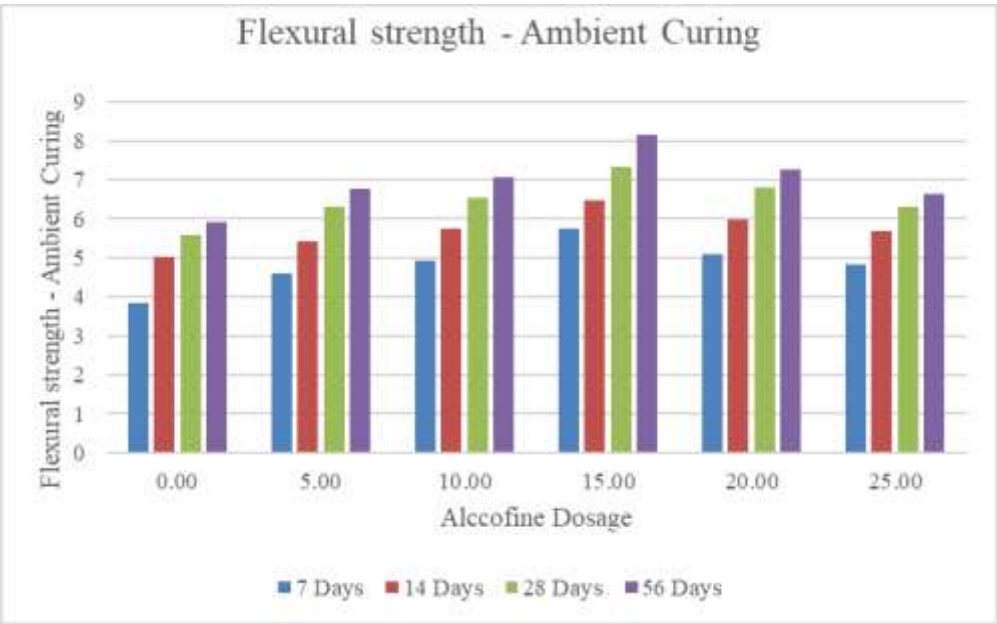

Fig. 4.25: Flexural Tensile Strength of Ambient Cured Geopolymer Concrete with Varying Percentages of Alccofine Replacement

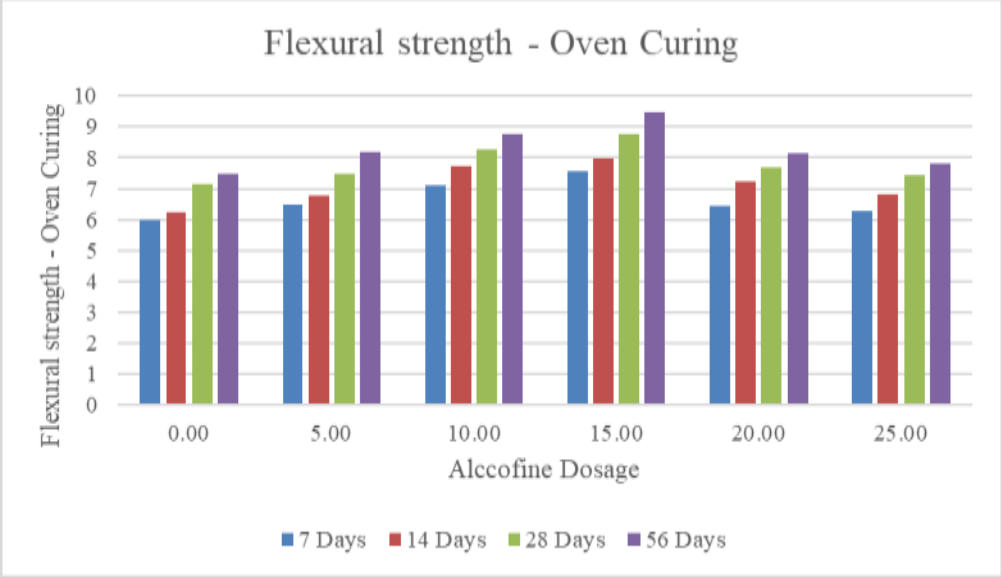

Fig. 4.26: Flexural Tensile Strength of Oven Cured Geopolymer Concrete with Varying Percentages of Alccofine Replacement

4.7.7 Rebound Hammer Strength

The inclusion of Alccofine in geopolymer concrete (GPC) significantly enhances rebound hammer strength due to the formation of a denser and more cohesive matrix. The ultra-fine particles and high pozzolanic activity of Alccofine improve geopolymerization, resulting in better interfacial bonding and reduced porosity, which contribute to higher surface hardness and rebound hammer strength. As shown in Fig. 4.27 and Fig. 4.28, the maximum rebound hammer strength for ambient-cured GPC was 50.98 MPa after 56 days at a 15% Alccofine dosage, while oven-cured specimens achieved 53.10 MPa at the same dosage, demonstrating enhanced geopolymerization and improved microstructure under higher temperatures. Beyond 15%, rebound hammer strength decreased, with ambient-cured and oven-cured values dropping to 41.55 MPa and 43.98 MPa, respectively, at a 25% dosage, due to reduced workability and compaction challenges caused by increased mix viscosity.

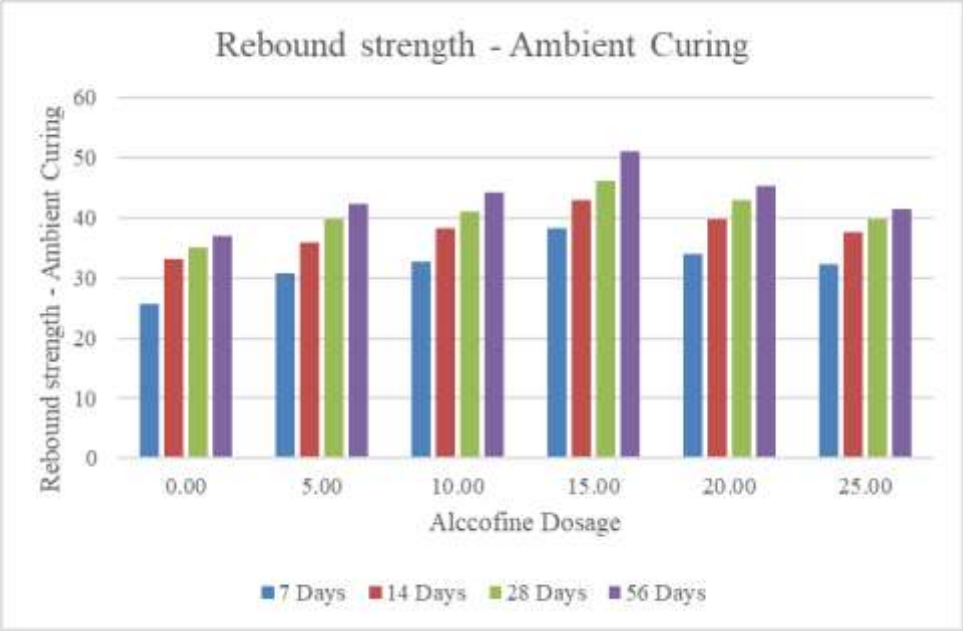

Fig. 4.27: Rebound Hammer Strength of Ambient Cured Geopolymer Concrete with Varying Percentages of Alccofine Replacement

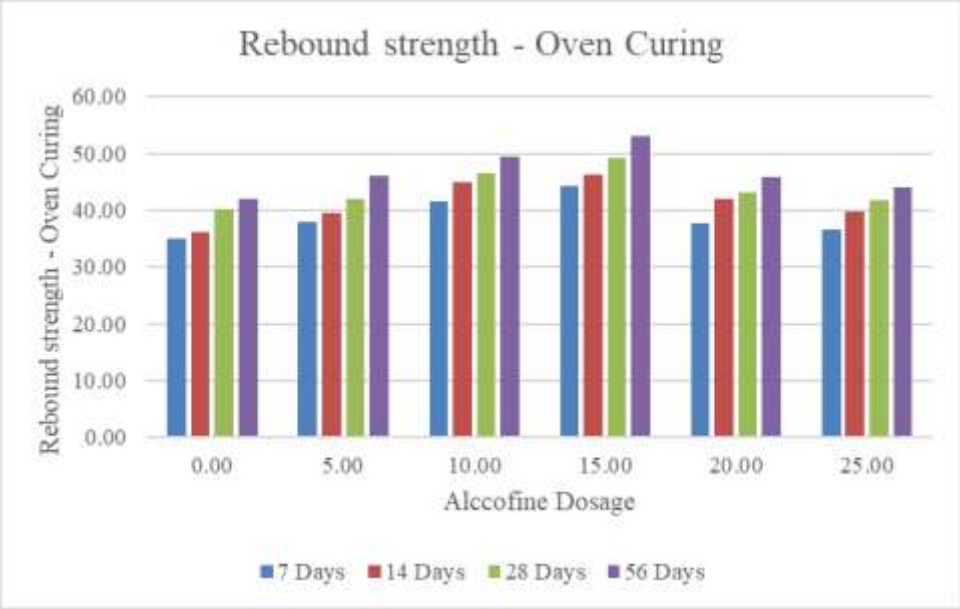

Fig. 4.28: Rebound Hammer Strength of Oven Cured Geopolymer Concrete with Varying Percentages of Alccofine Replacement

4.7.8 Modulus of Elasticity

The Alccofine-to-fly ash ratio significantly impacts the modulus of elasticity (MOE) of geopolymer concrete (GPC). Oven-cured GPC specimens consistently exhibit higher MOE due to enhanced geopolymerization under heat, resulting in a denser and more cohesive matrix. As shown in Fig. 4.29, the maximum MOE recorded for oven-cured GPC was 31.01 GPa at a 15% Alccofine dosage, while ambient-cured specimens reached 29.05 GPa at the same dosage. This reflects superior particle packing and increased interfacial bonding from Alccofine's ultra-fine particles. However, at a 25% dosage, the MOE decreased to 29.98 GPa (oven-cured) and 28.89 GPa (ambient-cured), likely due to reduced workability and potential compaction challenges from higher mix viscosity.

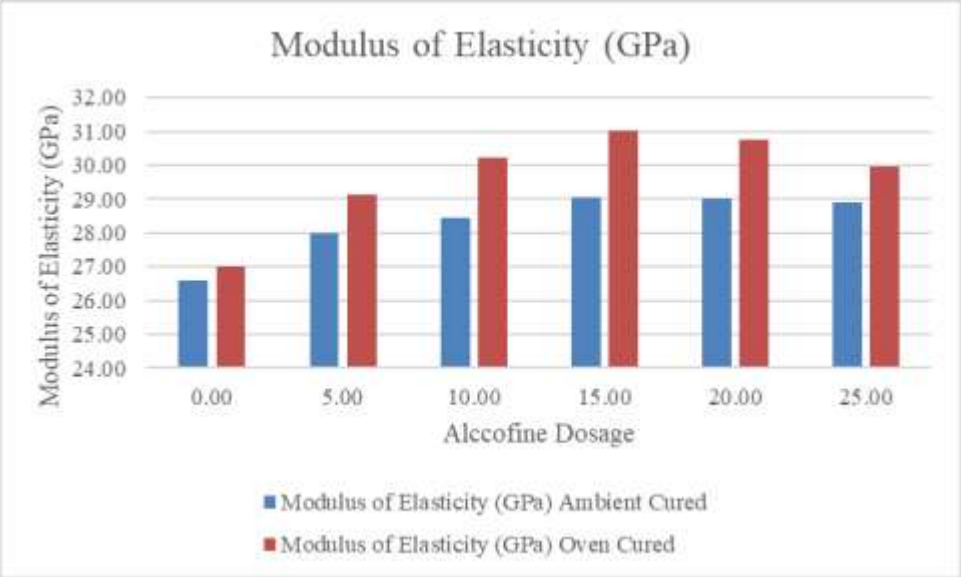

Fig. 4.29: Modulus of Elasticity of Geopolymer Concrete with Varying Percentages of Alccofine Replacement

4.8 Micro-Structural Analysis of Optimum Alccofine Percentage Geopolymer Concrete

The micro-structural analysis of geopolymer concrete with the optimum percentage of Alccofine was conducted using Fourier Transform Infrared Spectroscopy (FTIR), Scanning Electron Microscopy (SEM) and Energy Dispersive X-ray Spectroscopy (EDX). FTIR revealed the characteristic peaks indicating the formation of aluminosilicate gel, confirming the geopolymerization process. SEM analysis demonstrated a dense and compact microstructure with minimal voids, attributed to the enhanced particle packing due to Alccofine. EDX results provided elemental composition, highlighting the presence of silica (Si), aluminum (Al) and calcium (Ca), which are crucial for strength and durability.

4.8.1 Fourier Transforms Infrared (FT-IR) Spectroscopy

4.8.1.1 Fourier Transforms Infrared (FT-IR) Spectroscopy Of Alccofine

The Fig. 4.30 presents the FTIR spectrum of Alccofine, showcasing its chemical structure and functional groups. The x-axis indicates the wave number (cm^{-1}) and the y-axis represents the percentage transmittance (%T). The sharp peak near 1000–1100 cm^{-1} corresponds to Si-O-Si and Si-O-Al stretching vibrations, confirming the presence of silicate and alumina phases, which are essential for its pozzolanic and binding properties. The broad absorption band around 3400–3600 cm^{-1} is attributed to O-H stretching vibrations, signifying the presence of hydroxyl groups and moisture. The smaller peaks near 1500–1650 cm^{-1} correspond to H-O-H bending vibrations, indicating residual water. These characteristic peaks demonstrate Alccofine's high reactivity and its role as a supplementary cementitious material, enhancing the geopolymerization process and contributing to the strength and durability of geopolymer concrete.

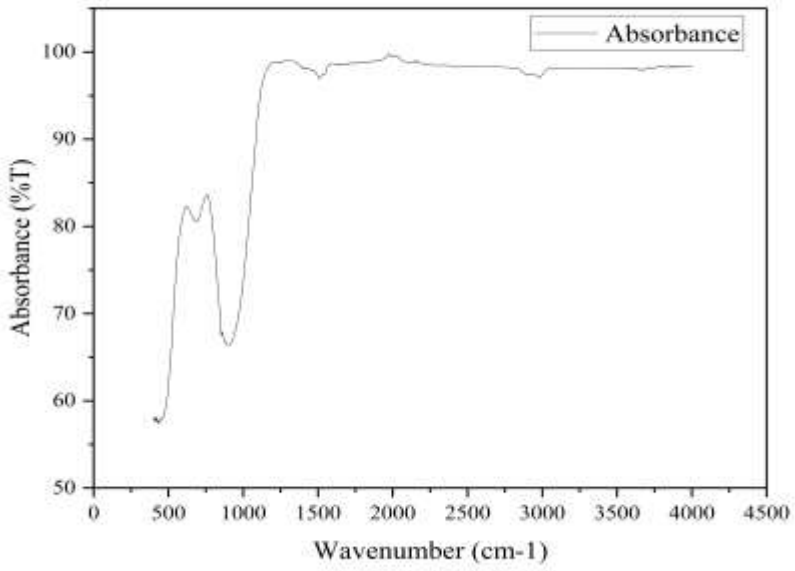

Fig. 4.30: Fourier Transforms Infrared (FT-IR) Spectroscopy Of Alccofine

4.8.1.2 Fourier Transforms Infrared (FT-IR) Spectroscopy Of Ambient Cured 15 % Alccofine Replacement Geopolymer Concrete

The FTIR spectra of geopolymer concrete with 15% Alccofine replacement reveal key insights into the chemical structure and functional groups under different curing conditions. Both oven-cured and ambient-cured samples as shown in Fig. 4.31 and Fig. 4.32 exhibit similar functional groups, with broad absorption bands around 3400–3600 cm^{-1} corresponding to O-H stretching vibrations, indicating the presence of hydroxyl groups and water molecules. The sharp peak near 1000 cm^{-1}, attributed to Si-O-Si asymmetric stretching, confirms the formation of aluminosilicate gel, a critical product of geopolymerization. The band near 1500–1650 cm^{-1}, representing H-O-H bending vibrations, highlights the presence of residual water. However, notable differences emerge between the curing methods. In oven-cured samples, the peaks around 1000 cm^{-1} are sharper and the O-H stretching region exhibits higher intensity, indicating enhanced geopolymerization and reduced residual moisture due to accelerated reaction kinetics. In contrast, ambient-cured samples show broader peaks and more prominent H-O-H bending vibrations, reflecting slower reactions and higher retained water. These differences emphasize that oven curing produces a denser and more uniform matrix, while ambient curing results in a less compact structure due to its slower geopolymerization process. These findings confirm the role of Alccofine as a sustainable additive that enhances the chemical and mechanical stability of both curing methods.

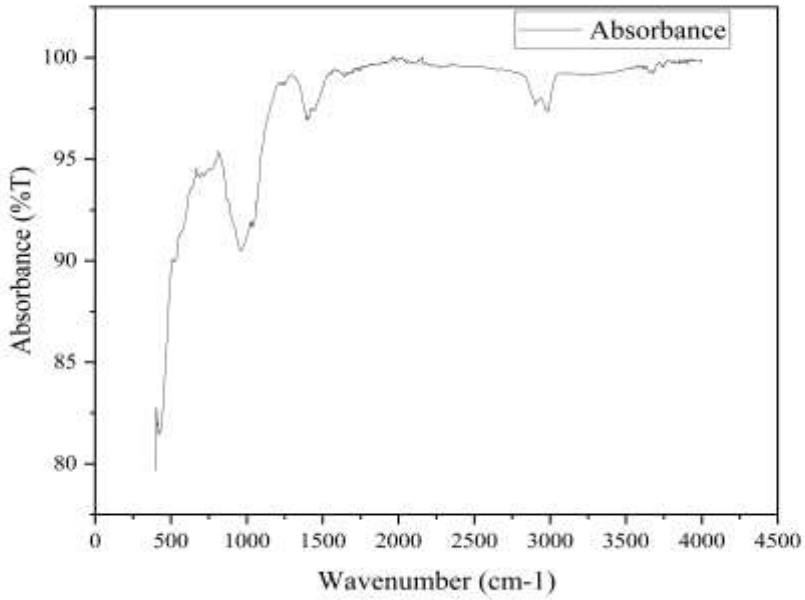

Fig. 4.31: Fourier Transforms Infrared (FT-IR) Spectroscopy of Oven Cured 15 % Alccofine Replacement Geopolymer Concrete

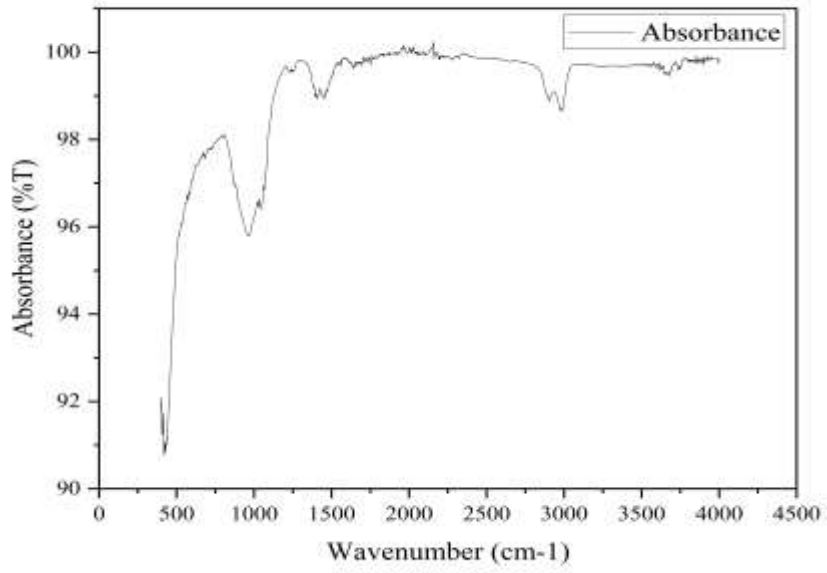

Fig. 4.32: Fourier Transform Infrared (FT-IR) Spectroscopy of Ambient Cured 15 % Alccofine Replacement Geopolymer Concrete

4.8.2 Scanning Electron Microscopy (*SEM*) and Energy Dispersive X-Ray analysis (*EDX*)

4.8.2.1 Scanning Electron Microscopy (*SEM*) and Energy Dispersive X-Ray (*EDX*) Analysis of Alccofine

The microstructural and elemental composition of alccofine were investigated using Scanning Electron Microscopy (SEM) and Energy Dispersive X-Ray (EDX) techniques. The SEM images, shown in Fig. 4.37, reveal the fine and uniform particle morphology of alccofine, which is critical for its high reactivity and ability to enhance concrete performance. The EDX analysis, illustrated in Fig. 4.38, provides the elemental composition, with carbon and oxygen being the predominant elements, accounting for weight percentages of 47.31% and 34.67%, respectively. Other essential elements include calcium (6.8%), silicon (6.25%), and aluminum (3.47%), which contribute to its pozzolanic activity and binding properties. The findings confirm the suitability of alccofine as a supplementary cementitious material, capable of improving the structural and durability characteristics of geopolymer concrete.

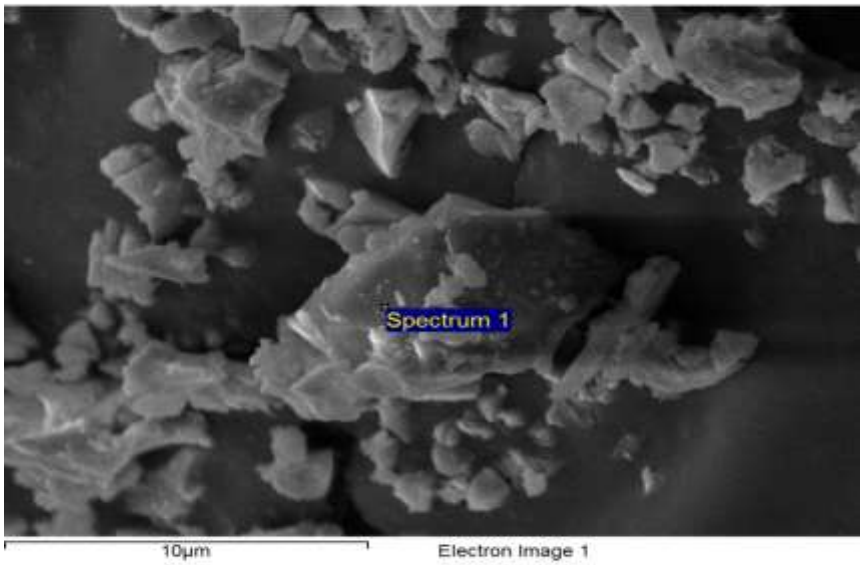

Fig. 4.33: Scanning Electron Microscopy Of Alccofine

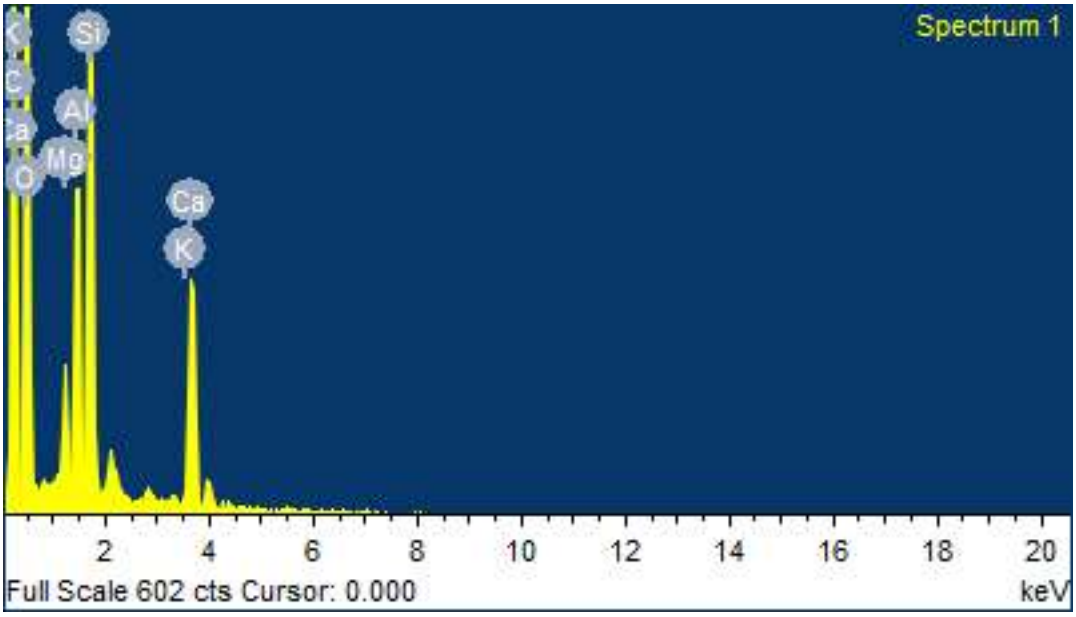

Fig. 4.34: Energy Dispersive X-Ray of alccofine

Table 4.4: Elemental Mass Percentage Of Alccofine

Elements	Atomic %	weight%
C K	33.35	47.31
O K	32.56	34.67
Mg K	1.9	1.33
Al K	5.5	3.47
Si K	10.31	6.25
K K	0.39	0.17
Ca K	16	6.8
TOTAL	100	

4.8.2.2 Scanning Electron Microscopy (*SEM*) and Energy Dispersive X-Ray (*EDX*) Analysis Of Ambient And Oven Cured 15% Alccofine Replacement Geopolymer Concrete

The SEM and EDX analyses reveal significant differences in the microstructure and elemental composition of oven-cured and ambient-cured geopolymer concrete with 15% Alccofine replacement, as presented in Fig. 4.35– Fig. 4.38 and detailed in Tables 4.5 and 4.6. The oven-cured sample demonstrates a compact and dense microstructure with minimal porosity, as evident from the SEM image (Fig. 4.35). The corresponding EDX analysis (Fig. 4.36) indicates a high oxygen content (43.15%) and carbon content (31.25%), along with significant levels of silicon (7.8%) and calcium (7.9%). These findings confirm enhanced geopolymerization, driven by elevated temperature curing, which facilitates the formation of a strong aluminosilicate network. This process promotes the development of stronger chemical bonds, resulting in reduced porosity, improved mechanical properties, and superior durability. In contrast, the ambient-cured sample exhibits a less dense microstructure with visible porosity, as shown in the SEM image (Fig. 4.37). The EDX analysis (Fig. 4.38) reveals a significantly higher oxygen content (60.13%) and markedly lower carbon content (2.07%), reflecting slower geopolymerization. Although silicon (15.16%) and calcium (6.07%) are present, their levels are lower than those observed in the oven-cured sample, leading to a weaker and less uniform matrix. The slower reaction kinetics under ambient curing conditions contribute to the increased porosity and reduced mechanical integrity. These observations highlight the critical influence of curing conditions on the microstructure and performance of geopolymer concrete. High-temperature oven curing significantly enhances geo-polymerization, promoting a denser and more durable matrix. In contrast, ambient curing, while capable of facilitating essential reactions, results in slower bond formation and inferior mechanical properties, underscoring the importance of optimizing curing conditions for improved concrete performance.

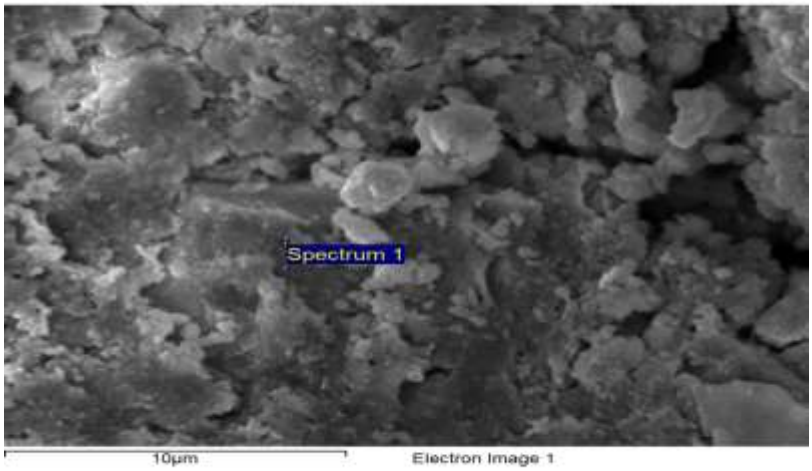

Fig. 4.35: Scanning Electron Microscopy of Oven Cured 15 % Alccofine Replacement Geopolymer Concrete

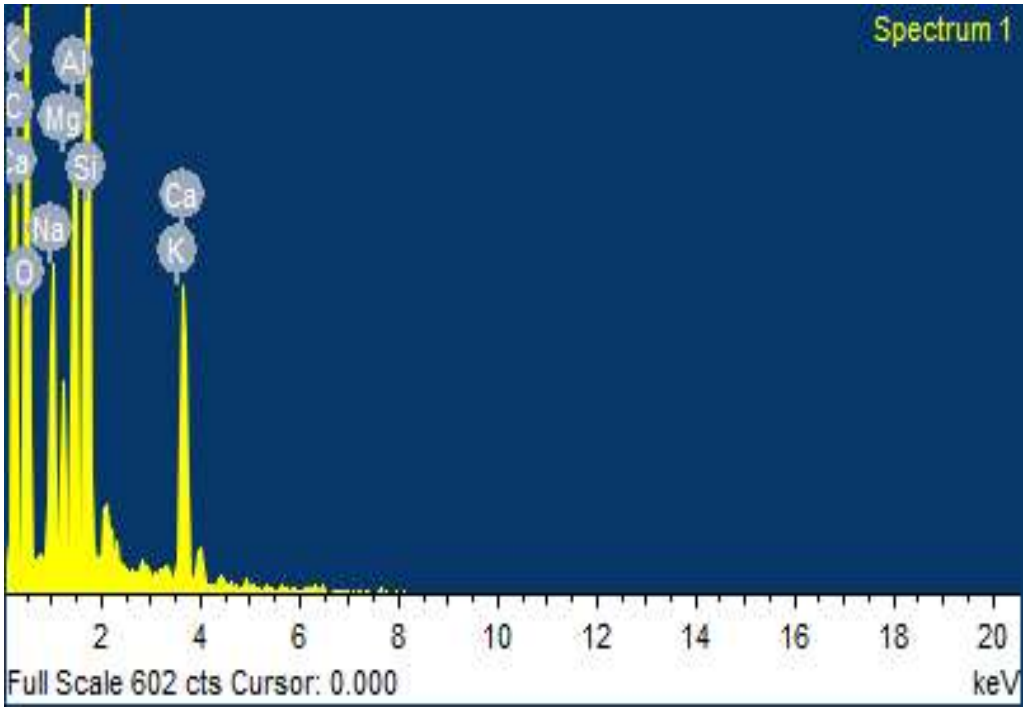

Fig. 4.36: Energy Dispersive X-Ray of Oven Cured 15 % Alccofine Replacement Geopolymer Concrete

Table 4.5: Elemental Mass Percentage Of Oven Cured 15 % Alccofine Replacement Geopolymer Concrete

Elements	Atomic %	weight%
C K	20.27	31.25
O K	37.28	43.15
N K	4.33	3.48
Mg K	2.51	1.91
Al K	6.32	4.34
Si K	11.84	7.8
K K	0.34	0.16
Ca K	17.10	7.90
TOTAL	100	

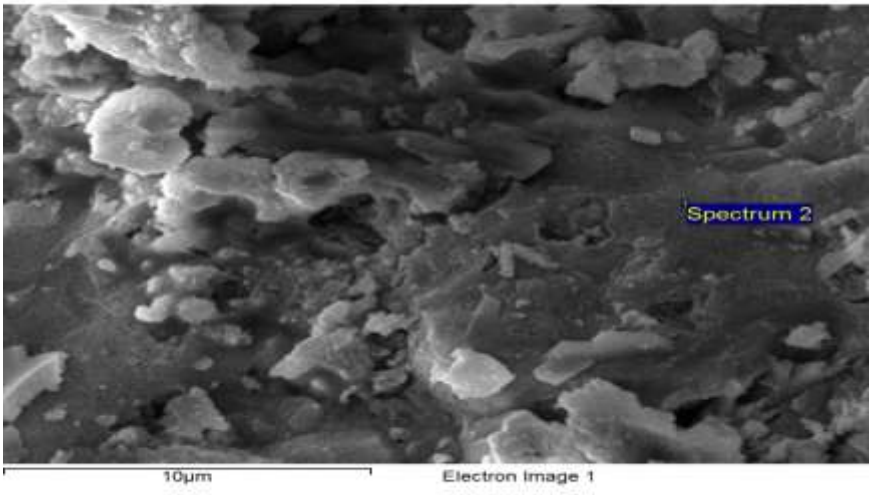

Fig. 4.37: Scanning Electron Microscopy of Ambient Cured 15 % Alccofine Replacement Geopolymer Concrete

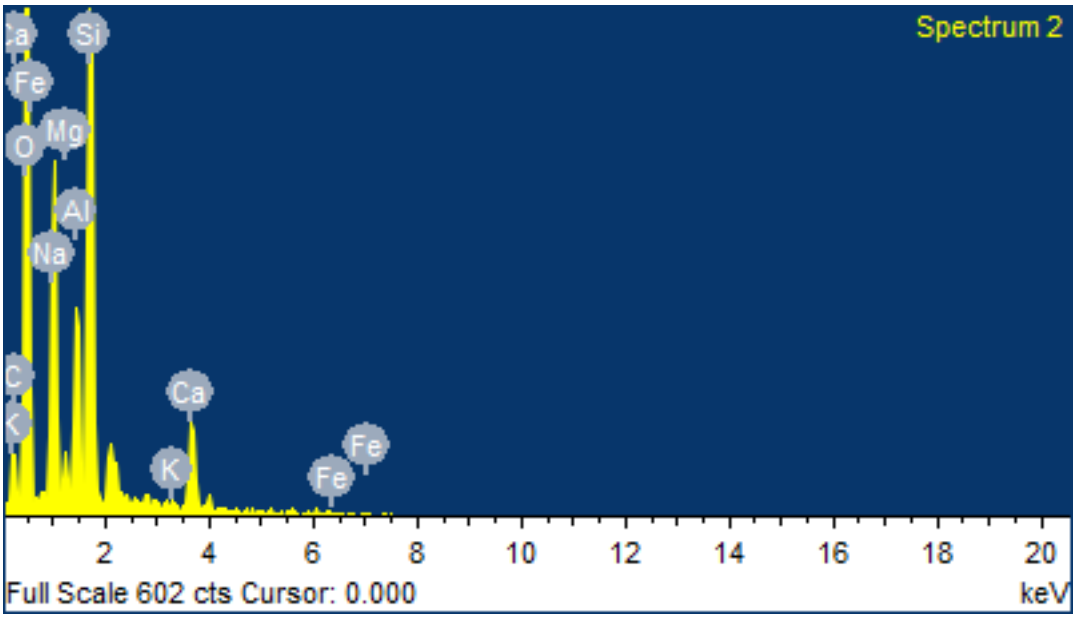

Fig. 4.38: Energy Dispersive X-Ray Of Ambient Cured 15 % Alccofine Replacement Geopolymer Concrete

Table 4.6: Elemental Mass Percentage Of Ambient Cured 15 % Alccofine Replacement Geopolymer Concrete

Elements	Atomic %	weight%
C K	1.2	2.07
O K	46.44	60.13
N K	11.46	10.33
Mg K	1.35	1.15
Al K	5.88	4.51
Si K	20.56	15.16
K K	0.42	0.22
Ca K	11.74	6.07
Fe L	0.94	0.35
TOTAL	100	

4.9 Durability Optimal Geopolymer Concrete (15% Alccofine)

The durability of the optimal geopolymer concrete (15% Alccofine) was assessed under severe conditions, including seawater exposure, acid attack, magnesium sulfate attack, and wetting-drying cycles.

4.9.1 Effect of Sea Water Condition

The seawater condition was simulated by preparing a saline solution in the laboratory that mimics seawater, following ASTM standards. Specimens of both geopolymer concrete (GPC) and conventional concrete were immersed in the solution for an extended duration. The GPC specimens were analyzed for weight loss and compressive strength at intervals of 6 weeks, 12 weeks, 18 weeks, and 24 weeks of exposure.

4.9.1.1 Density

The density and mass loss of geopolymer concrete (GPC) exposed to seawater are influenced by Alccofine dosage and curing conditions. Alccofine's high pozzolanic activity enhances matrix densification, reducing porosity and improving chemical resistance. Oven-cured specimens with 25% Alccofine achieved a maximum density of 2554 kg/m³ after 6 weeks, compared to 2551 kg/m³ for ambient-cured specimens. Strength and density increased until 12 weeks due to sodium ion interaction with the geopolymer matrix, enhancing binding and densification. After 12 weeks, these reactions stabilized, with density slightly decreasing by 18 weeks due to leaching and ion exchange, stabilizing at 2545 kg/m³ (oven-cured) and 2535 kg/m³ (ambient-cured). Higher Alccofine dosages mitigated mass loss and degradation by forming a dense microstructure with fewer pores.

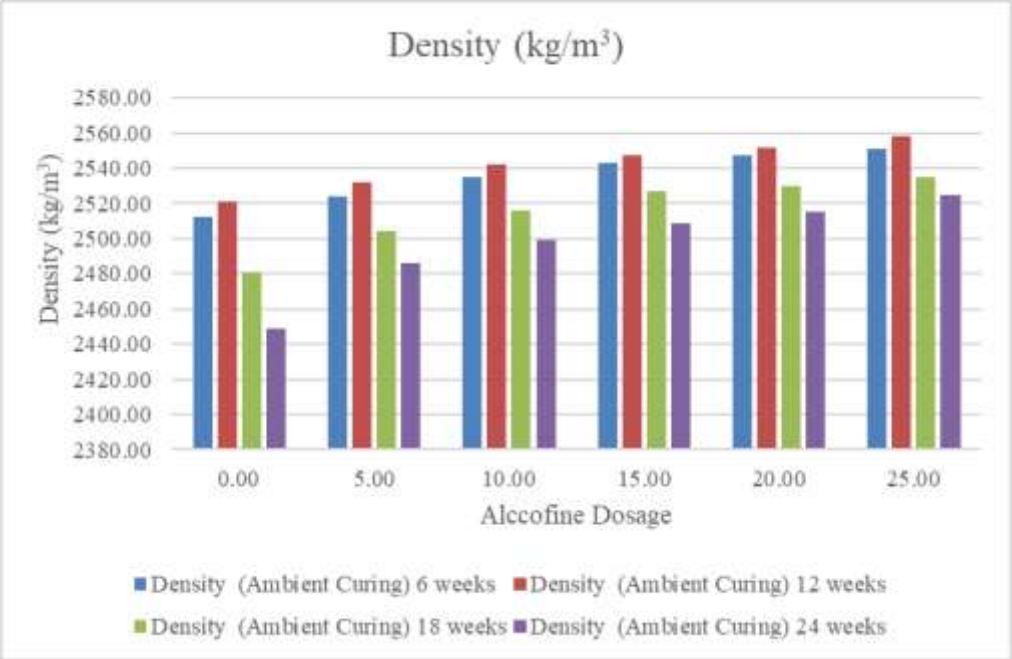

Fig. 4.39: Density of ambient-cured geopolymer concrete immersed in seawater with varying percentages of alccofine replacement

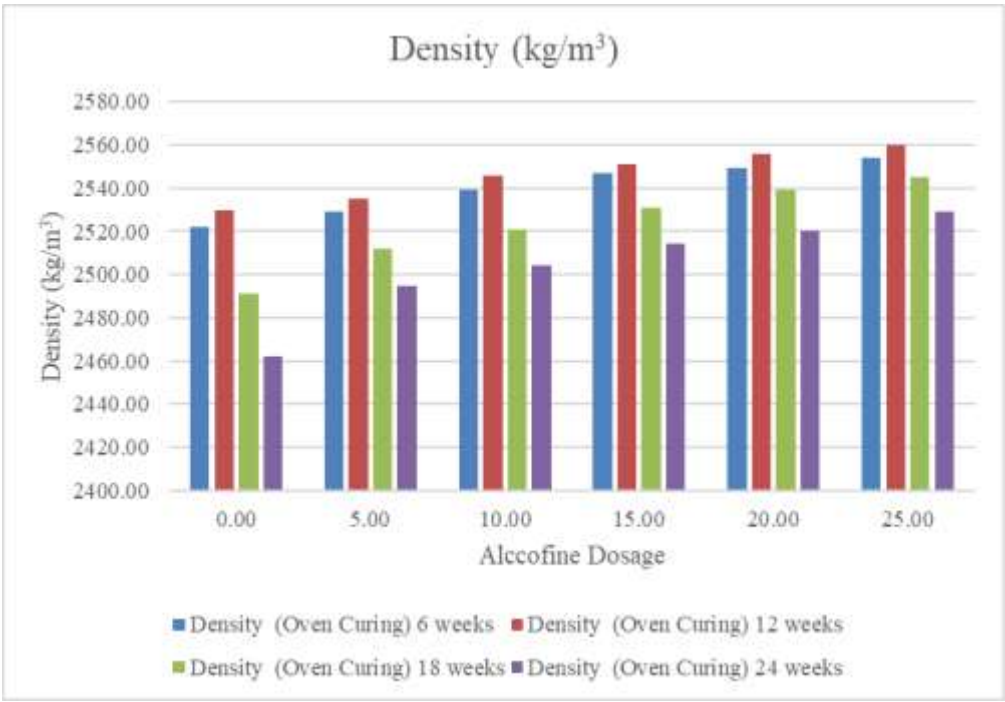

Fig. 4.40: Density of oven-cured geopolymer concrete immersed in seawater with varying percentages of alccofine replacement

4.9.1.2 Compressive Strength

The compressive strength and density of geopolymer concrete (GPC) exposed to seawater significantly depend on the dosage of Alccofine, a mineral admixture with fine particles and high pozzolanic reactivity. Alccofine promotes the formation of calcium silicate hydrate (C-S-H), enhancing resistance to seawater-induced degradation. As shown in Fig. 4.41 and Fig. 4.42, the maximum compressive strength for ambient-cured GPC was 49.88 MPa at a 15% Alccofine dosage after 12 weeks, while oven-cured specimens achieved 53.23 MPa under the same conditions. Strength increased until 12 weeks due to the interaction of seawater sodium ions with the geopolymer matrix, enhancing densification and binding. Oven curing accelerated these reactions, leading to higher strength and density. However, beyond 18 weeks, strength declined due to surface leaching and chloride penetration. At 24 weeks, ambient-cured specimens retained a compressive strength of 40.85 MPa, while oven-cured samples achieved 43.60 MPa. Despite this decline, the enhanced microstructure from Alccofine significantly mitigated long-term degradation, ensuring better durability than conventional concrete.

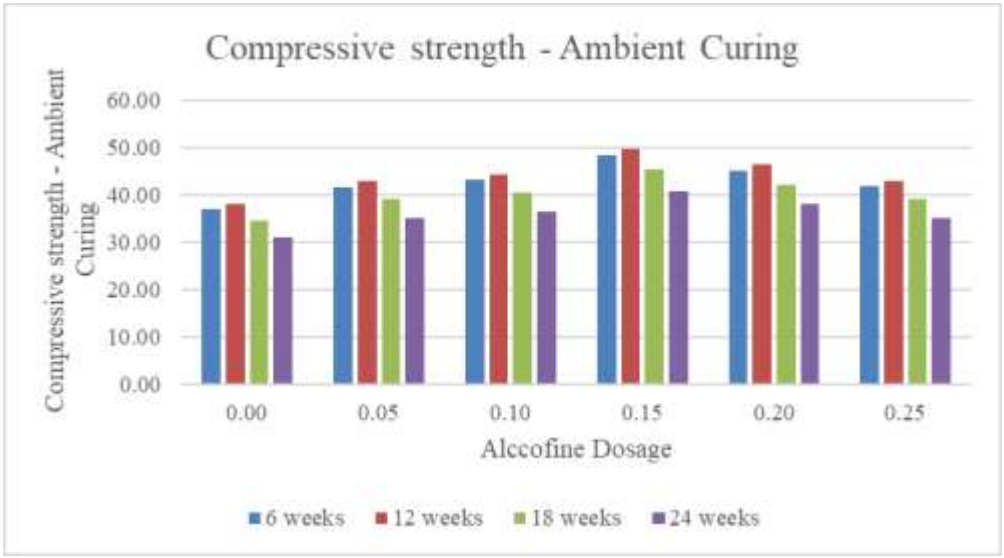

Fig. 4.41: Compressive strength of ambient-cured geopolymer concrete immersed in seawater with varying percentages of alccofine replacement

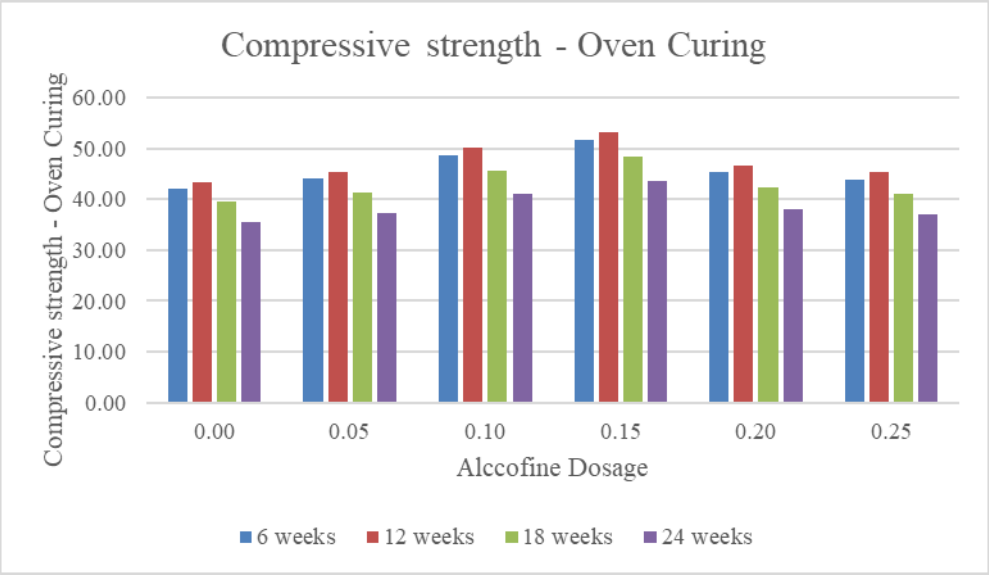

Fig. 4.42: Compressive strength of oven-cured geopolymer concrete immersed in seawater with varying percentages of alccofine replacement

4.9.2 Effect of sulphate attack

The sulfate attack test was conducted by preparing a sulfate solution in the laboratory, dissolving magnesium sulfate in tap water in accordance with ASTM guidelines. Geopolymer concrete (GPC) specimens were immersed in the solution for an extended period and evaluated for weight loss and compressive strength at intervals of 6 weeks, 12 weeks, and 18 weeks during exposure to the sulfate solution.

4.9.2.1 Density

The exposure of geopolymer concrete (GPC) to magnesium sulfate solutions affects its density and mass stability. Prolonged exposure of geopolymer concrete (GPC) to aggressive environments results in a reduction in density and mass loss, primarily due to chemical degradation and leaching processes. Oven-cured specimens with 25% Alccofine achieved a maximum density of 2520 kg/m³ after 12 weeks, compared to 2506 kg/m³ for ambient-cured specimens. Prolonged magnesium sulfate exposure reduced density, with oven-cured GPC stabilizing at 2505 kg/m³ and ambient-cured at 2481 kg/m³ after 18 weeks.

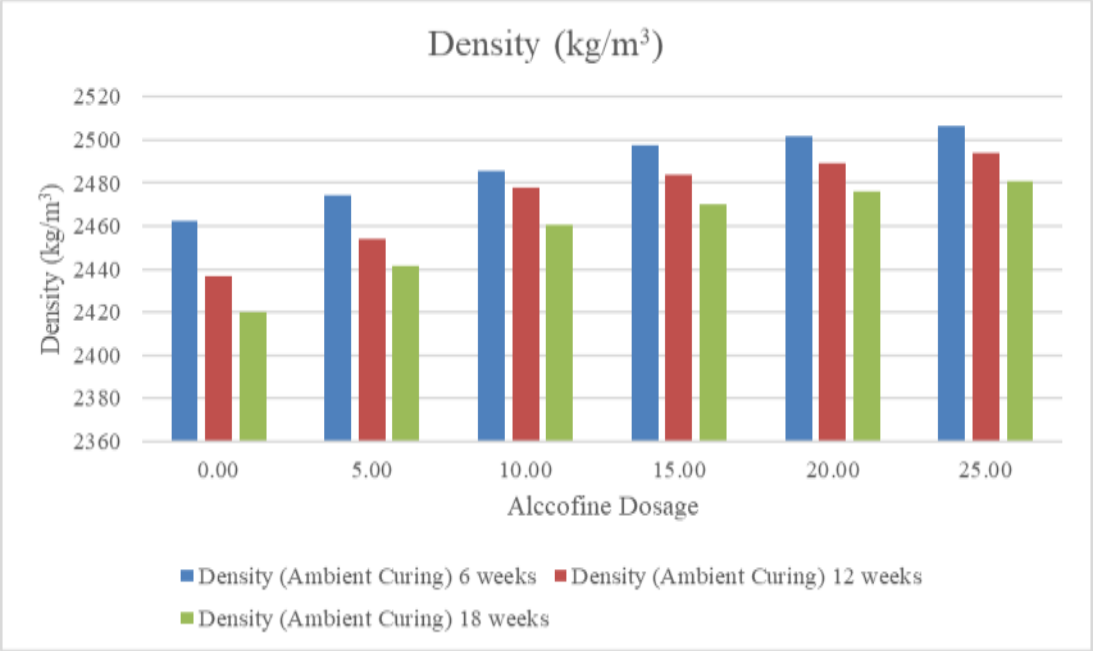

Fig. 4.43: Density of ambient-cured geopolymer concrete immersed in seawater with varying percentages of alccofine replacement

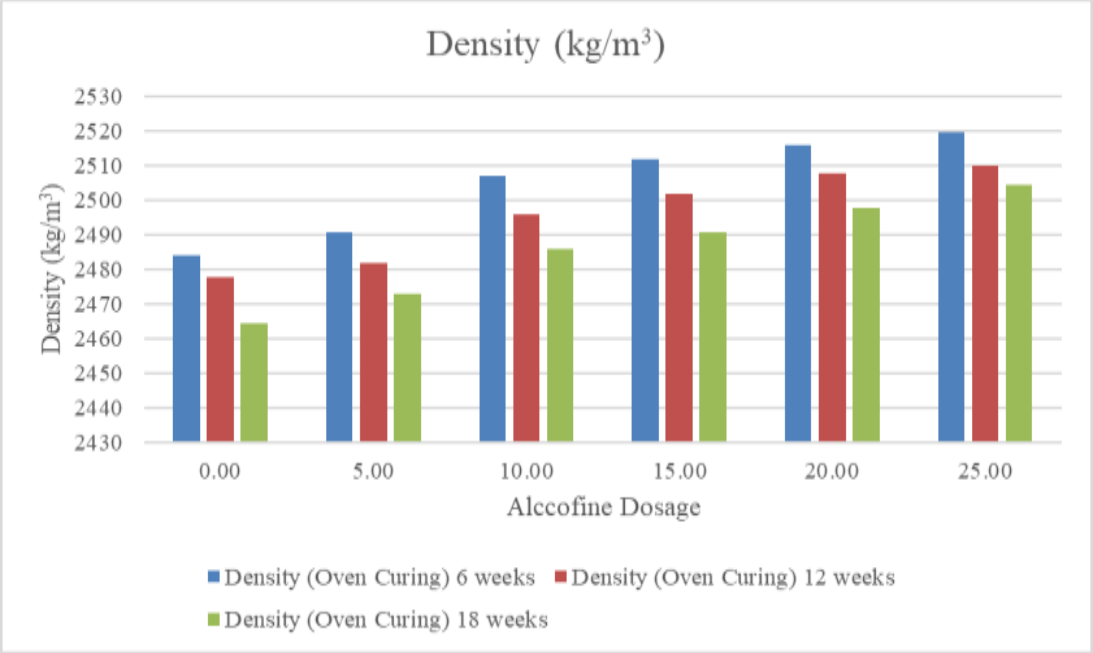

Fig. 4.44: Density of oven-cured geopolymer concrete immersed in seawater with varying percentages of alccofine replacement

4.9.2.2 Compressive strength

The compressive strength of geopolymer concrete (GPC) exposed to sulfate solutions is influenced by the dosage of Alccofine and the curing method. As shown in Fig. 4.45 and Fig. 4.46 ambient-cured GPC specimens achieved a maximum compressive strength of 42.47 MPa after 12 weeks at a 15% Alccofine dosage, while oven-cured specimens attained 45.53 MPa under the same conditions. However, prolonged sulfate exposure led to a gradual decrease in strength, with ambient-cured specimens stabilizing at 35.01 MPa and oven-cured samples at 39.30 MPa after 18 weeks. This reduction in compressive strength after extended exposure is attributed to chemical reactions such as the formation of ettringite and gypsum due to sulfate attack.

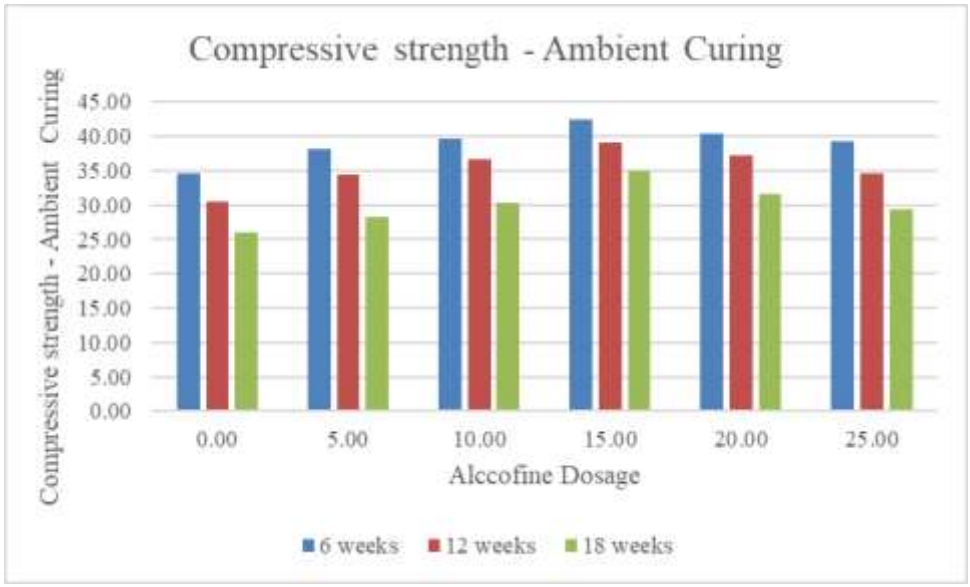

Fig. 4.45: Compressive strength of ambient-cured geopolymer concrete immersed in seawater with varying percentages of alccofine replacement

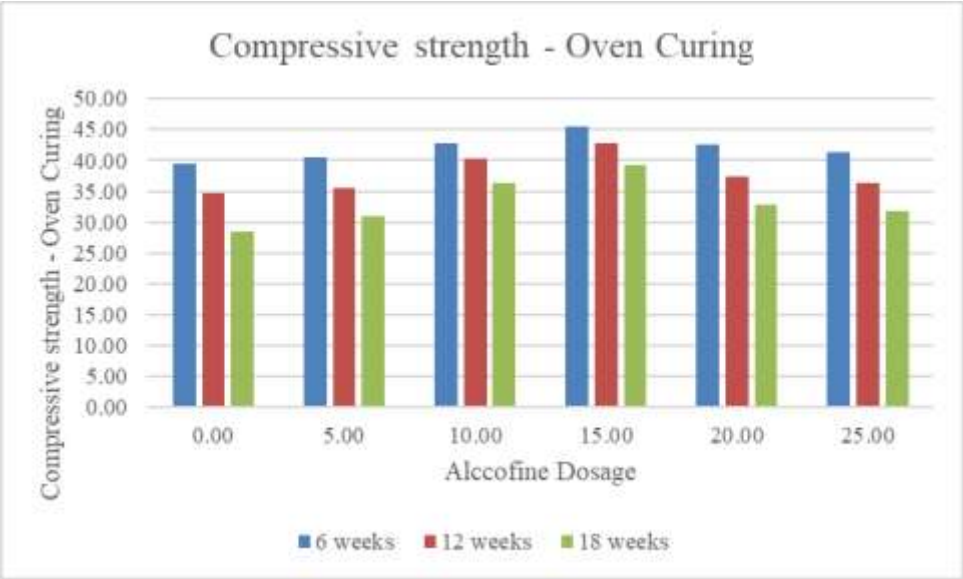

Fig. 4.46: Compressive Strength of Oven-Cured Geopolymer Concrete Immersed in Seawater with Varying Percentages of Alccofine Replacement

4.9.3 Effect of Acid Attack

The acid attack test was performed by preparing a 5% sulfuric acid solution in the laboratory, adhering to ASTM guidelines. Geopolymer concrete (GPC) specimens were submerged in the solution for an extended duration. The specimens were analyzed for weight loss and compressive strength at intervals of 6 weeks, 12 weeks, and 18 weeks while exposed to the acidic solution.

4.9.3.1 Density

The density and mass stability of geopolymer concrete (GPC) in acidic environments depend on Alccofine dosage and curing conditions. Alccofine showed superior resistance compared to fly ash-based GPC due to its dense, and enhanced calcium silicate hydrate (C-S-H) gel formation. Oven-cured specimens with 25% Alccofine achieved a maximum density of 2505.46 kg/m³ at 12 weeks. Ambient-cured specimens showed similar trends, with densities reducing to 2492 kg/m³.

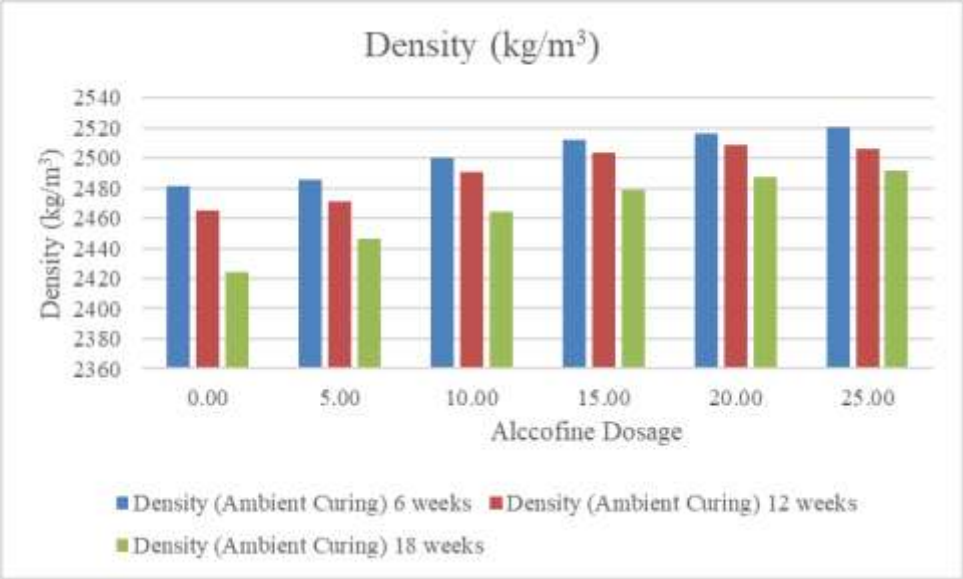

Fig. 4.47: Density of Ambient-Cured Geopolymer Concrete Immersed in Acid with Varying Percentages of Alccofine Replacement

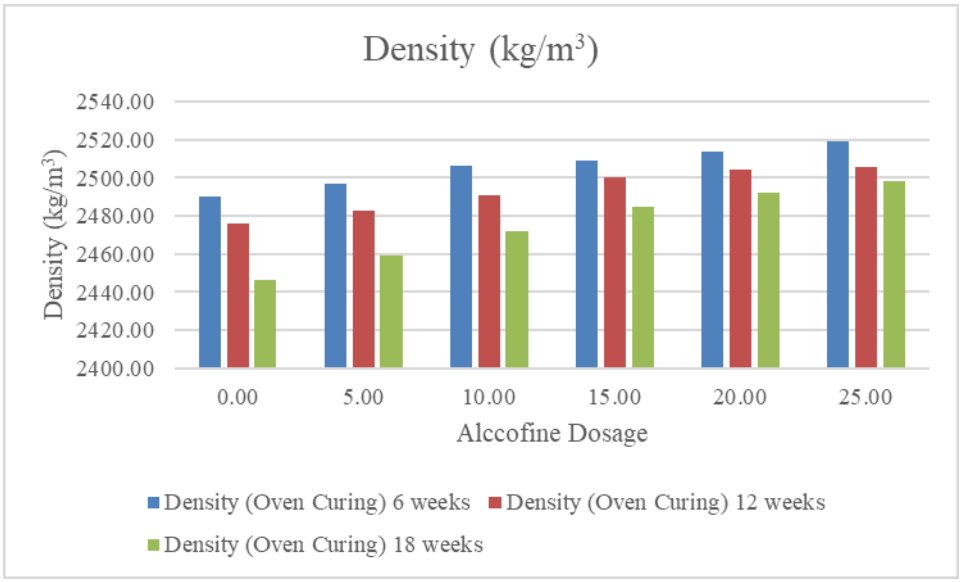

Fig. 4.48: Density of Oven-Cured Geopolymer Concrete Immersed in Acid with Varying Percentages of Alccofine Replacement

4.9.3.2 Compressive Strength

The effect of Alccofine dosage on the compressive strength of geopolymer concrete (GPC) exposed to acidic environments was evaluated under ambient and oven curing conditions. The results indicate a progressive decline in compressive strength over time (from 6 to 18 weeks) for all Alccofine dosages. An optimal dosage of 15% was identified, delivering the highest compressive strength in both curing methods: 39.08 MPa (ambient curing) and 41.89 MPa (oven curing) at 6 weeks. Beyond this dosage, compressive strength decreased. At 18 weeks, compressive strength for oven-cured specimens with 15% Alccofine remained higher (34.45 MPa) compared to their ambient-cured counterparts (31.58 MPa).

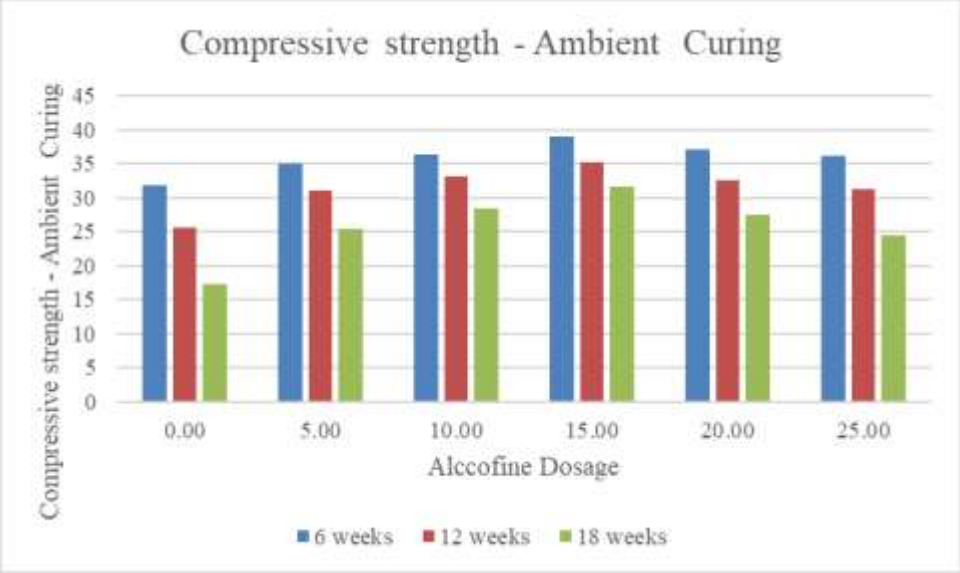

Fig. 4.49: Compressive Strength of Ambient -Cured Geopolymer Concrete Immersed in Acid with Varying Percentages of Alccofine Replacement

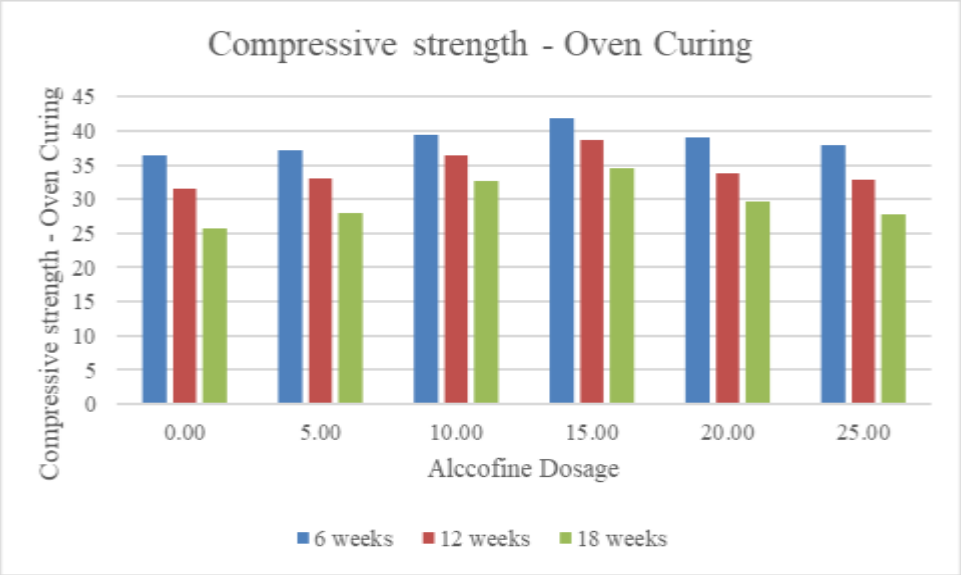

Fig. 4.50: Compressive Strength of Oven-Cured Geopolymer Concrete Immersed in Acid with Varying Percentages of Alccofine Replacement

4.9.4 Wetting-Drying Condition

The wetting-drying process was implemented through a repeated cycle, wherein the specimens were submerged in water for 24 hours, followed by exposure to ambient conditions for another 24 hours. This cycle was continuously repeated over an extended duration, up to a total of 90 cycles. Geopolymer concrete specimens underwent this procedure, and evaluations were conducted at specified intervals (30, 45, 60, 75, and 90 cycles) to assess mass loss and compressive strength.

4.9.4.1 Density

The density of geopolymer concrete (GPC) is affected by wetting and drying cycles due to moisture-induced expansion and contraction. Increased Alccofine dosage improved GPC resistance by enhancing microstructure and reducing permeability. After 30 cycles, the maximum density for oven-cured GPC with 25% Alccofine was 2478 kg/m³, slightly higher than ambient-cured specimens at 2473 kg/m³. Following 120 cycles, densities declined to 2459 kg/m³ (oven-cured) and 2462 kg/m³ (ambient-cured), reflecting cumulative matrix degradation.

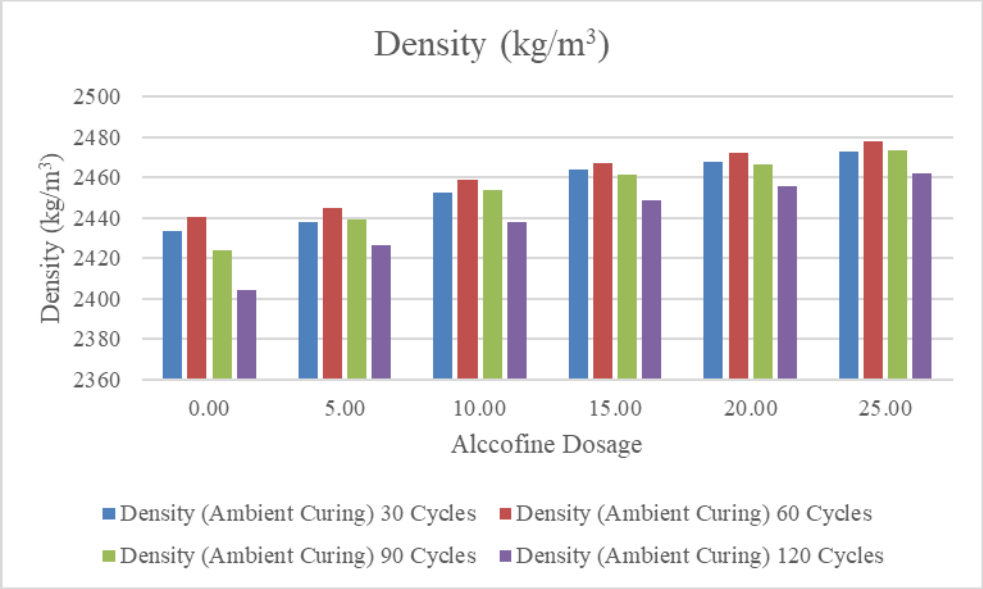

Fig. 4.51: Density of Ambient-Cured Geopolymer Concrete in Alternative Wetting-Drying with Varying Percentages of Alccofine Replacement

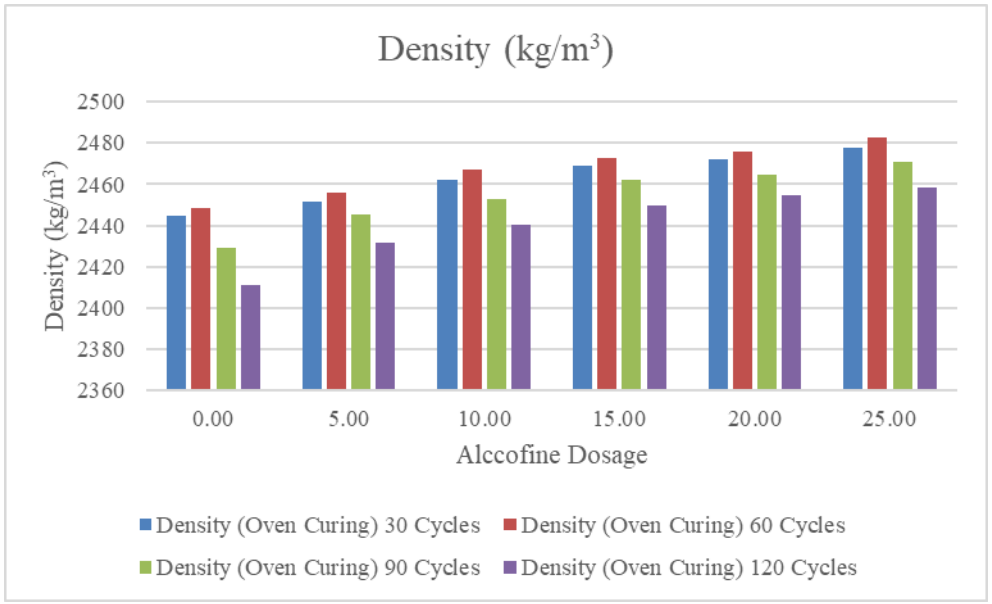

Fig. 4.52: Density of Oven-Cured Geopolymer Concrete in Alternative Wetting-Drying with Varying Percentages of Alccofine Replacement

4.9.4.2 Compressive Strength

The compressive strength of geopolymer concrete (GPC) under wetting-drying cycles is influenced by Alccofine dosage and curing conditions. These cycles cause alternating swelling and shrinkage, leading to micro-cracking and gradual strength reduction. However, GPC's chemical stability and dense matrix, enhanced by Alccofine, help mitigate these effects, maintaining higher long-term strength compared to conventional concrete in similar conditions. As shown in Fig. 4.53 and Fig. 4.54, the maximum compressive strength after 60 wetting-drying cycles was 36.85 MPa for oven-cured GPC at a 15% Alccofine dosage, while ambient-cured specimens achieved 34.66 MPa at the same dosage. After 90 cycles, compressive strength decreased to 34.45 MPa (oven-cured) and 32.14 MPa (ambient-cured), reflecting the impact of continuous wetting-drying-induced stress. After 120 cycles, oven-cured specimens retained 31.44 MPa, while ambient-cured samples stabilized at 30.32 MPa.

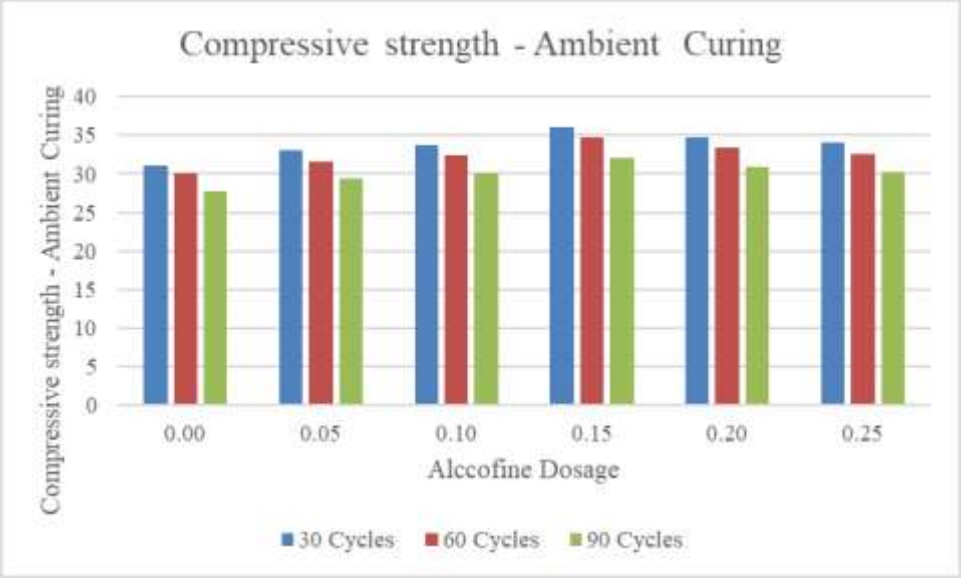

Fig. 4.53: Compressive Strength of Ambient -Cured Geopolymer Concrete in Alternative Wetting-Drying with Varying Percentages of Alccofine Replacement

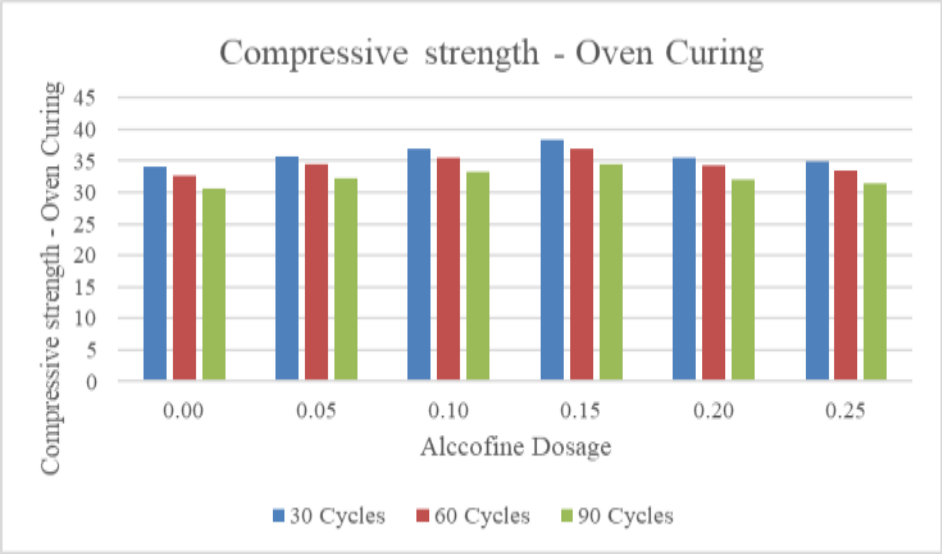

Fig. 4.54: Compressive Strength of Ambient -Cured Geopolymer Concrete in Alternative Wetting-Drying with Varying Percentages of Alccofine Replacement

4.10 Conclusion

This chapter comprehensively explores the effects of critical parameters and environmental conditions on the performance of geopolymer concrete (GPC), with a special focus on the role of Alccofine. The inclusion of Alccofine significantly enhances the mechanical and durability properties of GPC due to its fine particle size, high pozzolanic activity and contribution to calcium silicate hydrate (C-S-H) gel formation. Optimal Alccofine dosage, identified at 15%, improves compressive strength, flexural strength and splitting tensile strength under both ambient and oven curing conditions. Oven curing further amplifies these benefits by accelerating geopolymerization and creating a denser matrix. Environmental exposure tests reveal that GPC with Alccofine exhibits superior resistance to acid, sulfate and seawater attacks, as well as cyclic wetting-drying conditions. The addition of Alccofine mitigates mass loss and degradation, and enhances mechanical stability resulting in improved long-term durability. However, excessive Alccofine content may compromise workability and lead to segregation, emphasizing the importance of dosage optimization. In conclusion, the study confirms that Alccofine is a valuable additive for enhancing the performance of GPC.

Chapter 5

The Optimized Machine Learning Methods to Evaluate Compressive Strength of Geopolymer Concrete

5.1 Introduction

This chapter elaborates on the predictive modeling of the compressive strength of alccofine-based geopolymer concrete using machine learning algorithms applied to the data presented in Chapter 4. To account for the complex, non-linear interactions among factors affecting compressive strength, the basic and advanced machine learning methods Artificial Neural Networks (ANN), Support Vector Regression (SVR), Gene Expression Programming (GEP), Bidirectional Long Short-Term Memory (Bi-LSTM) networks and optimization algorithms like the Self-Improved Jelly Search (JS) optimizer were used to predict this compressive strength. Each model evaluates many significant aspects, including alccofine concentration, curing conditions, and mix proportions. A thorough comparison study was performed using statistical measures such as R^2, MAE, RMSE and MAPE to assess the predicted accuracy and dependability of each model.

5.2 Basic Machine Models

In this study, basic machine learning (ML) models, including Support Vector Regression (SVR), Gene Expression Programming (GEP), and Artificial Neural Networks (ANN), are implemented to perform predictive analysis and optimization effectively.

SVR excels in handling high-dimensional data and provides robust predictions for classification and regression tasks. GEP, an evolutionary algorithm, develops mathematical models that reveal complex variable relationships. ANN, inspired by the human brain, captures nonlinear patterns, making it particularly effective for predicting GPC's mechanical properties and performance. These models analyze experimental data, optimize mix designs, and deepen the understanding of GPC behavior. Their performance is evaluated using

statistical metrics like R^2, MSE, RMSE, MAE, and MAPE, ensuring accurate insights and hypothesis testing. This streamlined approach eliminates redundancy while maintaining clarity and focus.

5.2.1 SVM Model

The compressive strength of geopolymer concrete mixed with Alccofine was evaluated using a robust experimental dataset, split into training and testing sets in a 70:30 ratio using Python. Table 5.1 compares five Support Vector Regression (SVR) models (S1 to S5), highlighting differences in kernel functions, kernel scales, prediction speeds, and training times. The Linear SVR model (S1) demonstrated the fastest prediction speed (650 observations/second) and shortest training time (15.49 seconds). The Cubic SVR model (S3), while slightly slower at 610 observations/second with a training time of 16.27 seconds, balanced computational efficiency with superior predictive performance.

Table 5.1: Different Models Developed Using SVR

Model	Preset	Kernel function	Kernel scale	Prediction speed (obs/sec)	Training time (sec)
S1	Linear SVR	Linear	Automatic	650	15.49
S2	Quadratic SVR	Quadratic	Automatic	640	16.59
S3	Cubic SVR	Cubic	Automatic	610	16.27
S4	Fine Gaussian SVR	Gaussian	0.83	590	15.96
S5	Medium Gaussian SVR	Gaussian	3.3	630	15.66

Table 5.2 reveals that the third model, using a cubic kernel function in SVR, produces the most precise predictions for the compressive strength of alccofine mixed geopolymer concrete. This model has a high coefficient of determination (R^2 = 0.987), a low rootmean square error (RMSE = 0.766) and a minimum mean absolute percentage error (MAPE = 3.076) in comparison to other SVR models.

Table 5.2: Statistical Analyses of Models Developed Using SVR

Statistical parameters	Model 1	Model 2	Model 3	Model 4	Model 5
R^2	0.955	0.985	0.987	0.984	0.983
RMSE	1.933	1.098	0.766	0.923	1.176
MSE	3.738	1.207	0.587	0.852	1.384
MAE	1.541	0.886	0.634	0.797	0.952
MAPE	7.598	4.367	3.076	4.253	4.996

Fig. 5.1 shows scatter plots comparing predicted and actual values for all models. The Cubic SVR model (S3) exhibited the closest alignment, confirming its high accuracy and minimal prediction error. This analysis highlights the Cubic SVR model as the optimal choice for this study

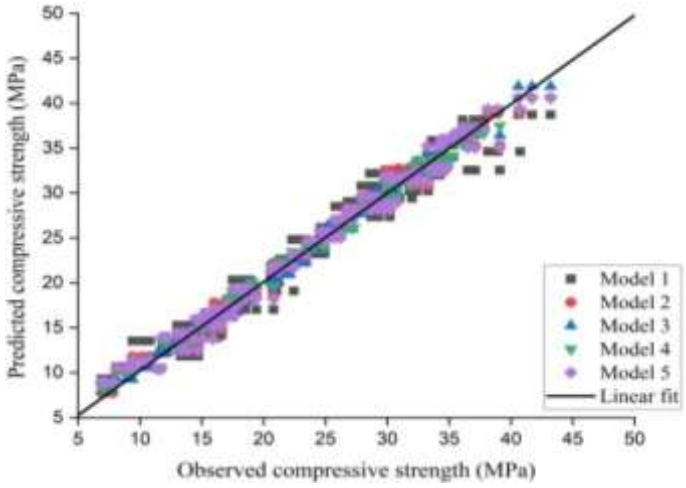

Fig. 5.1: Scatter Plots for Different Models Predicted Using SVM

5.2.2 GEP Model

The present study adopts a modelling approach where the compressive strength is treated as the dependent variable, and ten independent parameters serve as input variables, as described in Equation (5.1). The model was developed using GeneXproTools 5.0 (2020) with fundamental arithmetic operators (+, −, ×, /). High-quality datasets were randomly divided into training and testing phases, and multiple models were created by varying the dataset proportions, program sizes, and the number of iterations, as detailed in Table 5.3. The modelling process utilized the root-mean-squared error (RMSE) as the fitness function (Ei) to evaluate model performance. The fitness value (fi) was calculated using an equation derived from the expression tree (ET), which accounts for cumulative error relative to the target value. Genetic components were synthesized through addition to construct an effective model. Fig. 5.2 illustrates the expression tree for GEP Model 3, which predicts compressive strength. The input parameters are labelled d0 to d10, with G1c5 representing the constant for gene one. A mathematical formula (Equation 5.1) was derived from Model 3, establishing an explicit relationship between input variables and the output variable, offering a comprehensive representation of the expression tree.

$$f_{cs} = \left[\frac{EW}{L} + \frac{A}{B} - 7.617C - \frac{C}{M-10.248}\right] + \left[\frac{\frac{EW}{L}\times C - \frac{L}{A} + \frac{EW}{L}\times M^3 \times \frac{L}{A} - C_t \times \frac{L}{A} + \frac{Al}{F}\times\frac{L}{A}}{C}\right] + \left[M \times \frac{EW}{L} - 6.794 \times \frac{EW}{L} - \frac{7.707}{C_d \times \frac{EW}{L} - \frac{Al}{F}\times\frac{EW}{L} - \frac{EW^2}{L}}\right] + \left[\frac{28.773C_t - 28.773C_d + \frac{EW}{L} - 11.682M - 11.682\times C_t \times \frac{EW}{L} + 11.682\times C_d \times EW/L}{11.682(C_t - C_d)\times M \times EW/L}\right] + \left[\frac{C_d}{13.374\times\frac{EW^2}{L} + 6.619\times\frac{EW^3}{L} - 3.117\times M\times\frac{EW}{L}}\right] + \left[0.164 \times \frac{\text{NaOH}}{Na_2SiO_3} + C_d \times C + 10.053C - C_t \times \frac{L}{B} - C \times \frac{L}{B}^2\right] \quad (5.1)$$

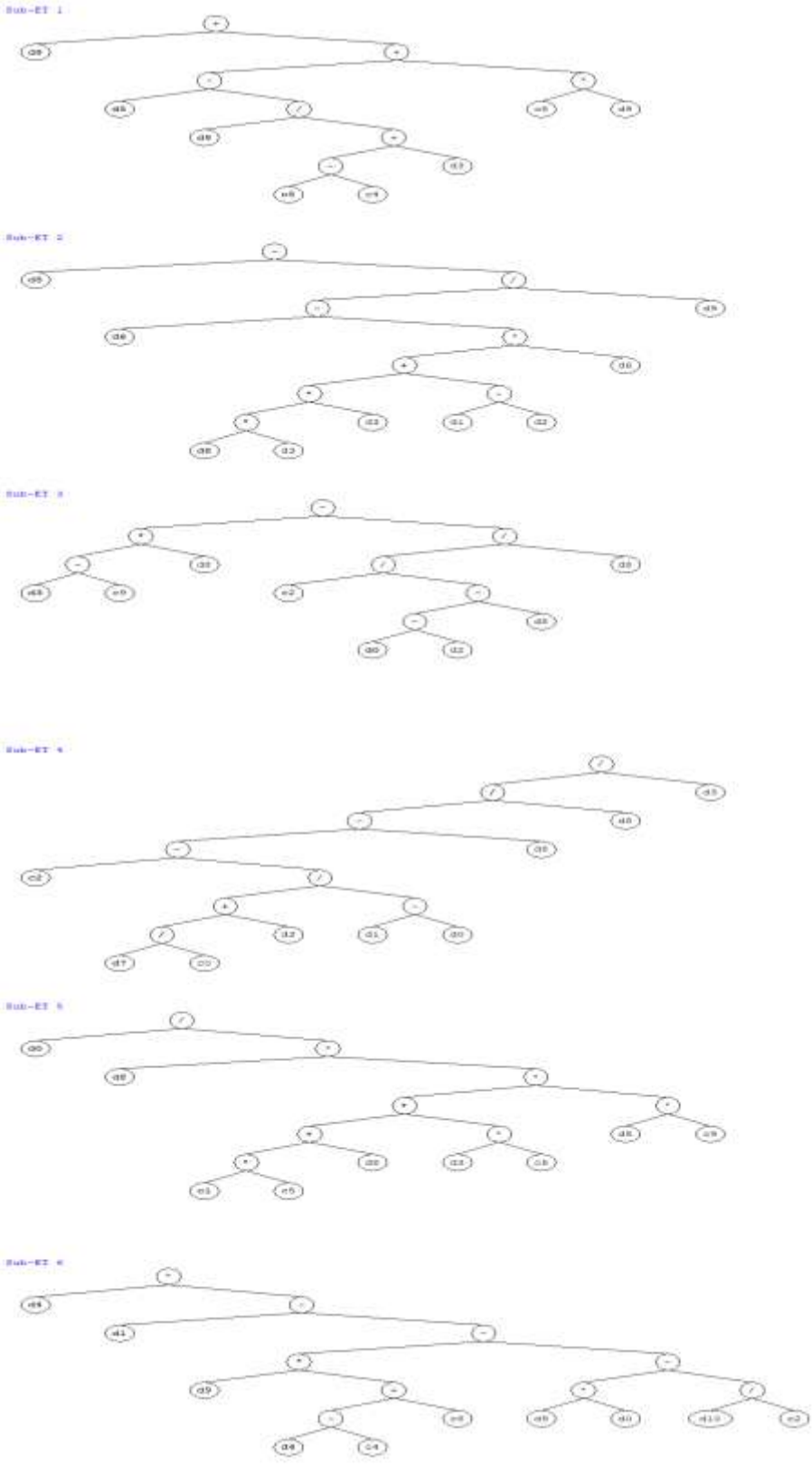

Fig. 5.2: GEP Formulated Expression Tree

Table 5.3 summarizes the models developed using Gene Expression Programming (GEP), detailing the configurations and data partitions for training and testing. Five models (M1 to M5) were generated, each with a distinct training-to-testing ratio. M1 used a 60:40 split, M2 employed a 50:50 allocation, M3 utilized 70:30, M4 adopted 80:20, and M5 designated 90% for training and 10% for testing. All models were configured with 35 chromosomes, a head dimension of 13, and 8 genes. The program sizes ranged from 97 to 108, influenced by these factors. The number of literals varied between 38 and 42, while the total number of generations exhibited significant variation, ranging from 163,512 for M3 to 356,685 for M1.

Table 5.3: Models Generated Using GEP

Model	Training data (in percent)	Testing data (in percent)	No. of chromosomes	Head size	No. of genes	Gene size	Program size	Literals	No. of generations
M1	60	40	35	13	8	40	108	42	356685
M2	50	50	35	13	8	40	97	38	270412
M3	70	30	35	13	8	40	105	39	163512
M4	80	20	35	13	8	40	105	40	260011
M5	90	10	35	13	8	40	98	39	275016

According to the data in Table 5.4, the fifth model of GEP, employing eight genes, thirteen head sizes and a 90 percent to 10 percent data distribution for training and testing, produced the most precise predictions for the compressive strength of alccofine mixed geopolymer concrete relative to other GEP models. The result is substantiated by the model's elevated R^2 value of 0.995, low RMSE of 1.012 and negligible MAPE of 3.776.

Fig. 5.3 presents scatter plots comparing the predicted and actual compressive strength values for the different models developed using Gene Expression Programming (GEP). Among these models, the third model (M3) demonstrates superior accuracy, showing closer

alignment between the predicted and actual values. This indicates that M3 achieves minimal error and provides better predictive performance compared to the other models.

Table 5.4: Statistical Analysis of Models Developed Using GEP

Statistical parameters	Model 1	Model 2	Model 3	Model 4	Model 5
R^2	0.977	0.978	0.995	0.974	0.987
RMSE	1.357	1.338	1.143	1.442	1.012
MSE	1.841	1.791	1.306	2.078	1.040
MAE	0.985	1.022	0.866	1.092	0.797
MAPE	4.631	4.867	4.141	5.599	3.776

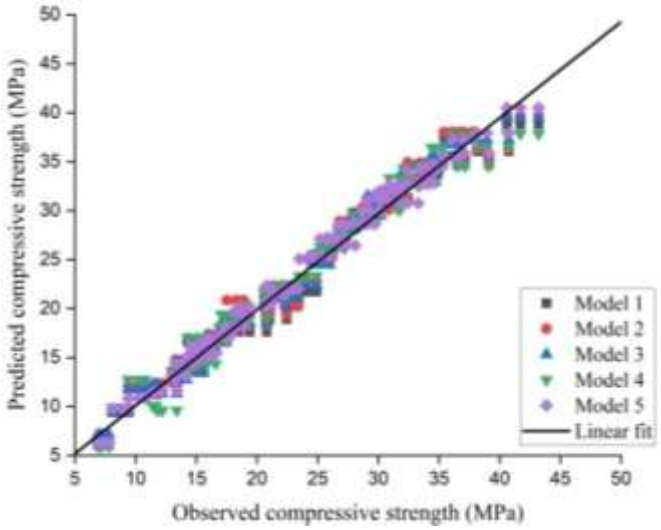

Fig. 5.3: Scatter Plots for Different Models Predicted Using GEP

5.2.3 ANN Architecture

The study utilized an artificial neural network (ANN) to predict the compressive strength of geopolymer concrete combined with alccofine. A feed-forward network was developed in Python using a back-propagation training algorithm. The ANN architecture consisted of 11

neurons in the input layer, a variable number of neurons in the hidden layer, and a single output neuron, as detailed in Table 5.5. Five ANN models (M1 to M5) were constructed using the TRAINLM training function, varying in hidden neurons, epochs, and performance metrics. Model M1, with 7 hidden neurons and trained over 22 epochs, achieved the best performance score of 0.92, a gradient of 0.480, and a Mu value of 0.100. The training process, illustrated in Fig. 5.4, exhibited a rapid decline in error during the initial phase, followed by convergence after 19 generations. Fig. 5.5 presents the error trends during training, testing, and validation, highlighting the progressive reduction in inaccuracies. This analysis underscores the significance of hidden neurons and training epochs in influencing model performance, offering critical insights for optimizing ANN design for accurate predictions.

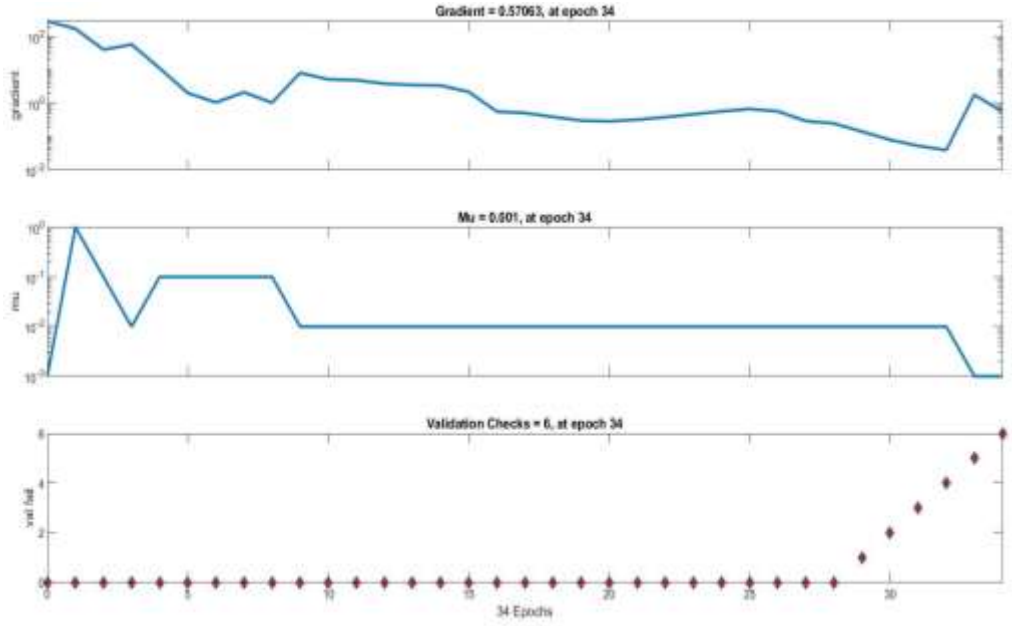

Fig. 5.4: Training Parameters During ANN Modeling

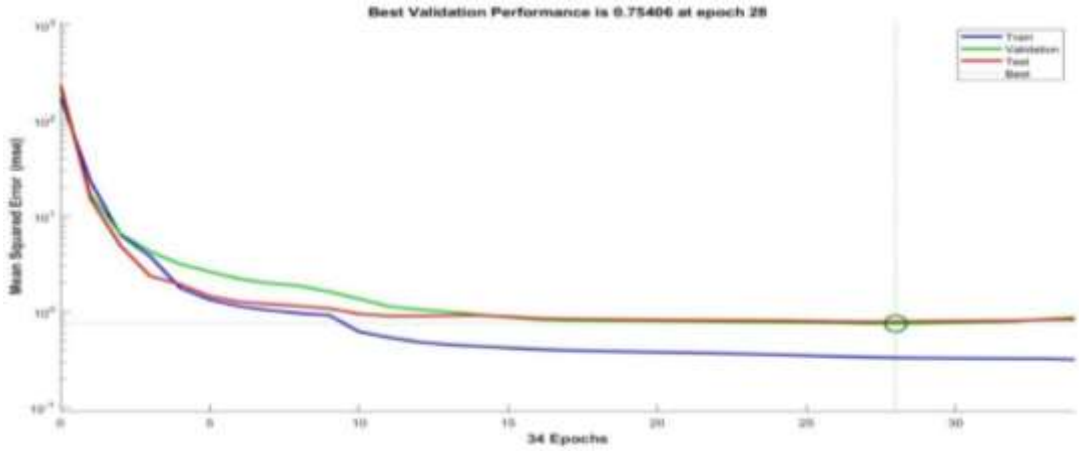

Fig. 5.5: Convergence Curve for the Training of Backpropgation Neural Network (BPNN)

Table 5.5: Models Developed Using Artificial Neural Network (ANN)

Model	Input Neurons	Hidden Neurons	Epochs	Performance	Gradient	Mu	Validation Checks	Training Function
M1	10	7	22	0.92	0.480	0.100	6	TRAINLM
M2	10	8	34	0.317	0.571	0.001	6	TRAINLM
M3	10	9	21	0.374	0.195	0.010	6	TRAINLM
M4	10	10	13	0.607	2.76	0.010	6	TRAINLM
M5	10	11	44	0.365	0.550	0.010	6	TRAINLM

The data in Table 5.6 clearly indicates that the second ANN model, employing eight neurons in the hidden layers and TRAINLM as the training function, produces the most precise predictions for the compressive strength of alccofine mixed geopolymer concrete, as demonstrated by its high R^2 value of 0.993, low RMSE value of 0.683 and low MAPE value of 2.492, surpassing the performance of the other ANN models.

Fig. 5.6 presents scatter plots illustrating the predicted versus actual compressive strength values of geopolymer concrete for various ANN models. Among these, the second ANN model demonstrates superior performance, with predicted values showing closer alignment to

the actual values. This reduced error and improved agreement indicate the model's effectiveness in accurately predicting the compressive strength of geopolymer concrete.

Table 5.6: Statistical Analysis of Models Developed Using ANN

Statistical Parameters	Model 1	Model 2	Model 3	Model 4	Model 5
R^2	0.981	0.993	0.990	0.983	0.990
RMSE	1.230	0.683	0.913	1.179	0.888
MSE	1.513	0.466	0.834	1.392	0.788
MAE	0.912	0.528	0.655	0.938	0.686
MAPE	4.699	2.492	3.199	4.854	3.707

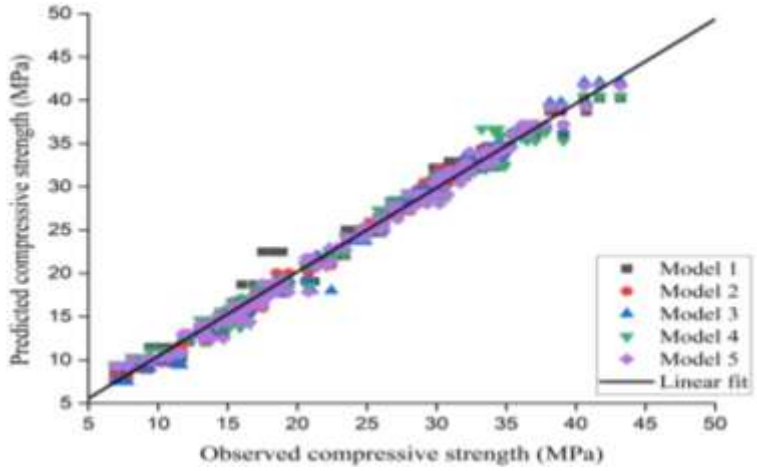

Fig. 5.6: Scatter Plots for Different Models Predicted Using ANN

The predictive effectiveness of the SVR, GEP, and ANN models is evident from their close alignment with the line representing positive agreement. Among the models, SVR Model 3,

GEP Model 3, and ANN Model 2 exhibit projected values that closely follow the optimal fitted line, while other models display a more scattered distribution. Notably, the GEP model demonstrates greater variability in its predictions compared to SVR and ANN. Fig. 5.7 provides a comparative analysis of the most effective models for predicting the compressive strength of alccofine-based geopolymer concrete, highlighting the strong alignment of the predicted values with the experimental data. The absence of overtraining syndrome further validates the robustness of these models. A detailed performance comparison, presented in Table 5.7, evaluates the models using statistical error metrics such as the coefficient of determination (R^2), mean square error (MSE), root mean square error (RMSE), mean absolute error (MAE), and mean absolute percentage error (MAPE). Among the models, GEP Model 3 demonstrates superior performance, outperforming all prior models constructed using SVR and ANN, thereby underscoring its effectiveness in predicting the compressive strength with greater accuracy and generalization potential.

Table 5.7: Statistical Analysis of Predicted Compressive Strength by Various Approaches

Statistical Parameters	SVR Model 3	GEP Model 5	ANN Model 2
R^2	0.987	0.995	0.993
RMSE	0.766	1.012	0.683
MSE	0.587	1.04	0.466
MAE	0.634	0.797	0.528
MAPE	3.076	3.776	2.492

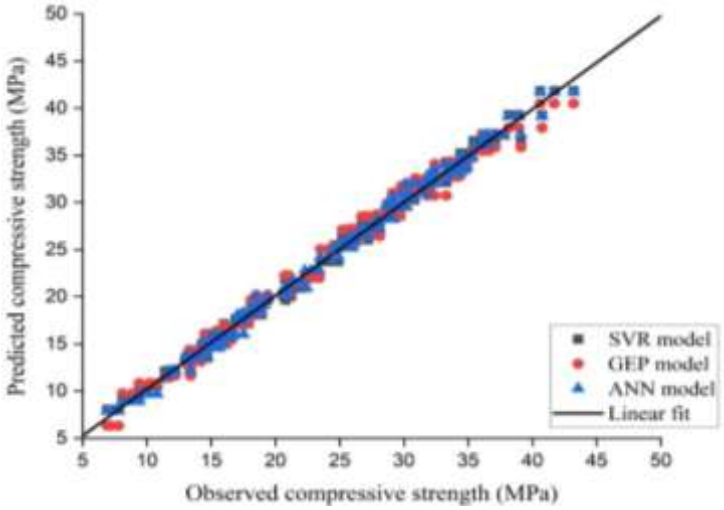

Fig. 5.7: Comparison of Best-Proposed Models

5.3 Advanced Machine Learning

Advanced machine learning models such as Bidirectional Long Short-Term Memory (Bi-LSTM) networks and optimization algorithms like the Self-Improved Jelly Search (JS) optimizer have emerged as cutting-edge tools in geopolymer concrete (GPC) research. Bi-LSTM, a variant of recurrent neural networks (RNNs), is adept at capturing long-range dependencies and contextual information in sequential data, making it particularly valuable for modelling time-dependent or process-driven behaviors in GPC properties. The JS optimizer, a novel met heuristic algorithm, enhances the search for optimal solutions by incorporating self-adaptive mechanisms, improving convergence speed and ensuring better global optimization. Together, these advanced methods provide powerful frameworks for predictive modelling, optimizing mix designs and uncovering intricate relationships within GPC data, contributing to the development of superior and sustainable concrete materials.

5.3.1 Simulation Setup

The proposed framework for predicting compressive strength was implemented and simulated using Python version 3.7. The simulation was conducted on a system equipped

with an 11th Gen Intel(R) Core (TM) i3-1115G4 processor, operating at a base frequency of 3.00 GHz, and a total installed RAM capacity of 8.00 GB.

5.3.2 Performance Analysis

In this analysis, the distinct labels were considered: Predicting Compressive Strength, the predictive analysis encompassed the assessment of Bi-LSTM+SIJSO and conventional approaches, with a thorough examination of various error metrics, including MAE, MAPE, MSE, MSLE and RMSE.

5.3.3 Error Analysis on Bi-LSTM1+SIJSO to Predict Compressive Strength

Fig. 5.8 illustrates the error assessment of our Bi-LSTM+SIJSO model in comparison to various other models, including Bi-LSTM+AOA, Bi-LSTM+BMO, Bi-LSTM+BOA, Bi-LSTM+BWO and Bi-LSTM+CA, for predicting Compressive strength. We conducted an analysis by varying the learning percentages and evaluating performance metrics such as MAE, MAPE, MSE, MSLE and RMSE. The objective was to achieve more accurate predictions of compressive strength by minimizing error ratings. As depicted in the graphical representation, our Bi-LSTM+SIJSO model consistently demonstrated lower error values, indicating its superior ability to precisely predict compressive strength. Primarily, when the training percentage is set at 70, the Bi-LSTM+SIJSO approach achieves an impressive MAPE of 0.007. In contrast, the conventional strategies yield higher MAPE values, with Bi-LSTM+AOA at 0.034, BI-LSTM+BMO at 0.028, Bi-LSTM+BOA at 0.021, Bi-LSTM+BWO at 0.024 and Bi-LSTM+CA at 0.033, respectively. In addition, the least MSE is attained using Bi-LSTM+SIJSO is 0.008 attaining rate 80, mean while the Bi-LSTM+AOA, Bi-LSTM+BMO, Bi-LSTM+BOA, Bi-LSTM+BWO and Bi-LSTM+CA scored greater MSE ratings. The exceptional performance exhibited by the Bi-LSTM+SIJSO approach underscores its capability to make precise predictions of compressive strength. This achievement is made possible through the improved normalization-based pre-processing and the final prediction accomplished with the aid of SIJSO.

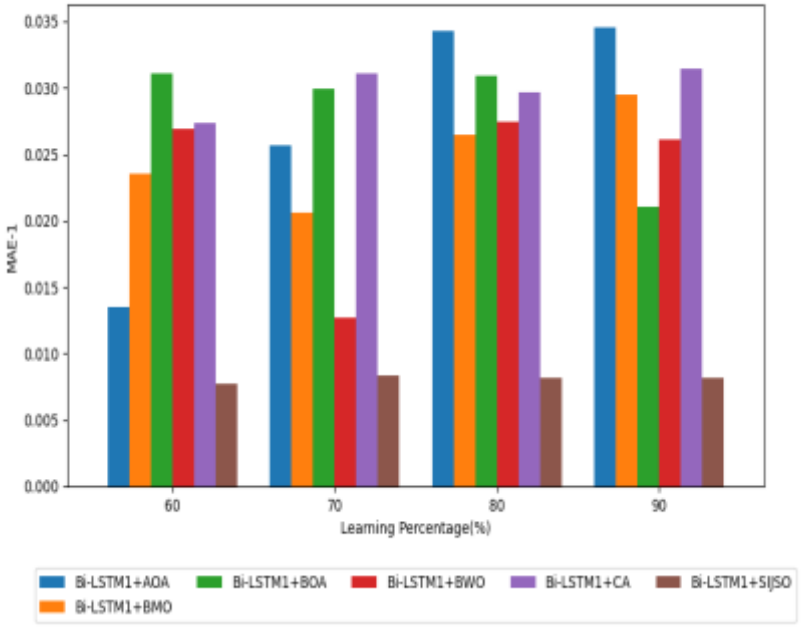
0.035
0.030
0.025
0.020
0.015
0.010
0.005
0.000
MAE-1
60
70
80
90
Learning Percentage(%)
Bi-LSTM1+AOA
Bi-LSTM1+BOA
Bi-LSTM1+BWO
Bi-LSTM1+CA
Bi-LSTM1+SIJSO
Bi-LSTM1+BMO

(a)

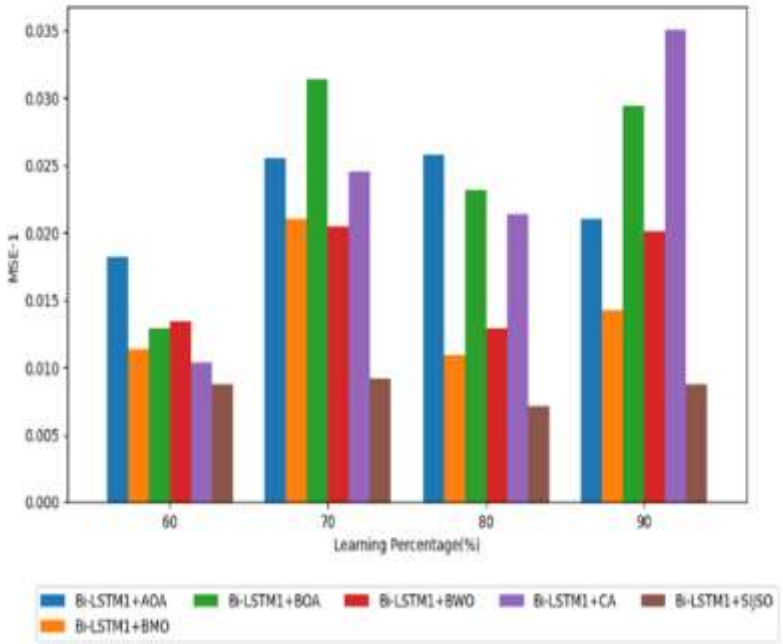
0.035
0.030
0.025
0.020
0.015
0.010
0.005
0.000
MSE-1
60
70
80
90
Learning Percentage(%)
Bi-LSTM1+AOA
Bi-LSTM1+BOA
Bi-LSTM1+BWO
Bi-LSTM1+CA
Bi-LSTM1+SIJSO
Bi-LSTM1+BMO

(b)

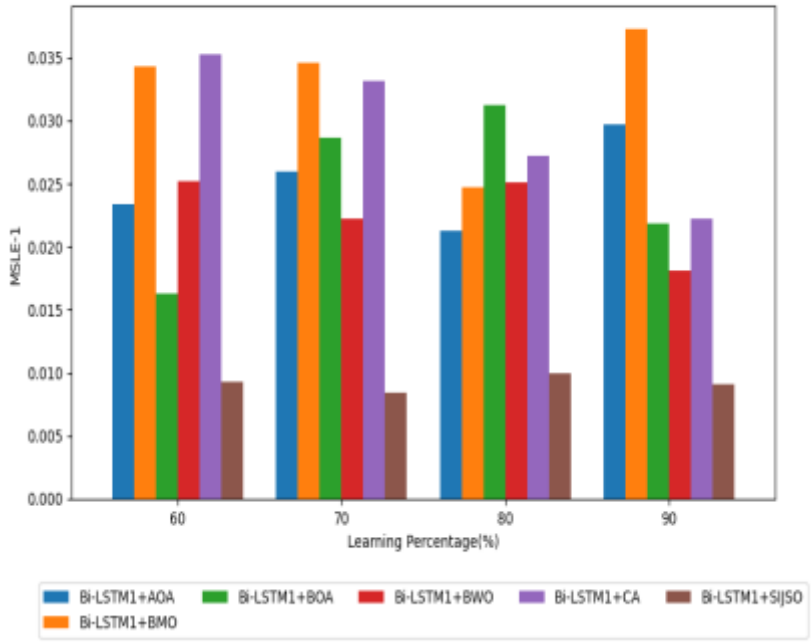
MSLE-1
0.035
0.030
0.025
0.020
0.015
0.010
0.005
0.000
60
70
80
90
Learning Percentage(%)
Bi-LSTM1+AOA
Bi-LSTM1+BOA
Bi-LSTM1+BWO
Bi-LSTM1+CA
Bi-LSTM1+SIJSO
Bi-LSTM1+BMO

(c)

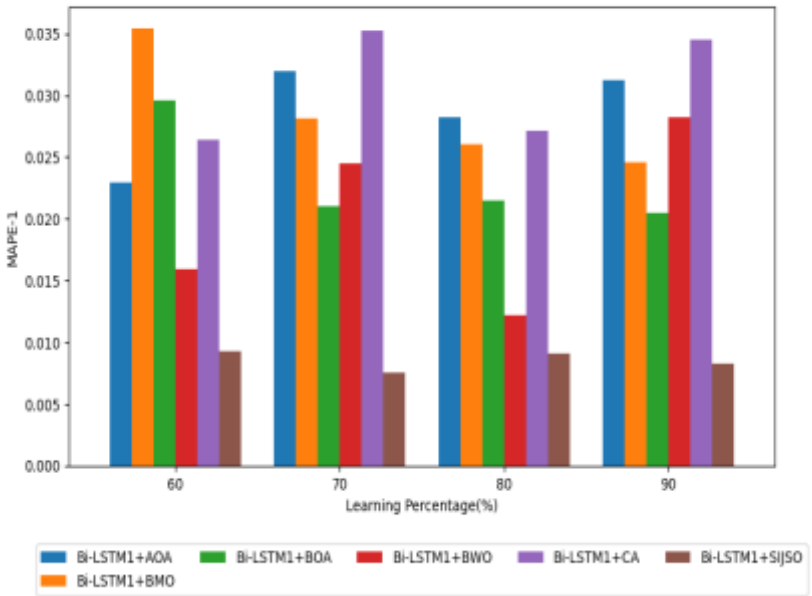
MAPE-1
0.035
0.030
0.025
0.020
0.015
0.010
0.005
0.000
60
70
80
90
Learning Percentage(%)
Bi-LSTM1+AOA
Bi-LSTM1+BOA
Bi-LSTM1+BWO
Bi-LSTM1+CA
Bi-LSTM1+SIJSO
Bi-LSTM1+BMO

(d)

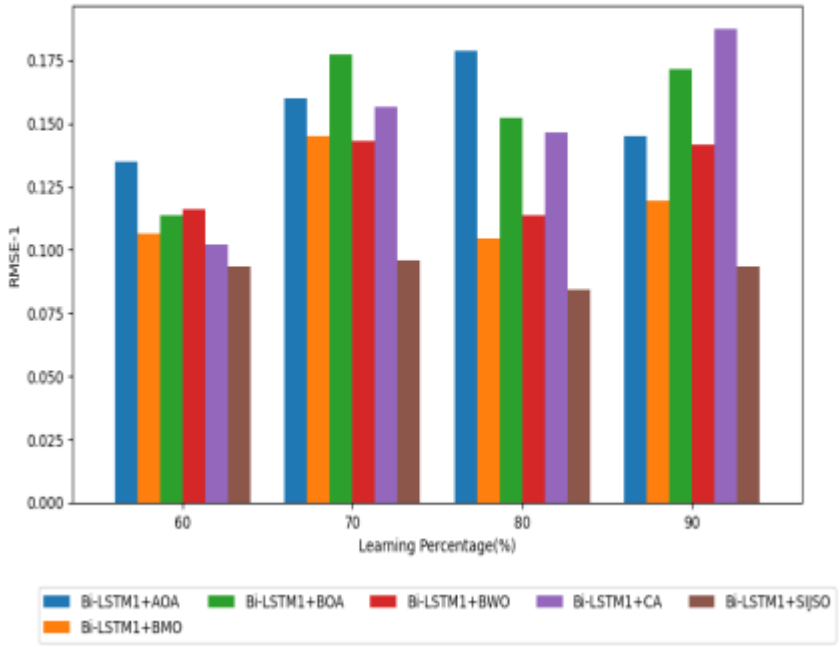

(e)

Fig. 5.8: Error Evaluation On Bi-LSTM-SIJSO and Conventional Schemes (a) MAE (b) MAPE (c) MSE (d) MSLE and (e) RMSE for the Prediction of Compressive Strength

Table 5.8 presents a comparison of classifiers between Bi-LSTM and conventional classifiers for prediction of compressive strength. Furthermore, we evaluate the performance of the proposed classifier (Bi-LSTM) against Bi-GRU, GRU, RNN, NN, CNN and LSTM. Mainly, the RMSE of the Bi-LSTM scheme is 0.092, whilst the Bi-GRU (0.260), GRU (0.229), RNN (0.213), NN (0.236), CNN (0.208) and LSTM (0.109) scored higher RMSE ratings.

Table 5.8: Classifier Comparison on Bi-LSTM and Conventional Classifiers for the Prediction of Compressive Strength

Metrics	Bi-LSTM	Bi-GRU	GRU	RNN	NN	CNN	LSTM
MSE	0.008	0.068	0.053	0.045	0.056	0.043	0.012
MAE	0.021	0.138	0.116	0.120	0.127	0.116	0.022
MSLE	0.005	0.034	0.026	0.020	0.028	0.021	0.006
MAPE	0.123	0.945	0.773	0.412	0.210	0.578	0.526
RMSE	0.092	0.260	0.229	0.213	0.236	0.208	0.109

5.3.4 Statistical Analysis on Error

Table 5.9 describes the statistical assessment on SIJO methodology is compared with AOA, BMO, BOA, BWO and CA for compressive strength prediction framework. In order to ensure the generation of highly precise calculations, each approach undergoes a comprehensive evaluation process. This evaluation involves a meticulous analysis of key statistical measurements, encompassing parameters such as minimum, mean, standard deviation, median and maximum values. When these metrics are combined, they provide a comprehensive insight into the effectiveness and consistency of the tactics being researched. Considering the mean statistical metric, the Bi-LSTM-SIJO scored the least error value of 0.032, whereas the Bi-LSTM-AOA, Bi-LSTM-BMO, Bi-LSTM-BOA, Bi-LSTM-BWO and Bi-LSTM-CA resulted in greater error ratings. Additionally, the SIJO approach yields the lowest error rate, which stands at 0.018 when considering the minimal statistical metric. Meanwhile, the error rates for other metrics are as follows: Bi-LSTM-AOA at 0.020, Bi-LSTM-BMO at 0.027, Bi-LSTM-BOA at 0.022, Bi-LSTM-BWO at 0.021 and Bi-LSTM-CA at 0.026.

Table 5.9: Statistical Evaluation on Error

Statistical Metrics	Bi-LSTM AOA	Bi-LSTM BMO	Bi-LSTM BOA	Bi-LSTM BWO	Bi-LSTM CA	Bi-LSTM SIJO
Mean	0.034	0.036	0.036	0.036	0.035	0.032
Minimum	0.020	0.027	0.022	0.021	0.026	0.018
Standard Deviation	0.009	0.005	0.006	0.008	0.006	0.010
Median	0.039	0.037	0.039	0.036	0.035	0.037
Maximum	0.043	0.043	0.043	0.043	0.043	0.043

5.3.5 Convergence Analysis

The convergence evaluation on Bi-LSTM-SIJO over Bi-LSTM-AOA, Bi-LSTM-BMO, Bi-LSTM-BOA, Bi-LSTM-BWO and Bi-LSTM-CA for compressive strength prediction framework is shown in Fig. 5.9. To enhance the prediction of compressive strength, it is vital for the model to achieve reduced error rates and demonstrate faster convergence. Initially, both the SIJO and traditional approaches demonstrated minimal error rates during the early iterations. However, as the iterations improved, the error rates decreased even more. It's important to highlight that the Bi-LSTM-SIJO approach consistently maintained a lower error rate in comparison to the conventional strategies. Specifically, at the 25th iteration, the error value for the SIJO method is 0.017, while alternative methods such as Bi-LSTM-AOA, Bi-LSTM-BMO, Bi-LSTM-BOA, Bi-LSTM-BWO and Bi-LSTM-CA yielded slightly higher error rates of 0.021, 0.028, 0.024, 0.022and 0.027, respectively. Therefore, the outstanding performance witnessed during the convergence evaluation highlights the potential of the SIJO method to achieve accurate predictions of compressive strength. This ability is directly attributable to the integration of improved normalization, Bi-LSTM classification strategy and the utilization of SIJSO for final predictions, all of which collectively contribute to an enhanced overall prediction performance.

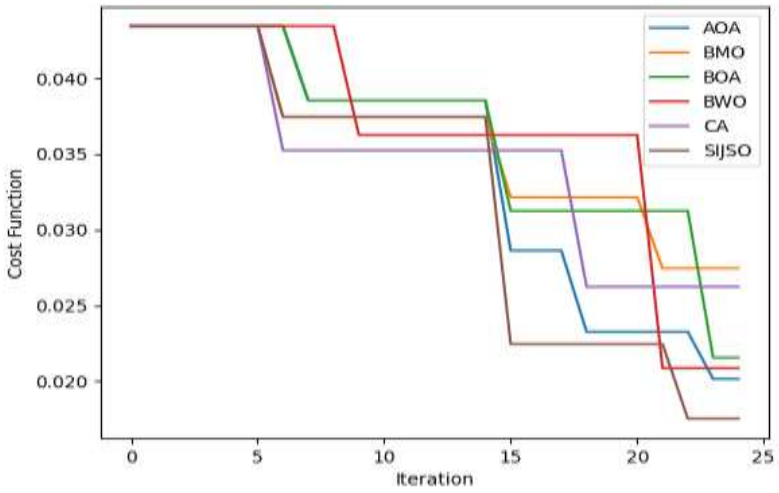

Fig. 5.9: Convergence Analysis on SIJO and Conventional Methods

5.4 Conclusion

This thesis has comprehensively demonstrated the potential of machine learning models, both basic and advanced, in predicting the compressive strength of alccofine-based geopolymer concrete and optimizing its mix designs. Among the basic models, ANN Model 2 stood out with a high R^2 value of 0.993, a low RMSE of 0.683 and a MAPE of 2.492, showcasing its robustness and predictive accuracy. SVM Model 3 with a cubic kernel achieved an R^2 of 0.987 and RMSE of 0.766, while GEP Model 3 displayed an R^2 of 0.995 with RMSE of 1.012, highlighting their effectiveness in capturing complex relationships. Advancing this work, the Bi-LSTM integrated with the Self-Improved Jelly Search Optimizer (SIJSO) further enhanced predictive performance, achieving a MAPE of 0.007, MSE of 0.008 and RMSE of 0.092, outperforming conventional Bi-LSTM models with alternative optimizers. Statistical and convergence analyses validated the SIJSO method, with the lowest mean error of 0.032 and a minimal error of 0.017 by the 25th iteration. These findings underscore the transformative potential of AI-driven approaches in designing eco-friendly and high-performance construction materials, laying a strong foundation for future research in sustainable material development and civil engineering advancements.

Chapter 6
Conclusion

6.1 General

This chapter presents the conclusions derived from the current research work. Based on the experimental results and subsequent discussions, conclusions have been drawn regarding the investigation and optimization of various control parameters, including the liquid-to-binder ratio, superplasticizer-to-liquid-binder ratio, molarity of the NaOH solution, sodium silicate-to-sodium hydroxide ratio (SS/SH), curing temperature, and alccofine replacement level, on the fresh, hardened, and durability properties of geopolymer concrete.

- The optimal liquid-to-binder (L/B) ratio for geopolymer concrete was found to be 0.55, balancing workability and strength. This ratio achieved a slump of 89 mm, indicating adequate workability while maintaining high compressive strength and density. Lower ratios such as 0.35 or 0.40 enhanced strength and density but reduced workability due to limited flowability.

- A dosage of 1.5% superplasticizer yielded superior compressive strengths of 36.00 MPa under ambient curing and 40.99 MPa under oven curing after 56 days. Exceeding this optimal dosage led to segregation and reduced density due to bleeding.

- The molarity of sodium hydroxide (NaOH) directly influenced the geopolymerization process. A 10M concentration was optimal, achieving maximum compressive strengths of 38.46 MPa under ambient curing and 41.16 MPa under oven curing. Higher molarities led to alkali saturation, while lower molarities compromised strength due to incomplete polymerization.

- The sodium silicate to sodium hydroxide (SS/SH) ratio significantly affected the geopolymer matrix. An SS/SH ratio of 2.00 provided the best results, yielding a

compressive strength of 37.50 MPa under ambient curing and 41.76 MPa under oven curing. This ratio ensured good workability, with a slump value of 91 mm, and enhanced strength through improved polymer bonding. Ratios above 2.00 increased viscosity, reducing workability and compactness.

- Curing temperature was a critical factor influencing strength and density. The optimal range was between 80°C and 100°C, achieving maximum compressive strength of 43.65 MPa and density of 2523 kg/m³. Temperatures above 100°C caused some micro-cracking due to excessive water loss and thermal stresses, while lower temperatures around 60°C produced only moderate strength due to slower geopolymerization.

- A dosage of 15% of alccofine was optimal, providing compressive strengths of 50.98 MPa under ambient curing and 53.10 MPa under oven curing after 56 days. This dosage enhanced particle packing, reduced voids. Higher dosages reduced strength due to decreased workability and incomplete reaction.

- In geopolymer concrete exposed to seawater conditions, an initial increase in strength and density is observed up to 12 weeks, attributed to continued geopolymerization. However, prolonged exposure beyond this period leads to degradation due to chemical interactions with seawater ions, causing strength reduction and mass loss.

- Geopolymer concrete subjected to acid and sulfate attacks exhibits notable mass and strength losses over time. The aggressive chemical environments deteriorate the microstructure by disrupting the polymeric chains and reducing durability.

- The study investigated compressive strength prediction in alccofine-based geopolymer concrete using machine learning models, including ANN, SVR, and GEP. Evaluation metrics such as R^2, RMSE, MAPE, assessed model performance. GEP showed superior predictive accuracy with an R^2 of 0.995 and RMSE of 1.012, while ANN (R^2: 0.993, RMSE: 0.683) and SVR (R^2: 0.987, RMSE: 0.766) also

performed well. GEP's strength lay in its ability to model complex, non-linear relationships.

- This thesis has successfully demonstrated the efficacy of advanced machine learning models, particularly Bi-LSTM integrated with the Self-Improved Jelly Search Optimizer (SIJSO), for accurately predicting the compressive strength of geopolymer concrete. The Bi-LSTM+SIJSO model achieved superior error metrics, including a MAPE of 0.007, MSE of 0.008, and RMSE of 0.092 at optimal training percentages, outperforming conventional approaches such as Bi-LSTM+AOA, Bi-LSTM+BMO, and others. Statistical analysis further validated the SIJSO method, recording the lowest mean error of 0.032 and a minimal error of 0.018 compared to alternative methods. Convergence analysis revealed the SIJSO model consistently maintained a lower error rate, achieving an error of 0.017 by the 25th iteration. These results highlight the advanced model's capacity for precise predictions and its potential to revolutionize the design of eco-friendly and high-performance construction materials.

6.2 Future Scope

- Exploring alternative supplementary cementitious materials such as metakaolin, silica fume, or rice husk ash in combination with Alccofine could enhance geopolymer concrete's mechanical and durability properties. Future research could focus on evaluating the long-term performance of geopolymer concrete under diverse environmental conditions, including freeze-thaw cycles, elevated temperatures, marine environments, and harsh chemical exposures. Investigating the impact of real-time environmental factors such as humidity, temperature, and curing conditions could further enhance model generalization and applicability, enabling more accurate predictions of geopolymer concrete performance in real-world scenarios.

- This research on geopolymer concrete using machine learning models such as SVR, GEP, and ANN highlights several promising directions for future exploration. Integrating hybrid models that combine the strengths of these algorithms could

significantly enhance prediction accuracy and reliability. Advanced optimization techniques like genetic algorithms, particle swarm optimization, and differential evolution could be employed to fine-tune model parameters for better performance.

List of Publications

(a) Papers in SCI/SCIE Journal (Published/Accepted)

S. No.	Title of the Paper	Name of the Authors	Name of the Journals	Indexing Status of Journal with Indexing Agency
1.	Prediction of Compressive Strength of Alccofine-Based Geopolymer Concrete	Diksha, Nirendra Dev and Pradeep Kumar Goyal	Iranian Journal of Science and Technology, Transactions of Civil Engineering DOI: https://doi.org/10.1007/s40996-023-01308-2	Science Citation Indexed Expanded, Clarivate
2.	Utilizing an Enhanced Machine Learning Approach for Geopolymer Concrete Analysis	Diksha, Nirendra Dev and Pradeep Kumar Goyal	Non-destructive Testing and Evaluation https://doi.org/10.1080/10589759.2024.2334434	Science Citation Indexed Expanded, Clarivate
3.	Predictive modeling and multi-parameter optimization of geopolymer mixes using SVM-GA hybrid approach.	Diksha, N. DKR Nirendra Dev and Pradeep Kumar Goyal	Multiscale and Multidisciplinary Modeling, Experiments and Design, 9(1), 1-23. https://doi.org/10.1007/s41939-025-01097-3	Emerging Sources Citation Index, Clarivate
4.	Optimized Alccofine-Based Geopolymer Concrete: Integrated Experimental Durability Assessment and Hybrid SVM–RF–PSO Predictive Modelling with Advanced Preprocessing Techniques	Under Review		

(b) Papers Presentation in the International Conference

S. No.	Title of the Paper(s)	Name of the Authors	Name of the Journals/ Conferences
1.	Use of XRD Technique in Characterizing different types of concrete	Diksha, Nirendra Dev and Pradeep Kumar Goyal	INNOVATIONS IN SMART AND SUSTAINABLE INFRASTRUCTURE (ISSI-2022) Organized by Civil Engineering, School of Technology, Pandit Deendayal Energy University, Gandhinagar during 23rd - 25th August, 2022
2.	Application of Brunauer–Emmett–Teller BET Theory in Characterization of Cementitious Materials (Cement, Supplementary Cementitious Materials/Aggregates/ Geopolymer)	Diksha, Nirendra Dev and Pradeep Kumar Goyal	International Conference on Advances in Civil Engineering 2022 held during 20th to 22nd December 2022, organized by Technology Research and Innovation Centre, India and hosted by LSKBJ College of Engineering, Chandwad, Nashik, India

References

- Adeleke, B. O., Kinuthia, J. M., Oti, J., & Ebailila, M. (2023). Physico-mechanical evaluation of geopolymer concrete activated by sodium hydroxide and silica fume-synthesised sodium silicate solution. Materials, 16(6), 2400.
- Alam, A., Verma, P., Tariq, M., Sarwar, A., Alamri, B., Zahra, N., & Urooj, S. (2021). Jellyfish search optimization algorithm for mpp tracking of pv system. *Sustainability*, *13*(21), 11736.
- Al-Amoudi, O. S. B., Abiola, T. O., & Maslehuddin, M. (2006). Effect of superplasticizer on plastic shrinkage of plain and silica fume cement concretes. *Construction and Building materials*, *20*(9), 642-647.
- Alameri, M., Ali, M. M., Elchalakani, M., & Sheikh, A. (2025). Optimizing slag-based geopolymer mix design for enhanced strength and durability. Journal of Building Engineering, 100, 111770.
- Alhazmi, H., Shah, S. A. R., Anwar, M. K., Raza, A., Ullah, M. K., & Iqbal, F. (2021). Utilization of polymer concrete composites for a circular economy: A comparative review for assessment of recycling and waste utilization. *Polymers*, *13*(13), 2135.
- Almutairi, A. L., Tayeh, B. A., Adesina, A., Isleem, H. F., & Zeyad, A. M. (2021). Potential applications of geopolymer concrete in construction: A review. *Case Studies in Construction Materials*, *15*, e00733.
- Altawil, H., & Olgun, M. (2025). Optimization of mechanical properties of geopolymer mortar based on Class C fly ash and silica fume: A Taguchi method approach. *Case Studies in Construction Materials*, *22*, e04332.
- Bakharev, T. (2005). Durability of geopolymer materials in sodium and magnesium sulfate solutions. *Cement and Concrete Research, 35*(6), 1233-1246.
- Benli, A., Öz, A., Kılıç, D., Tortum, A., Yıldız, İ., & Kaplan, G. (2025). Sustainable fly ash-based geopolymer composites: The influence of RAP aggregates and silica fume on strength, durability, and microstructural properties. Structural Concrete.
- Bhutta MAR et al (2014) Sulphate resistance of geopolymer concrete prepared from

blended waste fuel ash. J Mater Civ Eng 26(11):1–6

- Brencich, A., Bovolenta, R., Ghiggi, V., Pera, D., & Redaelli, P. (2020). Rebound hammer test: an investigation into its reliability in applications on concrete structures. *Advances in Materials Science and Engineering*, *2020*(1), 6450183.
- Buchwald, A., & Struble, L. (2009). Alkali-activated materials and geopolymers: Progress, challenges, and opportunities. *Journal of Materials in Civil Engineering, 21*(10), 457-469.
- Capacchione, C. (2021). Synthesis of new water reducer superplasticizers for building materials.
- Castillo, H., Collado, H., Droguett, T., Sánchez, S., Vesely, M., Garrido, P., & Palma, S. (2021). Factors affecting the compressive strength of geopolymers: A review. *Minerals*, *11*(12), 1317.
- Chalimourda, A., Schölkopf, B., & Smola, A. J. (2004). Experimentally optimal ν in support vector regression for different noise models and parameter settings. *Neural Networks*, *17*(1), 127-141.
- Chen, K., Wu, D., Xia, L., Cai, Q., & Zhang, Z. (2021). Geopolymer concrete durability subjected to aggressive environments–A review of influence factors and comparison with ordinary Portland cement. *Construction and Building Materials*, *279*, 122496.
- Chindaprasirt, P., Homwuttiwong, S., & Sirivivatnanon, V. (2005). Influence of fly ash fineness on strength, drying shrinkage, and sulfate resistance of blended cement mortar. *Cement and Concrete Research*, 35(6), 1155-1160.
- Dadsetan, S., Siad, H., Lachemi, M., Mahmoodi, O., & Sahmaran, M. (2022). Optimization and characterization of geopolymer binders from ceramic waste, glass waste and sodium glass liquid. *Journal of Cleaner Production*, *342*, 130931.
- Davidovits, J. (2002, October). years of successes and failures in geopolymer applications. Market trends and potential breakthroughs. In *Geopolymer 2002 conference* (Vol. 28, p. 29). Saint-Quentin, France; Melbourne, Australia: Geopolymer Institute.
- Davidovits, J. (1994, October). Properties of geopolymer cements. In *First international conference on alkaline cements and concretes* (Vol. 1, pp. 131-149).

- Deepa, C., & Gopalakrishnan, S. (2019). Predictive analysis of compressive strength of geopolymer concrete using ANN and SVM. *Materials Today: Proceedings*, 14, 457-463.
- Drucker, H., Wu, D., & Vapnik, V. N. (1999). Support vector machines for spam categorization. *IEEE Transactions on Neural networks*, *10*(5), 1048-1054.
- Duxson, P., Lukey, G.C., Separovic, F. and Van Deventer, J.S.J (2005). ‘‘Effect of alkali cations on aluminum incorporation in geopolymeric gels’’, Ind. Eng. Chem. Res., 44(4), pp. 832–839.
- Duxson, P., Provis, J.L., Lukey, G.C., & Van Deventer, J.S.J. (2007). The role of inorganic polymer technology in the development of ‘green concrete’. *Cement and Concrete Research, 37*(12), 1590-1597.
- Etxeberria, M., Vázquez, E., Marí, A., & Barra, M. (2007). Influence of amount of recycled coarse aggregates and production process on properties of recycled aggregate concrete. *Cement and concrete research*, *37*(5), 735-742.
- Frieda, F. S., & Greeshma, S. (2025). Effects on the strength and durability of graphene oxide modified geopolymer concrete using industrial waste bauxite tailings. *Case Studies in Construction Materials*, *22*, e04726.
- Girish, M., Prashanth, R., & Rajasekaran, C. (2020). Predictive modeling of compressive strength of fly ash-based geopolymer concrete using machine learning techniques. *Journal of Materials in Civil Engineering, 30*(8), 04018175.
- Girish, M., Prashanth, R., & Rajasekaran, C. (2021). Advances in machine learning for the prediction of geopolymer concrete properties. *Journal of Advanced Concrete Technology, 19*(3), 277-291.
- Girish, M., Prashanth, R., & Rajasekaran, C. (2023). Future directions in geopolymer concrete research: Challenges and opportunities. *Materials Today: Proceedings, 60*, 348-354.
- Gustavo W et al (2016) Fly ash slag geopolymer concrete: resistance to sodium and magnesium sulfate attack. J Mater Civ Eng 28(12):1–9
- Gougazeh, M., & Buhl, J. C. (2014). Utilization of local volcanic tuffs for producing high-performance blended cements: Pozzolanic activity and strength activity index. *Construction and Building Materials*, 52, 371-376.

- Rani, G. S., Jayan, S., & Alatas, B. (2023). Analysis of chaotic maps for global optimization and a hybrid chaotic pattern search algorithm for optimizing the reliability of a bank. *IEEE Access*, *11*, 24497-24510.
- Ghafoor, M. T., & Fujiyama, C. (2023). Mix design process for sustainable self-compacting geopolymer concrete. *Heliyon*, *9*(11).
- Guo, X., Shi, H., & Dick, W.A. (2020). Compressive strength and microstructural characteristics of class C fly ash geopolymer. *Cement and Concrete Research, 56*, 144-154.
- Gupta, R., & Kumar, S. (2020). Predictive modeling for the mix design of geopolymer concrete using machine learning. *Journal of Cleaner Production*, 264, 121689.
- Hanjitsuwan, S., Hunpratub, S., Thongbai, P., Maensiri, S., Sata, V., & Chindaprasirt, P. (2014). Effects of NaOH concentrations on physical and electrical properties of high calcium fly ash geopolymer paste. *Cement and Concrete Composites*, *45*, 9-14.
- Hardjito D, Wallah SE, Sumajouw DMJ, Rangan BV (2004). On the development of fly ash-based geopolymer concrete. ACI Mater J.; 101:467–472.
- Hardjito, D., & Rangan, B.V. (2005). Development and properties of low-calcium fly ash-based geopolymer concrete. *Research Report GC1, Faculty of Engineering, Curtin University of Technology*.
- Haque, M.N., Kayali, O., & Fawzy, M. (2014). Influence of type of aggregate on properties of geopolymer concrete. *Journal of Materials in Civil Engineering, 26*(7), 1095-1102.
- https://en.wikipedia.org/wiki/Long_short-term_memory
- https://www.analyticsvidhya.com/blog/2021/09/introduction-to-artificial-neural-networks/
- https://www.javatpoint.com/genetic-algorithm-in-machine-learning
- https://www.geeksforgeeks.org/genetic-algorithms/
- https://www.obitko.com/tutorials/genetic-algorithms/selection.php
- Hussein, R.A., Apasi, A., & Ibrahim, T. (2017). Long term performance of fly ash based geopolymer concrete in marine environment. *Construction and Building Materials, 147*, 533-544.

- Imbabi, M. S., Carrigan, C., & McKenna, S. (2012). Trends and developments in green cement and concrete technology. *International Journal of Sustainable Built Environment*, *1*(2), 194-216.
- Imtiaz, L.; Rehman, S.K.U.; Memon, A.S.; Khizar, K.M.; Faisal, J.M. A Review of Recent Developments and Advances in Eco-Friendly Geopolymer Concrete. *Appl. Sci.* 2020, *10*, 7838.
- Ismail SA, Bernal JL, Provis SH, Deventer JSJ (2013) Microstructural changes in alkali-activated fly ash/slag geopolymers with sulfate exposure. Mater Struct Constr 46:361–373
- Jin, L., Chen, M., Wang, Y., Peng, Y., Yao, Q., Ding, J., ... & Lu, S. (2023). Utilization of mechanochemically pretreated municipal solid waste incineration fly ash for supplementary cementitious material. *Journal of environmental chemical engineering*, *11*(1), 109112.
- Kadam, A. S., & Patil, S. S. (2018). Influence of Alccofine on strength and durability of high-performance concrete. Journal of Building Engineering, 18, 109-117.
- Kanagaraj, B., Priyanka, R., Anand, N., Kiran, T., Andrushia, A. D., & Lubloy, E. (2024). A sustainable solution for mitigating environmental corrosion in the construction sector and its socio-economic concern. Case Studies in Construction Materials, 20, e03089.
- Kore, S. D., & Vyas, A. K. (2015). Behavior of concrete using marble waste as coarse aggregate. In *UKIERI Concrete Congress–Concrete Research Driving Profit And Sustainability* (pp. 78-87).
- Koza, J. R. (1990). *Genetic programming: A paradigm for genetically breeding populations of computer programs to solve problems* (Vol. 34). Stanford, CA: Stanford University, Department of Computer Science.
- Kruse, R., Mostaghim, S., Borgelt, C., Braune, C., & Steinbrecher, M. (2022). Fundamental evolutionary algorithms. In Computational Intelligence: A Methodological Introduction (pp. 287-341). Cham: Springer International Publishing.
- Kryvenko, P., Rudenko, I., Sikora, P., Sanytsky, M., Konstantynovskyi, O., & Kropyvnytska, T. (2024). Alkali-activated cements as sustainable materials for repairing building construction: a review. *Journal of Building Engineering*, 109399.

- Kumavat, H. R., Chandak, N. R., & Patil, I. T. (2021). Factors influencing the performance of rebound hammer used for non-destructive testing of concrete members: A review. *Case Studies in Construction Materials*, *14*.
- Kumar, S., Kumar, R., & Mehrotra, S.P. (2021). Influence of mechanical activation on the physical properties of geopolymer concrete. *Journal of Cleaner Production, 17*(6), 847-853.
- Kumar, S., Kumar, R., & Mehrotra, S.P. (2023). Applications of geopolymer concrete in infrastructure: A case study approach. *Construction and Building Materials, 250*, 1187-1196.
- Li, H., Zhang, Z., Deng, Y., Xu, F., Hu, J., Zhu, D., ... & Shi, C. (2024). Geopolymer composites for marine application: structural properties and durability. *Cement and Concrete Composites*, *152*, 105647.
- Li, S., Si, W., Hui, J., & Ma, B. (2025). The effect and mechanism of superplasticizers on the efflorescence performance of alkali-activated slag-based materials. Case Studies in Construction Materials, 22, e04160.
- Liew, K.M., Sojobi, A.O., & Zhang, L.W. (2022). Cost-benefit analysis of geopolymer concrete in sustainable construction. *Journal of Cleaner Production, 300*, 123456.
- Liew, K.M., Sojobi, A.O., & Zhang, L.W. (2023). Smart construction materials: The integration of machine learning and IoT in geopolymer concrete. *Construction and Building Materials, 310*, 124567.
- Lloyd, N.A., & Rangan, B.V. (2010). Geopolymer concrete with fly ash. *In Second International Conference on Sustainable Construction Materials and Technologies*.
- Luhar, I., & Luhar, S. (2022). A comprehensive review on fly ash-based geopolymer. *Journal of Composites Science*, *6*(8), 219.
- Malhotra, V. M. (2002). *Introduction: Sustainable Development and Concrete Technology.* ACI Concrete International, 24(7), 22-26.
- Malhotra, V. M. (2004, January). Role of supplementary cementing materials and superplasticizers in reducing greenhouse gas emissions. In *Proceedings of ICFRC International Conference on Fiber Composites, High-Performance Concrete, and Smart Materials, Chennai, India* (pp. 489-499).

- Mastali, M., Kinnunen, P., Dalvand, A., Firouz, R. M., & Illikainen, M. (2018). Drying shrinkage in alkali-activated binders–a critical review. *Construction and Building Materials*, *190*, 533-550.
- Mccaffrey, R. (2002). Climate change and the cement industry. *Global cement and lime magazine (environmental special issue)*, *15*, 19.
- Rahman, M. M., Watanobe, Y., & Nakamura, K. (2021). A bidirectional LSTM language model for code evaluation and repair. *Symmetry*, *13*(2), 247.
- Mehta, P. K. (2002). Greening of the concrete industry for sustainable development. *Concrete international*, *24*(7), 23-28.
- Mehta, P. K., Monteiro, P. J. M., & Kumar, A. (2024). *Concrete: Microstructure, Properties, and Materials*. McGraw-Hill Education.
- Mishra, P., Shrivastava, A., & Yadav, S. (2022). Optimization of geopolymer concrete using machine learning techniques. *Journal of Building Engineering*, 48, 103872.
- Nandy, B., Saha, S., & Chakraborty, S. (2021). Comparative study of Alccofine in conventional and geopolymer concrete for sustainable construction. Construction and Building Materials, 298, 123930.
- Nagalia G, Park Y, Abolmaali A, Aswath P (2016) Compressive strength and microstructural properties of fly ash-based geopolymer concrete. J Mater Civ Eng.
- Nasir, M., Mahmood, A. H., & Bahraq, A. A. (2024). History, recent progress, and future challenges of alkali-activated binders–An overview. *Construction and Building Materials*, *426*, 136141.
- Nath, P., & Sarker, P.K. (2014). Effect of GGBFS on setting, workability and early strength properties of fly ash geopolymer concrete cured in ambient condition. *Construction and Building Materials, 66*, 163-171.
- Nath, P., Roy, T., & Kumar, M. (2021). Application of machine learning in predicting compressive strength of fly ash-based geopolymer concrete. *Construction and Building Materials*, 279, 122469.
- Nazari, A., & Sanjayan, J.G. (2020). Comparative study of the mechanical properties of geopolymer and traditional concrete. *Materials and Design, 60*, 564-569.
- Nazari, A., & Sanjayan, J.G. (2023). Understanding the variability in geopolymer

concrete properties: A comprehensive review. *Journal of Advanced Concrete Technology, 21*(2), 345-357.

- Nguyen, H. A. T., Pham, D. H., Ahn, Y., Oo, B. L., & Lim, B. T. H. (2025). Machine learning and sustainable geopolymer materials: A systematic review. *Materials Today Sustainability*, 101095.
- Neville, A. M., & Brooks, J. J. (2023). *Concrete Technology*. Pearson Education
- Okoye, F. N. (2017). Geopolymer binder: A veritable alternative to Portland cement. *Materials Today: Proceedings*, *4*(4), 5599-5604.
- Olivia, M., & Nikraz, H. (2011). Strength and water penetrability of fly ash geopolymer conrete. *Journal of Engineering and Applied Sciences*, *6*(7), 70-78.
- Oti, J., Adeleke, B. O., Mudiyanselage, P. R., & Kinuthia, J. (2024). A Comprehensive Performance Evaluation of GGBS-Based Geopolymer Concrete Activated by a Rice Husk Ash-Synthesised Sodium Silicate Solution and Sodium Hydroxide. *Recycling*, *9*(2), 23.
- Palomo, A., Grutzeck, M.W., & Blanco, M.T. (1999). Alkali-activated fly ashes: A cement for the future. *Cement and Concrete Research, 29*(8), 1323-1329.
- Paruthi, S., Rahman, I., Husain, A., Khan, A. H., Manea-Saghin, A. M., & Sabi, E. (2023). A comprehensive review of nano materials in geopolymer concrete: Impact on properties and performance. *Developments in the Built Environment*, *16*, 100287.
- Paruthi, S., Rahman, I., Khan, A. H., Sharma, N., & Alyaseen, A. (2024). Strength, durability, and economic analysis of GGBS-based geopolymer concrete with silica fume under harsh conditions. *Scientific Reports*, *14*(1), 31572.
- Patel, H., Sharma, S., & Dutta, P. (2024). *Effect of Alccofine on the durability and strength characteristics of concrete: A comprehensive study*. Construction and Building Materials, 361, 130184.
- Pratap, B., Mondal, S., & Rao, B. H. (2023, October). NaOH molarity influence on mechanical and durability properties of geopolymer concrete made with fly ash and phosphogypsum. In *Structures* (Vol. 56, p. 105035). Elsevier.
- Provis, J. L., & van Deventer, J. S. J. (2009). Geopolymers: Structure, processing, properties, and industrial applications. Elsevier.
- Provis, J. L. (2018). Alkali-activated materials. *Cement and concrete research*, *114*,

40-48.

- Qaidi, S.M.A.; Tayeh, B.A.; Zeyad, A.M.; de Azevedo, A.R.G.; Ahmed, H.U.; Emad, W (2022). Recycling of mine tailings for the geopolymers production: A systematic review. *Case Stud. Constr. Mater*, *16*.
- Raja, M. A., & Sujatha, S. J. (2024). Geopolymer concrete cured under ambient conditions using a single alkali activator. *Matéria (Rio de Janeiro)*, *29*(3), e20240281.
- Rajini, S., Suguna, K., & Nambiar, E.K.K. (2022). Deep learning techniques in the prediction and optimization of geopolymer concrete mix design. *Materials Today: Proceedings, 50*, 450-456.
- Rajput, B. S., Rajawat, S. P. S., & Jain, G. (2024). Effect of curing conditions on the compressive strength of fly ash-based geopolymer concrete. *Materials Today: Proceedings*, *103*, 32-38.
- Rangan, B.V. (2008). Low-calcium fly ash-based geopolymer concrete. *Research Report GC4, Curtin University of Technology, Perth, Australia*.
- Rangan, B. V. (2010). Fly ash-based geopolymer concrete. In Research Report GC4. Faculty of Engineering, Curtin University of Technology, Perth, Australia.
- Reddy, M. C., Reddy, N. S., & Kumar, A. (2019). Application of Alccofine in improving the properties of geopolymer concrete. Materials Today: Proceedings, 18, 2272-2278.
- Reddy, N., & Saha, R. (2021). ML applications for enhancing durability predictions of geopolymer concrete. *Materials Today: Proceedings*, 37, 2460-2467.
- Reddy, N. D. K., Diksha., Gupta, A. K., & Sahu, A. K. (2024). Evaluation of soil liquefaction potential using ensemble classifier based on grey wolves optimizer (GWO). *Soil Dynamics and Earthquake Engineering*, *182*, 108750.
- Ribeiro, F. R. C., Ruviaro, A. S., de Matos, P. R., & Kirchheim, A. P. (2025). Impact of different superplasticizers on hydration, rheology, mechanical strength, and environmental evaluation of LC3 cements. Case Studies in Construction Materials, e05347.
- Sarker, P.K., Kelly, S., & Yao, Z. (2013). Effect of fire exposure on cracking, spalling and residual strength of fly ash geopolymer concrete. *Materials and Design,*

63, 584-592.

- Sathish Kumar, T., Rao, S., & Reddy, B. (2020). Effects of Alccofine on mechanical properties of concrete. International Journal of Civil Engineering and Technology, 11(3), 372-380.
- Sharma, M., & Gupta, R. (2024). *The role of ultra-fine supplementary cementitious materials in enhancing concrete performance*. Materials Today: Proceedings, 91, 425-431.
- Shobeiri, V., Bennett, B., Xie, T., & Visintin, P. (2021). A comprehensive assessment of the global warming potential of geopolymer concrete. *Journal of Cleaner Production*, *297*, 126669.
- Sharma, S., Sharma, S., & Athaiya, A. (2017). Activation functions in neural networks. *Towards Data Sci*, *6*(12), 310-316.
- Sharma, D., Sharma, S., & Goyal, A. (2016). Utilization of waste foundry slag and alccofine for developing high strength concrete. *International Journal of Electrochemical Science*, *11*(4), 3190-3205.
- Singh, R., Kumar, A., & Bhardwaj, P. (2023). *Innovative applications of Alccofine in sustainable concrete development*. Journal of Building Engineering, 57, 104743.
- Sofi, M., van Deventer, J. S. J., Mendis, P. A., & Lukey, G. C. (2007). Engineering properties of inorganic polymer concretes (IPCs). Cement and Concrete Research, 37(2), 251-257.
- Songpiriyakij, S., Pulngern, T., Pungpremtrakul, P., & Jaturapitakkul, C. (2010). Sulfate resistance of blended fly ash geopolymer concrete. *Construction and Building Materials, 24*(12), 2355-2365.
- Sujitha, V. S., Raja, S., Rusho, M. A., & Yishak, S. (2025). Advances and Developments in High Strength Geopolymer Concrete for Sustainable Construction–A Review. *Case Studies in Construction Materials*, e04669.
- Sung G et al (2015) The mechanical properties of Fly ash-based geopolymer concrete with alkaline activators. Constr Build Mater 47:409–418
- Sun, Z., & Vollpracht, A. (2020). Leaching of monolithic geopolymer mortars. Cement and Concrete Research, 136, 106161.
- Topark-Ngarm P, Chindaprasirt P, Sata V (2015) Setting time, strength, and bond of

high-calcium fly ash geopolymer concrete. J Mater Civ Eng 27(7):1–7

- Temuujin, J., Van Riessen, A., & Williams, R. (2010). Influence of calcium compounds on the mechanical properties of fly ash geopolymer pastes. *Journal of Hazardous Materials, 167*(1-3), 82-88.
- Tayeh, B. A., Zeyad, A. M., Agwa, I. S., & Amin, M. (2021). Effect of elevated temperatures on mechanical properties of lightweight geopolymer concrete. *Case Studies in Construction Materials*, *15*, e00673.
- Thatikonda, N., Mallik, M., Sarella, V. R., & Dubey, S. (2024). Evaluation of self-compacting geopolymer concrete properties containing different water glass solutions. *Sustainable Chemistry and Pharmacy*, *41*, 101680.
- Thomas, B.S., & Gupta, R.C. (2016). Performance of high-strength geopolymer concrete incorporating recycled aggregate. *Construction and Building Materials, 114*, 992-1000.
- Upreti, K., Verma, M., Agrawal, M., Garg, J., Kaushik, R., Agrawal, C., ... & Narayanasamy, R. (2022). Prediction of mechanical strength by using an artificial neural network and random forest algorithm. *Journal of Nanomaterials*, *2022*(1).
- Van Deventer, J. S., Provis, J. L., & Duxson, P. (2012). Technical and commercial progress in the adoption of geopolymer cement. *Minerals Engineering*, *29*, 89-104.
- Van Jaarsveld, J. G. S., Van Deventer, J. S. J., & Lorenzen, L. (1997). The potential use of geopolymeric materials to immobilise toxic metals: Part I. Theory and applications. *Minerals engineering*, *10*(7), 659-669.
- Verma, M., & Dev, N. (2021). Sodium hydroxide effect on the mechanical properties of flyash-slag based geopolymer concrete. *Structural Concrete*, *22*, E368-E379.
- Volaity, S. S., Aylas-Paredes, B. K., Han, T., Huang, J., Sridhar, S., Sant, G., ... & Neithalath, N. (2025). Towards decarbonization of cement industry: a critical review of electrification technologies for sustainable cement production. *npj Materials Sustainability*, *3*(1), 23.
- Wang, J., & Zhang, Y. (2025). Artificial intelligence in high-entropy materials. *Next Materials*, *9*, 100993.
- Wu, X., Shen, Y., & Hu, L. (2022). Performance of geopolymer concrete activated by sodium silicate and silica fume activator. *Case Studies in Construction Materials*, *17*.

- Xie, J., & Kayali, O. (2016). Effect of superplasticiser on workability enhancement of Class F and Class C fly ash-based geopolymers. *Construction and Building Materials*, *122*, 36-42.
- Xie, T., & Liew, K.M. (2019). A comprehensive review on computational modeling of geopolymer concrete. *Journal of Cleaner Production, 260*, 120872.
- Xie, J., Zhao, J., Wang, J., Wang, C., Huang, P., & Fang, C. (2019). Sulfate resistance of recycled aggregate concrete with GGBS and fly ash-based geopolymer. *Materials*, *12*(8), 1247.
- Xie, T., & Liew, K.M. (2021). Application of machine learning in assessing the durability of geopolymer concrete. *Cement and Concrete Composites, 120*, 104006.
- Xu, H., & Van Deventer, J. S. J. (2000). The geopolymerisation of alumino-silicate minerals. *International journal of mineral processing*, *59*(3), 247-266.
- Xu, H., & van Deventer, J. S. J. (2002). Geopolymerisation of multiple minerals. Minerals Engineering, 15(12), 1131-1139.
- Zhang, Z., Provis, J. L., Reid, A., & Wang, H. (2014). Geopolymer foam concrete: An emerging material for sustainable construction. *Construction and Building Materials*, *56*, 113-127.
- Zhang, Z., Provis, J.L., Reid, A., & Wang, H. (2022). Geopolymer concrete: Advanced insights into microstructure and mechanical properties. *Construction and Building Materials, 143*, 50-63.
- Zhang, Z., Provis, J.L., Reid, A., & Wang, H. (2023). Integration of IoT and machine learning for the monitoring and prediction of geopolymer concrete performance. *Construction and Building Materials, 300*, 124003
- Zhang, Z., Provis, J.L., Reid, A., & Wang, H. (2024). Long-term durability of geopolymer concrete: A critical review. *Journal of Cleaner Production, 400*, 130045
- Zhang, Z., Provis, J.L., Reid, A., & Wang, H. (2024b). Smart construction materials: The integration of machine learning and IoT in geopolymer concrete. *Construction and Building Materials, 310*, 124567.
- Zhou, S., Zhang, W., & Li, H. (2018). The influence of fly ash on the mechanical properties and microstructure of geopolymer concrete. *Journal of Cleaner Production, 190*, 524-532.

- Zhou, S., Zhang, W., & Li, H. (2024). Long-term durability of geopolymer concrete: A critical review. *Journal of Cleaner Production, 400*, 130045.
- Zuhua, Z., Xiao, Y., Huajun, Z., & Yue, C. (2009). Role of water in the synthesis of calcined kaolin-based geopolymer. *Applied clay science*, *43*(2), 218-223.